DETERMINATION OF DIFFUSION WEIGHTED MAGNETIC RESONANCE IMAGING BASED BIOMARKERS OF MILD COGNITIVE IMPAIRMENT IN PARKINSON'S DISEASE

by

Özge Can Kaplan

B.Sc., Biomedical Engineering, Işık University, 2015

Submitted to the Institute of Biomedical Engineering
in partial fulfillment of the requirements
for the degree of
Master of Science
in
Biomedical Engineering

Boğaziçi University
2017

ACKNOWLEDGMENTS

I would like to express my gratitude for those who has broaden my point of view and contributed to my thesis and other work during my M.Sc. period. Firstly, I would like to thank Asst. Prof. Dr. Esin Öztürk Işık for guiding me through all my research. Apart from this, and beyond, being a role model as an advisor and academician, I feel lucky to have met such a unique person. I also want to thank Assoc. Prof. Aziz Müfit Uluğ for his valuable advice that helped me a lot while interpreting my results and reshaping my pathway.

My deepest appreciation and thanks from heart goes to Ali Demir, M.Sc. for patiently answering my questions, and guiding me. His mentoring has always been a motivation for me to move on, even when I suspect if I am on the right path or not. Again, I want to share my very special thanks to Doğan Dalva, M.Sc. from Işık University Department of Electrical and Electronics Engineering, for helping me to initiate my studies with his expertise. I would also like to thank my laboratory colleagues for their warmest affection. Firstly to G. Hale Hatay, M.Sc. for helping me when I am stuck, and sharing her time with me to improve my work. Secondly to Dilek Betül Arslan, M.Sc. for sharing her experiences, knowledge and advice that eased my work. I will never forget her remindings that lifted my spirits up and Sevim Cengiz, M.Sc. for sharing her knowledge. Very special thanks to Ozan Genç and Ayhan Gürsan for their friendship and support.

Last but not least, thanks to my mother, for embracing me no matter where she is and keeping me in harmony. Another special thanks to Tümay Solak, for his gentle and patient nature. Without his partnership, this two years period would never be completed. I would like to dedicate my study to my granddad, who is not amongst us but will always be remembered delicately.

ACADEMIC ETHICS AND INTEGRITY STATEMENT

I, Özge Can Kaplan, hereby certify that I am aware of the Academic Ethics and Integrity Policy issued by the Council of Higher Education (YÖK) and I fully acknowledge all the consequences due to its violation by plagiarism or any other way.

Name :

Signature:

Date:

ABSTRACT

DETERMINATION OF DIFFUSION WEIGHTED MAGNETIC RESONANCE IMAGING BASED BIOMARKERS OF MILD COGNITIVE IMPAIRMENT IN PARKINSON'S DISEASE

Parkinson's Disease (PD) results in structural changes on white matter (WM) of the brain, creating cognitive deficits in addition to motor problems generally ending up with Parkinson's disease dementia (PDD). Mild cognitive impairment (MCI) is the middle stage of this cognitive decline. There is a need for finding non-invasive biomarkers for early diagnosis of PD-MCI. In this study, 27 cognitively intact PD (PD-CI), 32 PD-MCI and 18 healthy controls (HC) were included to assess the structural differences. Diffusion weighted magnetic resonance images (DW-MRI) were obtained at a Philips 3T clinical scanner. Fractional anisotropy (FA) and mean diffusivity (MD) maps were estimated from DW-MRI via FMRIB Software Library (FSL) tools. Mean FA and MD values were calculated at regions of Johns Hopkins University (JHU) 81 WM atlas and Montreal Neurological Institute (MNI) atlas. For each region, a Kruskal Wallis test was applied to detect statistically significantly FA or MD differences between the three subject groups, followed by a Mann Whitney rank sum test for pairwise comparisons. FA and MD maps were also fed into tract based spatial statistics (TBSS) tool of FSL and permutation tests were applied. Region based results showed that mean FA and MD values significantly differed in some WM regions mostly between PD-MCI and HC groups. TBSS results showed that there was a statistically significant difference between PD-MCI and HC FA maps at all of the regions assessed. Less number of regions had significant FA differences between PD-MCI and PD-CI groups, but no regions were found to be different between PD-CI and HC. The results obtained with this study may contribute into an early detection of PD-MCI.

Keywords: Parkinson's disease, mild cognitive impairment, diffusion weighted magnetic resonance imaging.

ÖZET

PARKİNSON HASTALIĞI HAFİF KOGNİTİF BOZUKLUĞUNUN DİFÜZYON AĞIRLIKLI MANYETİK REZONANS GÖRÜNTÜLEME TEMELLİ BİYOİŞARETLEYİCİLERİNİN BELİRLENMESİ

Parkinson hastalığı (PH) beyin ak maddesinde yarattığı yapısal değişimler sebebiyle, motor problemlere ek olarak, genelde Parkinson hastalığı demansa (PHD) dönüşen bilişsel kayıplara sebep olur. Parkinson hastalığı hafif kognitif bozukluğu (PH-HKB), bu bilişsel düşüşün orta seviyesidir. PH-HKB'nin teşhisinde invaziv olmayan biyoişaretleyicilerin bulunması gerekmektedir. Gruplar arası istatistiksel anlamlı farkların belirlenmesi için, 32 PH-HKB, 27 Parkinson kognitif normal hastası (PH-KN) ve 18 sağlıklı kontrol (SK) çalışmaya dahil edilmiştir. Difüzyon ağırlıklı manyetik rezonans görüntüleme görüntüleme (DA-MRG) verileri 3T Philips klinik MR tarayıcı ile alınmıştır. DA-MR görüntülerinden FMRIB yazılım kütüphanesi (FMRIB's Software Library - FSL) araçları kullanılarak, fraksiyonel anizotropi (FA) ve ortalama difüzivite (MD) haritaları çıkarılmıştır. Johns Hopkins Üniversitesi (JHU) 81-DTG atlası ve Montreal Nöroloji Enstitüsü (MNI) atlası bölgeleri üzerinde ortalama FA ve MD değerleri hesaplanmıştır. Her bölgede, gruplar arası istatistiksel anlamlı farkların belirlenebilmesı için Kruskal Wallis testi ve ikili karşılaştırmalar için, Mann Whitney sıra toplam testi uygulanmıştır. Ayrıca, FA ve MD haritaları, FSL'in yolak bazlı uzamsal istatistik (Tract Based Spatial Statistics - TBSS) yöntemiyle incelenmiş, permütasyon testi uygulanmıştır. Bölgesel sonuçlar, FA ve MD değerlerinin, PH-HKB ve SK arasındaki birçok bölgede anlamlı farkların bulunduğunu göstermektedir. TBSS sonuçlarında ise, PH-HKB ve SK arasında bütün bölgelerde fark görülürken, PH-KN ve SK arasında hiçbir bölgede fark bulunamamıştır. Bu çalışmada ulaşılan sonuçlar, PH-HKB'nin erken belirlenmesinde yardımcı olabilir.

Anahtar Sözcükler: Parkinson hastalığı, hafif kognitif bozukluk, difüzyon ağırlıklı manyetik rezonans görüntüleme.

TABLE OF CONTENTS

LIST OF FIGURES

LIST OF TABLES

LIST OF SYMBOLS

B_0	Magnetic Field
B_1	The Radio Frequency Magnetic Field
T_1	Spin Lattice Relaxation Time
T_2	Spin Spin Relaxation Time
γ	Gyromagnetic Ratio
λ	Eigenvalue
ω	Larmor Frequency (rad/sec)
Δ	Delta
π	3.1415...

LIST OF ABBREVIATIONS

2D	Two-dimensional
4D	Four-dimensional
ACE-R	Addenbrooke's Cognitive Examination Revised Test
AD	Axial Diffusivity
ADC	Apparent Diffusion Coefficient
BET	Brain Extraction Tool
D	Diffusion Coefficient
DICOM	Digital Imaging and Communications in Medicine
DLB	Dementia with Lewy bodies
DTI	Diffusion Tensor Imaging
DWI	Diffusion Weighted Image
EPI	Echo Planar Imaging
FA	Fractional Anisotropy
FID	Free Induction Decay
FSL	FMRIB Software Library
GDS	Geriatric Depression Scale
GRE	Gradient Echo
GUI	Graphical User Interface
HC	Healthy Control
Hz	Hertz
ICBM	International Consortium of Brain Mapping
JHU	Johns Hopkins University
M	Mega (10^6)
MD	Mean Diffusivity
mm	milimeters
MMSE	Mini Mental State Examination
MNI	Montreal Neurological Institute
MR	Magnetic Resonance

MRI	Magnetic Resonance Imaging
MS	Multiple Sclerosis
NIfTI	Neuroimaging Informatics Technology Initiative
NMR	Nuclear Magnetic Resonance
T	Tesla
TBSS	Tract Based Spatial Statistics
TE	Echo Time
TFCE	Threshold-Free Cluster Enhancement
TR	Repetition Time
PD	Parkinson's Disease
PD-CI	Parkinson's Disease - Cognitively Intact
PDD	Parkinson's Disease Dementia
PD-MCI	Parkinson's Disease - Mild Cognitive Impairment
RD	Radial Diffusivity
RF	Radio Frequency
s	seconds
SDMT	Symbol Digit Modalities
SE	Spin Echo
std	Standard Deviation
QOL	Quality of Life
UPDRS	Unified Parkinson Disease Rating Scale

1. INTRODUCTION

1.1 Principles of Magnetic Resonance Imaging

Magnetic Resonance Imaging (MRI) is an imaging technique, providing high soft tissue contrast. Studies on the field has started with electromagnetism in late 18^{th} century. However, the turning point of MRI started with the discovery magnetic resonance phenomenon by F. Bloch, and E. Purcell. Magnetic resonance is defined as some atomic nuclei absorbs or emits radio waves under strong magnetic field. Until 1970's MRI was used for chemical and physical analysis. In the year of 1971, R. Damadian showed that relaxation times of tissues and tumors differ under a magnetic field. Afterwards, first NMR image was acquired by P. Lauterbur. Evolution of MRI continued with, phase and frequency encoding, development of antenna coils, development of first fast imaging technique, EPI (Echo Planar Imaging) that reduced five hours of scan time to minutes. When it came to 1980's MRI modalities began to emerge. One of the first MR modalities introduced by D.Le Bihan was DWI (Diffusion Weighted Imaging) [1], that will be discussed in the latter sections.

MRI hardware consists of many equipments. A schematic of an MRI system is presented in Figure 1.1 [2]. These can be classified as the ones located in the control center, used by the operator and the others located the imaging room, shielded with copper and some other material due to magnetic field homogeneity and sound insulation issues. The control center, houses the host computer, providing a graphical user interface (GUI) for the operator [2]. The imaging room contains the hardware to generate and receive MR signals.

Magnets are the essentials of an MRI system. The main magnet, made up of superconducting metal-alloy, creates a constant magnetic field, B_0. Amplitude of magnetic field is measured in terms of Tesla and MRI systems used in clinics nowadays are either 1.5T or 3T.

A patient undergone an MRI scan is first exposed to the B_0 main magnetic field. On the other hand, in order to determine some certain coordinates on the subject, gradient coils located in orthogonal directions are used. Gradient coils generate magnetic fields in x, y, z directions, yet as their name implies, the strength of their magnetic field changes gradually.

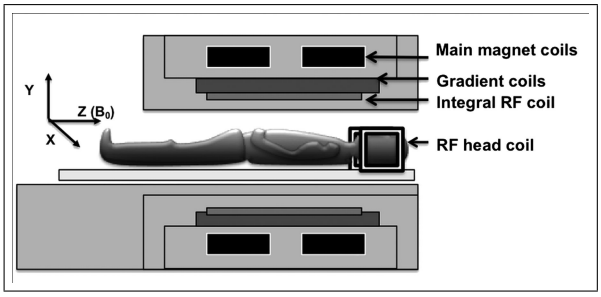

Figure 1.1: Basic MRI hardware.

RF Coils, which are located beneath the gradient coils can be considered as the antenna of an MRI system [2]. They have two functions: the first one is to transmit RF energy to the tissue of interest and the second one is to receive the RF signal back from the tissue of interest [3]. When an RF pulse, also called B_1 magnetic field, is applied, it is combined with B_0 magnetic field and as a result an MR signal is formed, that will be explained in detail in the following paragraphs. RF coils are separately assigned to perform transmission and receive RF signals, yet some coils do both of the tasks on a single device.

Apart from the pieces explained above, there are shimming coils, that ensure the homogeneity of magnetic field inside the coils. Homogeneity of magnetic field is required because it provides better image quality, but it is disturbed because of objects placed within the B_0 magnetic field.

1.1.1 Origins of MR Signal

The primary origin of the MR signal used to generate almost all clinical images comes from hydrogen nuclei [2]. A hydrogen atom, consists of a single proton and one

electron moving around the nucleus. The atom spins around itself, creating a small magnetic field around the atom (Figure 1.2a). The magnetic field for each proton is known as a magnetic moment [2], where for a normal group of atom magnetic moments are aligned randomly (Figure 1.2b). When an external magnetic field is applied, magnetic moments align either parallel or anti-parallel to B_0, depending on the energy state of the atom, yet, net magnetization is always in the same direction of B_0 magnetic field (Figure 1.2c). Apart from that, the group of atoms that are being exposed to the external magnetic field, precess about B_0. The most frequent explanation of precession is movement of a spinning top, and the imaginary main axis of the top forms a cone shape. A schematic of precession of a single atom around B_0 is shown in Figure 1.2d.

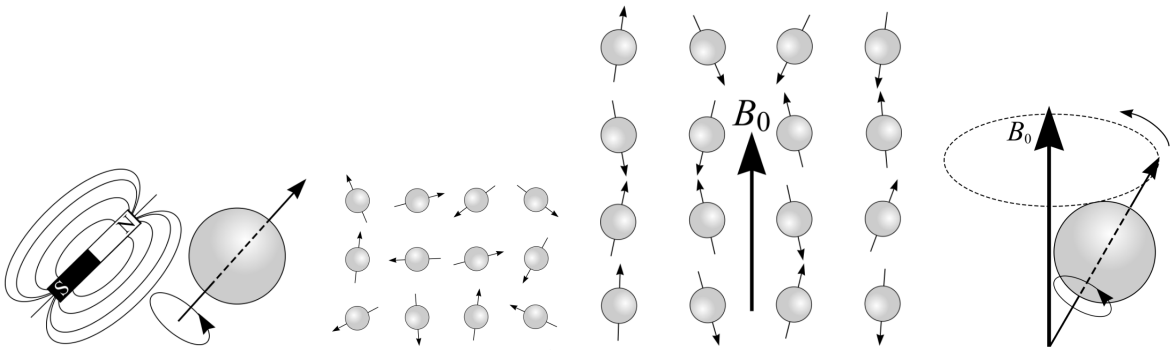

(a) Spin movement of an atom.

(b) Spins are aligned randomly.

(c) Under a magnetic field, spins align parallel or anti-parallel to the main magnetic field but net magnetization vector is always towards the main magnetic field.

(d) Precession movement.

Figure 1.2: Spin movement of atoms in natural state and under B_0 effect.

The frequency of precession in MHz is called Larmor frequency (ω_0). The Larmor frequency is calculated by the following equation,

$$\omega_0 = \gamma B_0, \tag{1.1}$$

stating that, rate of precession (i.e. frequency) is directly proportional to the strength of the main magnetic field. γ indicates the gyromagnetic ratio of the atom under

interest (the gyromagnetic ratio of hydrogen = 42.68 MHz/T [2]). As protons under align with B_0, they form a net magnetization M_0. Next, an RF pulse is applied at Larmor frequency, with an aim of distracting the alignment of spins. The net magnetization is tilted towards the transverse plane with a flip angle of α with respect to the main axis. As the RF pulse pushes the net magnetization vector off the main axis, this results in a reduction of the longitudinal magnetization and growth of the transverse magnetization. RF pulse, also causes protons to move in phase (i.e. same direction, at the same time) [2]. When RF pulse is turned off, spins relax while the phase harmony fades and the net magnetization returns to the beginning state, causing a longitudinal magnetization regrowth. This process is called T_1 relaxation. At the same time, transverse magnetization reduces, which is called as T_2 relaxation. These parameters are the main cause of contrast in MR images (see Figure 1.3, [4]) since the signal intensity varies for different type of tissues due to their varying relaxation times.

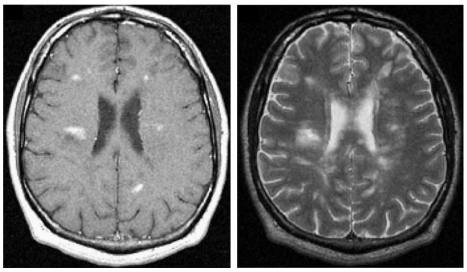

Figure 1.3: T_1 (left) and T_2 (right) weighted MR images of human brain.

In physics, it has been stated that if a closed loop is placed around a changing magnetic field, an electric current is induced on the closed loop. The same principle is used in MR signal receiving as well. The motion of transverse magnetization creates an alternating magnetic field inducing a potential difference across the conductive receiver coil, resulting in an electric current. This current is what we call an MR signal.The vectorial summation of longitudinal and transverse magnetization components is called free induction decay (FID). (Figure 1.4 [2]).

Echo is another type of MR signal formed as a result of the interaction of two or more RF pulses. There are two main types of echo signals, spin echo (SE) and gradient echo (GRE). RF pulse sequences differ according to the type of echo we would like to

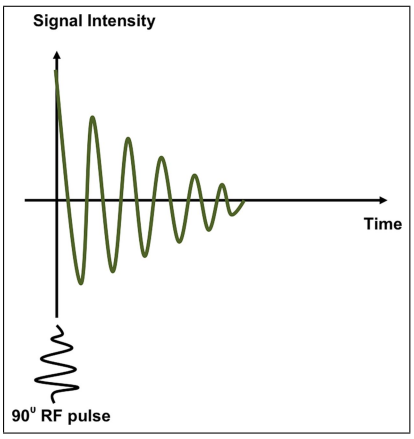

Figure 1.4: Basic MR signal, FID, formed after an RF pulse.

acquire, yet, further details would be out of scope of this study. The factors influencing MR signal intensity that enables us to differentiate between tissues are, proton density, T_1, T_2 relaxation times, flow of liquids like water or blood, repetition time of pulse sequences, echo time, inversion time and magnetic susceptibility [2].

1.2 Diffusion Weighted Magnetic Resonance Imaging

In MRI we create the contrast due to the different properties of tissues. The composition or flow of the tissue can be used as contrast mechanisms. While magnetic characteristics of tissues make them vary in relaxation times (i.e.T_1, T_2), molecular differences add spectroscopic features and fluid movement creates differentiation in terms of perfusion and diffusion. Proton density weighted MR images, T_1, T_2 weighted MR imaging, MR spectroscopic imaging, perfusion and diffusion weighted MR imaging (DWI) are MRI techniques with discrete characteristics. The scope of this study covers DWI, for this reason, an overview of this technique will be presented.

The advantage of DWI is that deductions drawn are very sensitive due to the fact that water diffusion apply on much smaller length scales than the nominal image resolution [5].

Apart from the usage in brain, DWI is used in other applications, like characterization of renal disease and measuring cartilage intensity [6]. As a side note, we should add that, one step further of DWI is diffusion tensor imaging (DTI), that is used in 3D visualization of neural pathways [7]. To construct a DTI image, DWI images acquired with at least six directions are required. The technique is used to observe white matter (WM) integrity in normal brain or diseases like multiple sclerosis (MS), stroke, dementia, and schizophrenia [7]. Likewise, it is a valuable technique for presurgical evaluation, primarily in patients with tumors and epilepsy [5].

1.2.1 Physics of Diffusion Weighted Imaging

In order to understand how the diffusion weighted images are acquired by using MRI, the concept of "diffusion" must be understood first. Diffusion is transfer of one material from one spatial location to another [8]. In numeric perspective, diffusion, D, is described by a probability density function given as,

$$D = \frac{<\Delta t^2>}{2\Delta t}, \tag{1.2}$$

where t is time, and it is assumed that there are no boundaries that would prevent motion. This type of diffusion is called "isotropic". When there are some structures that directs motion along an axis, the motion becomes "anisotropic". At this point, the expression becomes a multivariate normal distribution given as [8],

$$P = (\Delta\vec{r}, \Delta t) = \frac{1}{\sqrt{(4\pi t)^3|D|}} exp \frac{-\Delta\vec{r}^T Dm1\Delta\vec{r}}{4\Delta t}. \tag{1.3}$$

A schematic comparing isotropic and anisotropic motion is given in Figure 1.5 [9]. The term anisotropy was first introduced by Basser et al. [8]. Each material has its' own diffusion coefficient depending on molecular shape, size, viscosity or the medium

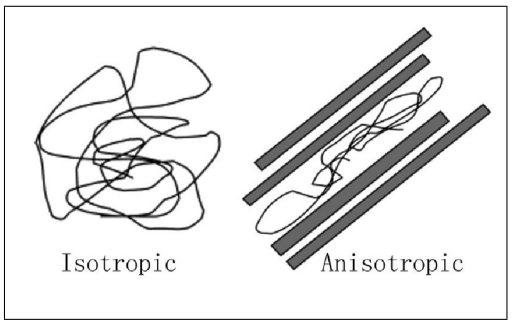

Figure 1.5: A schematic of isotropic vs. anisotropic motion.

it is located in. It is described by Einstein's diffusion coefficient equation given as [8],

$$D = \frac{< \Delta r^2 >}{2n\Delta t} \tag{1.4}$$

which states that diffusion coefficient is a function of mean square displacement divided by the number of dimensions and time elapsed [8]. As water is the most abundant compound in the human body, it moves in between, within, outside or through the cells, even in postmortem brain [8, 10]. In biological tissues, diffusion is mostly anisotropic. If the motion is restricted by any tissue, water moves within the remaining space. If we could detect mobile and stationary water, then we could have a clue on the structure of the surrounding area. Diffusive motion is also modified as structure of the tissue changes [8]. For this reason, by observing the water motion in a region over time, it is possible to detect any morphological change that have occurred. Based on its principle, information that DTI provides is more structural than physiological [10].

Diffusion tensor is a matrix, where diffusion coefficients are shown in all directions [8]. When diffusion movement is perfectly isotropic, diffusion tensor matrix becomes zero, except diagonal elements that are equal (see Equation 1.5). This means, diffusion in x, y, z axes are in equal rate, thus, motion is symmetrical. On the other hand, when there is anisotropy, due to the inequality in diffusion rates in different directions, diagonal elements are unequal and off-diagonal elements change as well

(Equation 1.6).

$$D = \begin{bmatrix} D_{xx} & 0 & 0 \\ 0 & D_{yy} & 0 \\ 0 & 0 & D_{zz} \end{bmatrix} \tag{1.5}$$

$$D = \begin{bmatrix} D_{xx} & D_{xy} & D_{xz} \\ D_{yx} & D_{yy} & D_{yz} \\ D_{zx} & D_{zy} & D_{zz} \end{bmatrix} \tag{1.6}$$

1.2.2 Diffusion Weighted Image Acquisition

DTI uses water as a probe to infer the neuroanatomy [10] and motion of water is detected by the phase difference, described in Section 1.1. MRI can be sensitized to diffusion process by some pulse sequence alterations [5]. First, a diffusion gradient is applied and the frequency of water molecules change with respect to their location. This is called the "dephasing gradient" and when it ends, although the frequencies go back to Larmor frequency, phases of spins remain different. After 10-100 ms of dephasing gradient, another "rephasing" gradient is applied in the opposite direction. In case of no water motion, rephasing pulse is able to unwind the phase of the spins. If water moves in between these two pulses, rephasing pulse could not unwind phase differences, and some signal loss occurs due to dephasing [8, 10] (Figure:1.6 [8, 10]).

So, how exactly do we proceed to measure the diffusion coefficients, if the pulse sequence gives measures of the signal loss due to water motion? This could be achieved by a simple method proposed by Stejskal and Tanner, by obtaining two images of the same tissue with two different b values given as [11],

$$Experiment1 : S_1 = S_0 e^{-b_1 D} \tag{1.7}$$

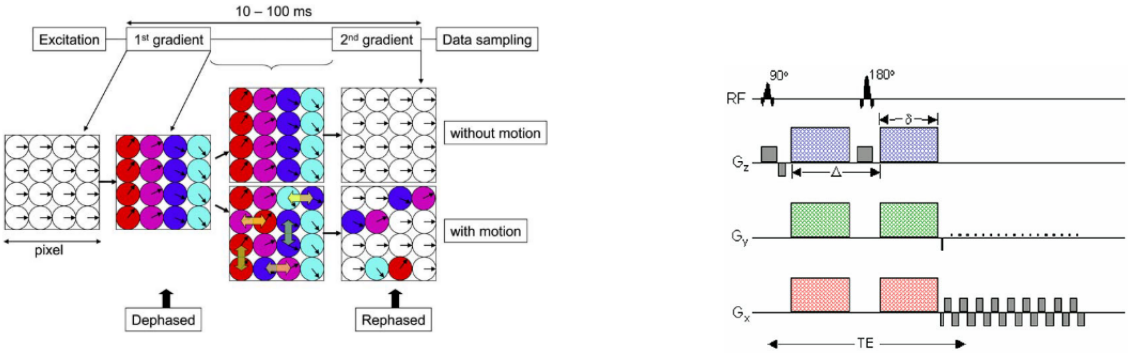

(a) Spin alignment in DWI.

(b) DWI-EPI pulse sequence.

Figure 1.6: DWI acquisition.

$$Experiment2 : S_2 = S_0 e^{-b_2 D} \tag{1.8}$$

Taking the ratio of these signals, the S_0 term cancels out and the equation becomes,

$$\frac{S_1}{S_2} = e^{-(b_2 - b_1)D} \tag{1.9}$$

We could then estimate the diffusion coefficient, D, by taking the natural logarithm of both sides as,

$$D = \frac{-ln(\frac{S_2}{S_1})}{(b_2 - b_1)}. \tag{1.10}$$

1.2.3 Diffusion Weighted Image Parameters

Many diffusivity-based measures derived from DWI have been proposed [12–15] and some of them are the essential parameters of our study. For this reason, some of these will be discussed in detail.

DTI metrics are usually derived from a mathematical combination of the three eigenvectors [16]. Calculation of diffusivity value, for a single voxel is shown in Figure 1.2.2. If diffusivity is calculated for each voxel, an apparent diffusion coefficient (ADC)

map is derived. ADC measures the freedom of water molecules encircled by a tissue. In other words, it measures the axial diffusivity (AD) in one direction, either x, y or z, represented by a single λ. Radial diffusivity (RD) is the mean diffusion in one of the cartesian planes. When considered in physiological aspect, it can be defined as the diffusivity perpendicular to the fibers/myelin content [17]. Because we are dealing on a 2D basis, the equation becomes [17]:

$$RD = \frac{\lambda_2 + \lambda_3}{2} \tag{1.11}$$

Mean diffusivity (MD), reflects the average degree of diffusion. Mean diffusivity of a voxel is the average of its eigenvalues [8],

$$MD = \frac{\lambda_1 + \lambda_2 + \lambda_3}{3} \tag{1.12}$$

in $\frac{mm^2}{s^-2}$ units [17]. Fractional anisotropy (FA) is the most widely used DTI based parameter [7]. Derived from eigenvalues, FA values vary in a range of 0 to 1, and it is widely used for white matter anisotropy [5]. On a FA map, areas with high signal intensity (i.e. areas appearing white) shows the regions with anisotropic motion (FA value of 1 means the motion is fully anisotropic), while low signal intensity (areas appearing in black) refers to the regions that are fully isotropic. FA value for a voxel is calculated as [5],

$$FA = \sqrt{\frac{3}{2}} \sqrt{\frac{(\lambda_1 - \overline{\lambda})^2 + (\lambda_2 - \overline{\lambda})^2 + (\lambda_3 - \overline{\lambda})^2}{2(\lambda_1^2 + \lambda_2^2 + \lambda_3^2)}} \tag{1.13}$$

An example set of FA, MD, AD and RD maps of a 28-years old healthy female volunteer are given in Figure 1.7 [18].

1.3 Parkinson's Disease

Parkinson's disease (PD) is a neurodegenerative disorder, following Alzheimer's disease (AD) in terms of frequency [19]. Major cause of the disease is thought to be the

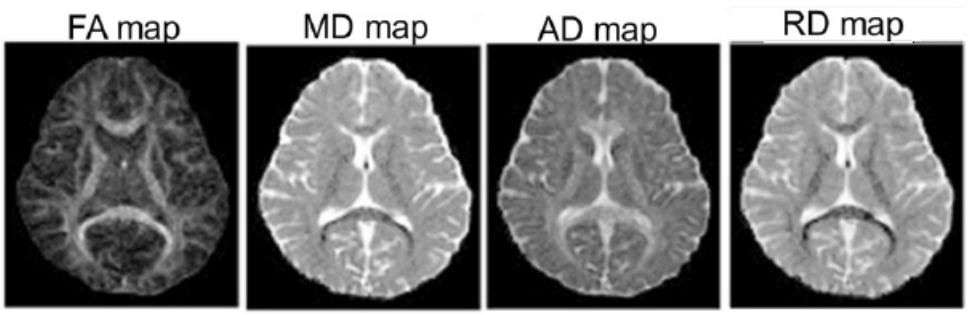

Figure 1.7: An example set of FA, MD, AD and RD maps.

striatal dopamine depletion, i.e. loss of dopaminergic function, that results in characteristic motor symptoms of PD [20, 21]. Also the presence of Lewy bodies (LB), which is intracellular cytoplasmic aggregation composed of protein, lipid and other materials, is considered as another cause of the disease [22,23]. Further evidence shows the disease has a pattern beginning in the brain stem and proceeds to higher cortical levels [23,24]. The disease itself is well known with a motor phenotype of tremor, postural instability and gait disorders [19,20]. Additionally, PD has a large range of non-motor symptoms, that is recognized broadly [25–27] but often missed in clinical practice [19]. Existence of these are related with neuromodulators adenosine, enkephalins and neurotransmitters of glutamergic, cholinergic, serotonergic and adrenergic system [28]. The non-motor symptoms can be classified as sleep disorders, oddly opposite types like insomnia or excessive daytime somnolence. Autonomic symptoms include bladder disturbances, sweating, and sexual difficulties. Gastrointestinal symptoms like bowel incontinence, sensory symptoms of pain, olfactory disturbance or visual dysfunction are also sometimes observed. Another type of non-motor symptoms is neuropsychiatric ones. The spectrum of cognitive deficits ranges from mild cognitive impairment (MCI) to PD-Dementia (PDD), starting with symptoms of executive dysfunction. Researchers have shown that, 30%-40% of PD patients suffer from dementia [29]. These cognitive impairments might cause confusion or attention loss. At the latest stages, PDD causes cognitive symptoms like hallucination, mood disorders, anxiety, apathy, and depression. Beside the disability it creates, it doubles the mortality risk [30].

PD-MCI is the middle stage of the cognitive decline. By definition, it is the

cognitive decline from a previous performance baseline that is considered abnormal for the patients age, but with a retention of normal daily functioning [29]. Its progression has been linked to age, late disease onset, severity of PD and lower educational level [31].

PD-MCI can be categorized according to the affected cognitive domain. Amnestic MCI causes memory deficits, non-amnestic MCI affects other cognitive domains like executive, visiospatial, attention or language. While cases only memory domain is affected is called "single domain" MCI, if an additional non-memory domain is affected.the disease is called "multiple domain" MCI [32–34].

PD-MCI to PDD is progressive. There are many studies searching on this gradual decline. Considering the fact that these studies do not have the same sample size, drawing a general conclusion by comparing results is not simple yet some numeric data can be presented [35]. Statistics has shown that 27% (ranging in between 19%-38%) of PD patients have MCI, and upto 80% of these patients tend to develop PDD [34]. Community based studies indicated that 20-35% of PD population would develop PD-MCI and 10% would progress to PDD per year [29,36]. A similar study showed that cumulative incidence of developing cognitive impairment was 8.5% within 1 year follow up [37]. According to a 5 year follow up study of Broeders and a Norwegian Park West study carried by Pedersen, it was concluded that within 5 years after diagnosis, 25-50% of patients with PD developed PD-MCI or PDD, and likewise, PD-MCI progressed to PDD [38, 39].

Diagnosis of PD and subtypes might be challenging. Disorders of motor features may not present approximately until 50 to 80% of dopaminergic neurons are lost, meaning that a serious disease progression exists [40, 41]. Additionally there are more than 15 diseases showing similar symptoms like AD, basal ganglia tumor, cerebrovascular disease or dementia with LB [19, 20]. Diagnosis criteria of PD-MCI and PDD are defined in clinical, cognitive and functional aspects [34, 35]. There are some diagnostic criteria of PD-MCI that is based on the definition of MCI and some specificities of PD [42]. According to the MDS Task Force written by Litvan et al., a four step diagnosis criteria is defined. First step is inclusion criteria. As much as inclusion criteria

are ensured, probability of patient to be diagnosed with PD-MCI increases and second step is exclusion criteria, where ensurance prevents mis-diagnosis. To start with inclusion criteria, in order for a patient to be diagnosed with MCI, he must be diagnosed with PD according to UK PD Brain Bank criteria [34]. Secondly, a cognitive decline should be measured either by the patient himself or a caregiver. The final criteria is that cognitive decline should not prevent daily activities [19, 42].

Exclusion criteria are, diagnosis of PDD, which is already the end point of cognitive problems and the patient should no longer be assessed in PD-MCI category. Secondly, if there are some other explanations of current problems like stroke, depression, trauma or adverse effects of medication, patient is excluded of the PD-MCI group [34].

Third step of diagnosing PD-MCI is to define the category, whether level I or level II. Level I subtype shows symptoms of impairment in a cognitive domain. Global test scores derived from neuropsychological tests give information on cognitive profile of the subject. Some common tests are Montreal Cognitive Assessment (MCA), Parkinson's Disease Cognitive Rating Scale, Scales for Outcomes of Parkinson's Disease Cognition and Mattis Dementia Rating Scale [34]. Level II subtype of PD-MCI requires a detailed assessment to be diagnosed. Application of two neuropsychological tests for each cognitive domain is a necessity [34] and at least two of them are supposed to result in impairment.

Fourth step of diagnosis is understanding the type of PD-MCI, in terms of single or multiple domain. For this reason, again, neuropsychological tests for at least two of each cognitive domain are used. Failure of two tests for one domain, as long as others are unimpaired is necessary. If at least one impaired result in more than one domain is concluded, PD-MCI can be said to be multiple domain [34].

The important fact is non-motor symptoms tend to emerge much before motor symptoms. This makes cognitive complaints especially important on watching the progression of the disease. If a drug therapy is effective on PDD, it might also be

effective on PD-MCI, but this hypothesis has not been tested on large clinical trials [19]. Furthermore, another view states that drug intervention might be even more effective on slowing the disease progression if applied at earlier stages [33].

When quality of life (QOL) decreases due to motor complications caused by further neurodegeneration and medication effects [25,27], it can be considered that MCI might be progressing into PDD. Structural brain imaging could demonstrate certain patterns of atrophy, vascular pathology, or inflammatory changes [43] and could be used for early diagnosis of PD-MCI.

1.4 The Objective of the Study

There are dozens of studies on PD-MCI that differ in terms of MR modalities used, methods of analysis or stages of disease they compare. Moreover, while some researches focus on gray matter atrophies and cortical thickness, some others assess WM disintegrity at different regions. Even these studies vary according to the brain region labels they use, since there are many brain atlases where boundaries or naming of regions slightly differ. On the other hand, there have been a few studies that compared PD-MCI, cognitively intact PD (PD-CI) and healthy control (HC) groups by using voxel based morphometry (VBM) and tract based spatial statistics (TBSS) analysis, but none of these studies were conducted at a 3T clinical MR scanner.

The aim of this study is to find possible biomarkers of PD-MCI by comparing DW-MRI between PD-MCI, PD-CI and HC groups, using region based parcellation and TBSS methods at 3T.

2. MATERIALS and METHODS

2.1 Subjects

We recruited 77 subjects for this study. All subjects provided written informed consent. The patients showing depression symptoms, antidepressant drug users or those having less than 5 years of education were excluded from the study. All the subjects were identified according to their disease status, age, gender and background. 32 of the subjects were PD-MCI, 27 were PD-CI and 18 were HC. The age range was 45-79, yet the distribution peaked at around 60s. The group had an average of 9.6 years of education. Majority of the subjects were male. The demographic information of the subjects is provided in Table 2.1.

2.2 Diagnostic Assessment

In clinics, in order to detect cognitive impairment, neuropsychological tests are applied. Similarly, in our study, all participants were examined in order to check their motor system status and cognitive profile. According to the test scores subjects were classified as PD-CI or PD-MCI.

In order to measure the stage of the disease, Unified Parkinson's Rating Scale (UPDRS), which is a very common scale to measure severity of PD, was applied. UPDRS measures mental state, daily living activities, motor examination and therapeutic complications [44].

The next test applied was Addenbrooke's Cognitive Examination Revised (ACE-R) test, which is a very common and inexpensive test that is widely used to assess one's cognitive profile. Among 40 types of dementia screening tests, its sensitivity and better performance, makes it effective for different types of dementia, including PDD,

Table 2.1: The demographic information of subjects included in this study.

#	STATUS	AGE	GENDER	EDUCATION	#	STATUS	AGE	GENDER	EDUCATION
1	PD-MCI	63	M	5	40	PD-N	56	M	5
2	PD-MCI	68	M	5	41	PD-N	65	M	7
3	PD-MCI	67	M	15	42	PD-N	58	M	5
4	PD-MCI	66	M	15	43	PD-N	50	M	5
5	PD-MCI	78	M	11	44	PD-N	72	M	15
6	PD-MCI	60	M	7	45	PD-N	48	M	11
7	PD-MCI	67	M	5	46	PD-N	60	M	13
8	PD-MCI	63	M	5	47	PD-N	63	M	5
9	PD-MCI	57	M	11	48	PD-N	66	M	5
10	PD-MCI	59	M	11	49	PD-N	66	M	11
11	PD-MCI	54	M	11	50	PD-N	69	F	8
12	PD-MCI	55	M	5	51	PD-N	51	F	11
13	PD-MCI	76	M	11	52	PD-N	81	F	11
14	PD-MCI	61	M	5	53	PD-N	52	F	15
15	PD-MCI	60	M	8	54	PD-N	58	F	5
16	PD-MCI	69	M	5	55	PD-N	63	F	15
17	PD-MCI	45	M	11	56	PD-N	56	F	5
18	PD-MCI	77	M	11	57	PD-N	72	F	15
19	PD-MCI	71	M	8	58	PD-N	70	F	11
20	PD-MCI	62	M	11	59	PD-N	61	F	5
21	PD-MCI	70	M	15	60	HC	56	M	8
22	PD-MCI	70	M	5	61	HC	56	M	15
23	PD-MCI	68	M	5	62	HC	52	M	14
24	PD-MCI	79	M	15	63	HC	57	M	5
25	PD-MCI	45	F	5	64	HC	52	M	11
26	PD-MCI	67	F	5	65	HC	56	M	13
27	PD-MCI	60	F	11	66	HC	55	M	11
28	PD-MCI	55	F	11	67	HC	70	M	8
29	PD-MCI	54	F	5	68	HC	60	M	15
30	PD-MCI	57	F	5	69	HC	63	M	11
31	PD-MCI	63	F	5	70	HC	68	M	15
32	PD-MCI	59	F	5	71	HC	72	M	13
33	PD-N	68	M	10	72	HC	67	F	8
34	PD-N	53	M	15	73	HC	51	F	5
35	PD-N	68	M	15	74	HC	46	F	15
36	PD-N	47	M	15	75	HC	60	F	11
37	PD-N	59	M	12	76	HC	60	F	5
38	PD-N	47	M	12	77	HC	55	F	11
39	PD-N	51	M	12					

Alzheimer's disease dementia (ADD), fronto temporal dementia (FTD) and progressive supranuclear palsy [45, 46]. An ACE-R test takes approximately 15 minutes, and it is scored out of 100 that is being shared by 5 cognitive domains being tested, which are attention/orientation, memory, fluency, language and visuospatial domains. This test does not require a high educational level and it is available in many languages [46].

In order to diagnose depression, 15 item Geriatric Depression Scale (GDS) was applied. There are numerous studies reporting up to 40% of people with PD having major depression [47]. GDS is usually applied on elderly, due to the fact that most people having medical co-morbidities, like cognitive co-morbidity, might be affected in terms of cognitive processing. On the other hand, GDS is applied effectively on general adult population too [48].

Examination of attention and working memory were done by Stroop color and word test [34]. Introduced in 1935, it is used to assess psychiatric disorders, cognition and stress response [49]. A typical test consists of 3 pages: a word page with color names written in black, a color page of meaningless words written colored, and a color-word page with color names from first page written in the colors of second page but none of them are written in the color that they imply. Subjects were asked to read the words or say the name of the color [49].

Benton's Judgment of Line Orientation (BJLOT) test was also applied. This test was developed in 1978, and it examines visuospatial function [34, 50]. Basically, it asks to pair line segments having similar angular orientation [51]. It does not require major motor response, thus, it is applicable on a large range of subjects and limits the application time to 5 to 10 minutes [50].

Another similar test that was applied was symbol digit modalities test (SDMT), assessing attention, visual scanning and motor function [52]. In an SDMT, subject is asked to name nine symbols corresponding to the numbers 1-9 and write the correct number to the blank space provided below the symbol. Conducted both in written and oral form, test is completed in 90 seconds and two types of scores, measuring distinct

types of functioning are evaluated [53].

2.3 Data Acquisition and MR Protocol

After motor and cognitive assessments, diffusion weighted images (DWI) and T1-Weighted MR data were acquired by using a clinical 3T MR scanner (Philips Medical Systems, Best, Holland) and a 32-channel head coil at Hulusi Behçet Life Sciences Research Center, Istanbul University. DWI were acquired by using a 32 directional echo planar imaging (EPI) sequence (flip angle= 90°, FOV= 240x240x180mm, voxel size= 2x2x2mm, b=1000s/mm^2). T1-weighted MR images were acquired by using a 3D TURBO gradient echo sequence (TR/TE= 8.3/3.8 ms, flip angle= 8°, FOV= 250x250x180mm, voxel size= 1x1x1 mm).

2.4 Image Processing of Experimental Data

Most of the image processing steps of this study were carried out by using FMRIB Software Library, V5.0 (FSL)(https://fsl.fmrib.ox.ac.uk/fsl/fslwiki), which is a library of analysis tools [54]. In addition to DTI derived from DWI, it allows processing of fMRI and MRI data as well. Analysis of the images can be done either by using graphical user interface (GUI) (Figure 2.1) or the command line. However, in order to avoid any mistakes, a script based approach was adopted and all the scripts were written as automatized as possible. Steps that were thought to be sequential were gathered in for loops, that would include whole subjects within the same groups or the whole dataset.

Before processing, all subjects were given an index number. Next, by using MATLAB, images were converted from digital imaging and communications in medicine format (DICOM) to neuroimaging informatics technology initiative (NiFTI) format, as FSL works with images in NiFTI. Also, in order to acquire b value and b

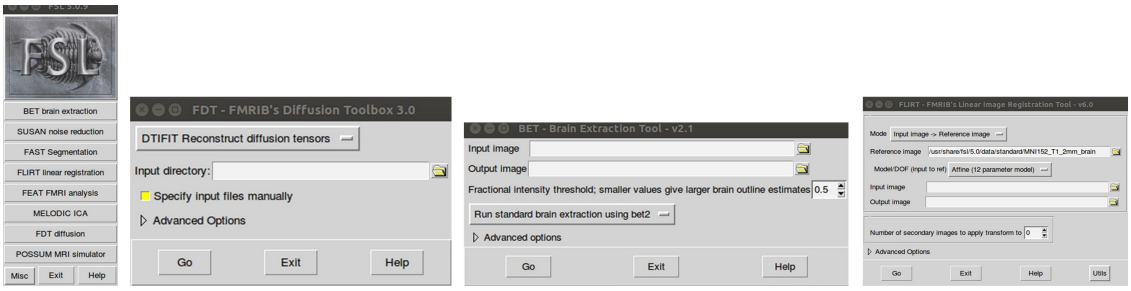

(a) (b) (c) (d)

Figure 2.1: Graphical user interfaces of the tools used within this study.
a) Main GUI, b) FDT GUI, c) BET GUI, d) FLIRT GUI

vector files, MRIcron was used, that is a NiFTI format image viewer, that also converts a multi layered DICOM image stack into a 4D NifTI file. The program also outputs a b value and b vector file.

Second step was extraction of b_0 images from DWI and save them as a separate file. This was required because b_0 images were used in registration process and they provided the best template of diffusion weighted images where no diffusion gradient was applied. For this purpose, again a MATLAB script was used.

Data was now ready to be fed into FSL. Analysis of DWI were done by FSL's Diffusion Tool (FDT), that includes preprocessing, local diffusion modeling and tractography tools. They are "eddycorrect", "dtifit", "bedpostx" and "probtrackx". The first two are the ones that were used in our study. An image of FDT GUI is presented in Figure 2.2.

The first processing step was eddy current correction applied both on DWI and b_0 images of each subject. Eddy current effect occur during DWI acquisition due to rapidly switching magnetic field gradients. This alterations induce eddy currents in the electrically conductive parts of the MR scanner [55], which is reflected as contours around the image [55]. (Figure 2.3, [56].)

The second step was brain extraction. For this purpose, FDT's brain extraction

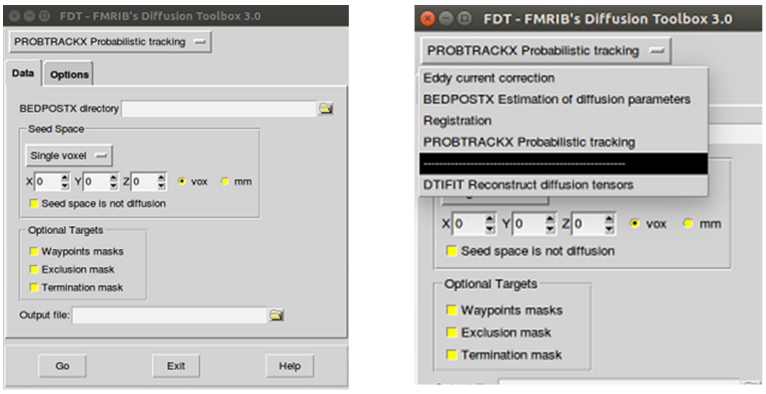

Figure 2.2: FMRIB's diffusion toolbox (FDT).

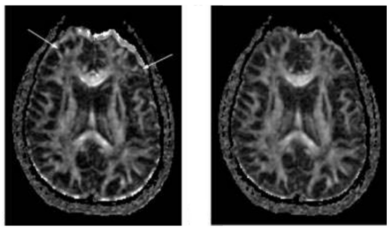

Figure 2.3: Brain MRI before (left) and after (right) eddy current correction.

tool (BET) was used. As its name implies, BET is used for segmentation of brain from non-brain structures, like skull and spine. Removal of these structures is necessary for true image registration. Figure 2.4, shows image of a healthy brain before and after brain extraction. In our study, instead of directly using BET on DWI images, a two

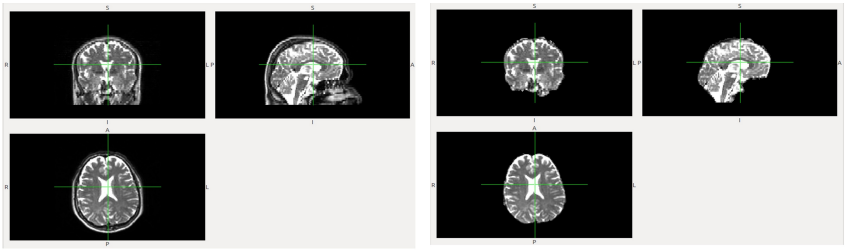

(a) Before BET applied. (b) After BET applied.

Figure 2.4: Brain extraction tool example on a healthy brain.

staged strategy was followed: first, brain extraction was applied on b_0, then, brain mask of b_0 acquired as a result of brain extraction was multiplied with eddy current corrected DWI.

Estimation of FA and MD maps was carried out by using FDT's tensor fitting tool (DTIFIT), where the tool matches tensors to each voxel of a DWI. After brain is extracted and eddy currents were corrected, DTIFIT was used. The tool uses gradient directions (i.e. bvec file) and gradient magnitudes (i.e. bval file) as input parameters. Additionally a brain mask is fed into the tool (for our case b_0 brain mask was used). As a result, eigenvalue files (V1, V2,V3), eigenvector files (L1,L2,L3), FA and MD maps, mode of anisotropy (MO) file and raw T2 signal (S0) with no diffusion weighting are estimated. Figure 2.5 shows the outputs of DTIFIT on a healthy volunteer brain. Our study used FA and MD maps.

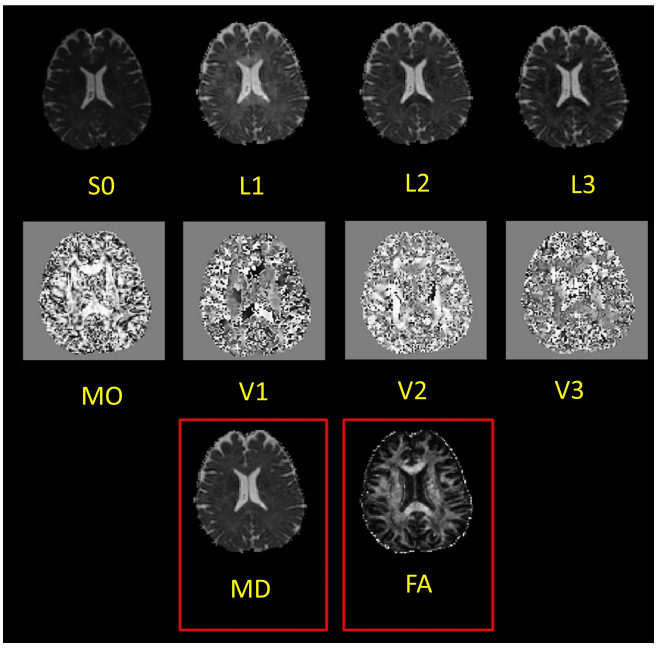

Figure 2.5: Outputs of tensor fitting tool.

After estimating the FA and MD maps for our subjects, we needed to align them onto a common template to evaluate these maps altogether. Image registration is fitting an image to another standard image to align them. It is useful because it enables group comparisons by aligning MR images of same or different MR modalities to a common space [54]. Two types of linear transformations are rigid-body and affine transformation. Rigid-body transformation is the simplest type of registration, where rotations and translations are allowed. This enables us to make translations, rotations and scaling [57]. When voxel locations of an image is represented in a matrix form, these transformations are then represented in a transformation matrix. Multiplication

of these two matrices gives the new coordinates of regarding voxels in the new space (Equation 2.1).

$$\begin{bmatrix} y_1 \\ y_2 \\ y_3 \\ 1 \end{bmatrix} = \begin{bmatrix} m_{11} & m_{12} & m_{13} & m_{14} \\ m_{21} & m_{22} & m_{23} & m_{24} \\ m_{31} & m_{32} & m_{33} & m_{34} \\ 0 & 0 & 0 & 1 \end{bmatrix} \begin{bmatrix} x_1 \\ x_2 \\ x_3 \\ 1 \end{bmatrix} \tag{2.1}$$

Compared to rigid body transformation, affine transformation offers a better sensitivity. This time, lengths and angles are not preserved. In our study, we used linear affine transformation that is provided by FMRIB's linear registration tool (FLIRT) in order to bring all the subjects to the same space. As reference image we used MNI152 Brain Atlas that is shown in Figure 2.6

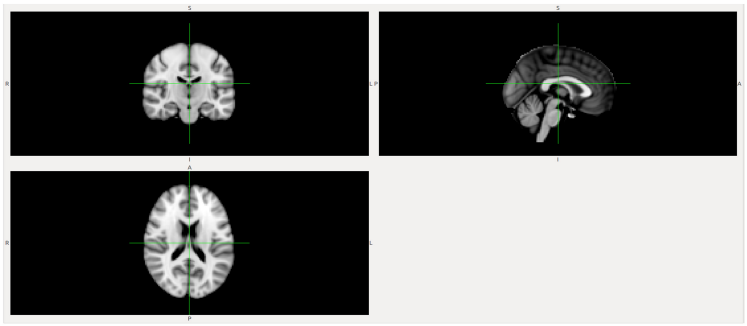

Figure 2.6: MNI152 brain atlas.

Our aim was to register FA and MD maps to MNI space, however the differences between MNI brain and acquired maps caused us to follow a differentiated pipeline apart from what has been proposed in studies examining DWI via FSL. First, b_0 brain images were linearly registered to MNI152 brain atlas. By doing this, a transformation matrix was acquired. Afterwards, FA and MD maps were linearly registered to MNI152 map by using the transformation matrix acquired in the previous step. As a result, we had FA and MD maps of all subjects aligned in the same space.

After registration of FA and MD maps, in order to calculate mean FA and

MD values, we used masks acquired from ICBM-JHU-DTI-81-WM labels. This is a structural WM atlas, developed at Johns Hopkins University, Laboratory of Brain Anatomical MRI, and provided to FMRIB, including 81 subjects (M:42,F:39) with mean age of 39 [58]. DTI-81 atlas, divides the brain WM into 48 regions and each region is indexed by a different number. In order to have a general conclusion of brain regions, we also generated masks from MNI atlas, that segments brain into 9 main regions. By using "fslmaths" function of FSL, we thresholded the atlas, so that each region, represented by an index became distinguishable. Afterwards, each region was binarized again using the same function. Each FA and MD map was multiplied with 48 region masks of DTI-81, and 9 mask of MNI atlas. Figure 2.7 shows an example output of multiplication. By using MATLAB, pixels whose values were greater than zero were averaged. Standard deviations were also calculated and all data were saved in .xls format.

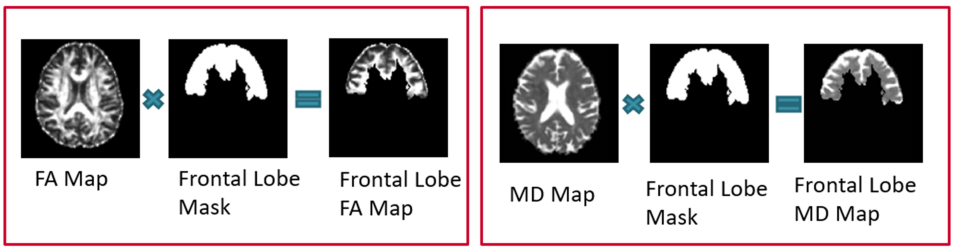

Figure 2.7: Left: Horizontal view of an FA map after multiplication with frontal lobe mask. Right: Horizontal view of an MD map after multiplication with frontal lobe mask.

2.5 Statistical Methods

2.5.1 Tract Based Spatial Statistics (TBSS)

Apart from processing tools that have been previously discussed, we should note that, DTI analyzing tools are based on 3 distinct categories. These are region of interest (ROI) analysis, voxel based analysis (VBA) (also known as voxel based morphometry (VBM)), and tract based analysis [59].

Tract based spatial statistics (TBSS) is one of the tract based analysis tools that was developed by Smith et al. [60]. It solves the issues of DTI analysis researchers often face with, like smoothing issues or misalignment problems of voxel based analysis. It also enables whole brain investigation that is not used in region of interest based approaches (ROI). So, TBSS could be considered as an improved version of the predecessors by bringing the advantages of each style [60]. What it basically does is aligning all white matter tracts for multiple subjects' FA maps, that enables us to make multiple subject voxelwise comparisons.

TBSS has four essential steps. Although MD maps can also be fed into the TBSS pipeline, FA maps are generally used for theoretical explanations. All the functions (except "stats") are used with "tbss" prefix and the sequenced numbers, that eases following up the procedure. The first step is preprocessing, named tbss_1_preproc, where FA maps are slightly eroded and end slices are extracted. Processed FA maps are carried to a working directory, by default to a folder named FA.

Second step is non-linear registration of FA images into a standard space carried by tbss_2_reg function. Since main aim of TBSS is to project aligned WM tracts on to a mean skeleton, it is important not to change natural alignment of tracts, which makes registration vital. Therefore, choosing right degree of freedom (DoF) is important. If low DoF is used, alignment does not reflect the correct structure even of the largest tracts. On the contrary, high DoF may cause excess warping of images, that would result in unrelated tracts to overlap, multiple bundles may seem as a thick one or a thick bundle may be divided into two [60].

For non-linear registration, choosing target image is also another discussion topic. While target could be automatically chosen as the most typical subject within the study, it can be predefined as well. Moreover, FSL's FMRIB58FA image can also be chosen (Figure 2.8). For our study, we preferred FMRIB58FA as the target, due to processing time considerations.

After registration process is completed, post registration process starts. The

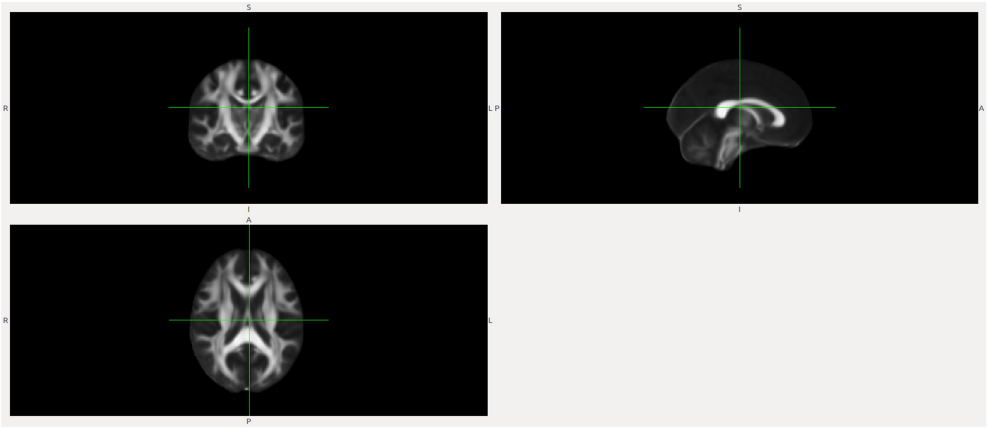

Figure 2.8: FSL's FMRIB58 FA image.

tbss_3_postreg function, affine aligns the target to MNI152 space. Then each image is affine aligned to the target and affine transform to MNI152 space is applied. That means, each of our FA images are now aligned to the MNI space. The results are merged into a 4D image file, named all_FA, and mean of these are calculated as another file and named mean_FA. mean_FA image is skeletonised (i.e. thinned) and an image showing centers of all common tracts of the group of maps being assessed [61], mean_FA_skeleton is acquired (Figure 2.9, shown in green).

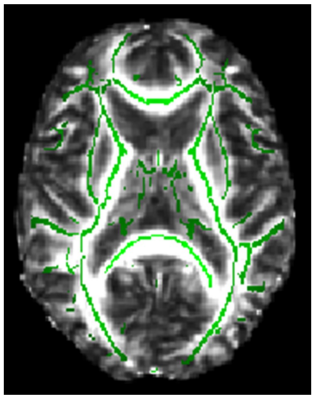

Figure 2.9: Mean FA skeleton projected on all FA image.

Last TBSS step is named prestats (and carried by the function tbss_4_prestats), which projects each subjects' aligned FA image to the

mean_FA_skeleton at a chosen threshold, which is 0.2 by default. This is achieved by filling the skeleton with FA from the nearest relevant tract center [60]. The output image is named all_FA_skeletonised.

In our study, we fed FA maps acquired at the end of DTIFIT into TBSS. The reason we did not use registered FA maps is, TBSS already applies non-linear registration to the input image and as the number of registrations increase, data losses occur. For each FA image, preprocessing and nonlinear registration were carried out. Afterwards, folders for three pairwise-comparison groups were created (i.e. PD-MCI vs. PD-CI, PD-MCI vs. HC and PD-CI vs. HC groups) and related images were copied to these directories. These files were outputs of non-linearly registered FA maps (output of second step of TBSS). For each folder containing two groups, post registration and prestats were repeated and it resulted in all FA skeletonized image of three pairwise-comparison groups.

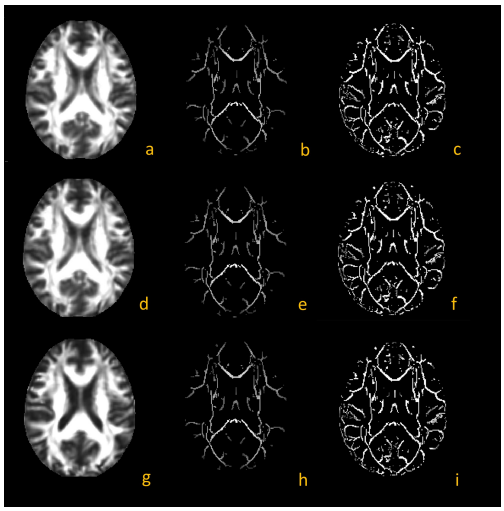

Figure 2.10: a,d,g: all FA images, b,e,h: mean FA skeleton images, c,f,i: all FA skeletonised images of PD-MCI/HC, PD-CI/HC, and PD-MCI/CI groups, respectively.

After acquisition of skeletonised image of all FA maps (i.e. projection of all FA maps onto mean skeleton of the group), data was ready for voxelwise analysis that is comparison of a group of image, voxel by voxel. First step of statistics wa using the randomise tool of FSL. randomise uses a design matrix file, design.mat (and also a related contrast matrix file, design.con) as input, in addition to all FA skeletonised image. Controlled by a GUI, a design matrix can also be created simply by the command

design_ttest2. For a two group comparison, number of subjects for each group must be specified. By using the inputs given, randomise tool carries out permutation based statistics.

Permutation based statistics is a type of non-parametric test [62]. To explain briefly, as it is in all statistical tests, the null hypothesis is, there is no difference between the groups being compared, according to an experimental condition. In this case assigning any subject either one of the groups randomly does not change the test statistic and this is called randomization. Grouping the subjects also means we label them and as long as the difference in between the groups is statistically insignificant, one can say that labels are exchangeable [62]. For a group of subjects, each possible permutation results in a statistical value. Significance is tested by comparing distribution of all of these values. What is being observed is the frequency of difference mean to exceed the difference found without permutation [63].

In randomise tool we can define the number of permutations. Also, usage of threshold-free cluster enhancement (TFCE), is strongly recommended by FSL for correction of family-wise error [64]. At the end of TBSS and statistics, image showing test statistics of each voxel is presented. Name of the output image is a stat image of raw t statistics "tbss_tstat1" or "tbss_tstat2". Suffix 1 or 2 depends on the number of subjects that the test group includes. If number of subjects in first test group is greater than second one, "tbss_tstat1" should be taken into account, or vice versa. Corrected p values image is presented as "tbss_corrp_tstat1". The resulting image shows voxels differing between 2 groups of subjects. In order to visualize the test statistics, FSLs' image viewer, FSL View is used. In Figure 2.11a an example of test statistics image that is also represented in official FSL website is provided, so that we can have a clue on what our final image looks like. Figure 2.11a shows mean_FA_skeleton overlaid on MNI brain, and "tbss_corrp_tstat1" image is projected onto the two. As long as t stat image is thresholded at 0.95, it shows p values that are less than 0.05. Figure 2.11b, on the other hand shows the same t stat image, where t-stat image is thickened by "tbss_fill" function.

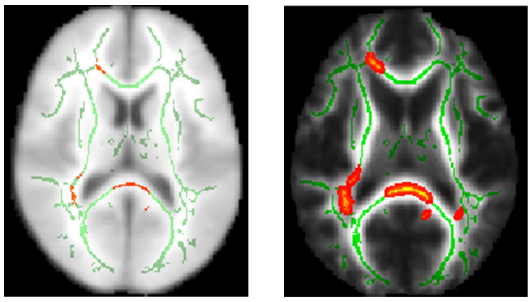

(a) Non-filled Version. (b) Filled version.

Figure 2.11: Output of TBSS: voxelwise test statistics.

Our aim was to examine statistically significant differences between groups. To start with FA maps, we multiplied our skeletonised FA map by the JHU and MNI atlases' region masks. For pairwise comparisons, t statistics were calculated by using randomise tool of FSL. Number of permutations was set to 5000.

2.5.2 Statistical Analysis of DWI Parameters and Neuropsychological Test Scores

Our data groups differed from each other in terms of disease stage, where HC's had no PD at all, PD-CI patients had PD but there was no cognitive decline, and PD-MCI patients had cognitive decline. Due to the possiblity of insufficient sample size, we assumed all the data to be not normally distributed. In such cases, usage of distribution free methods (non-parametric methods) is a necessity [65], where rank of observations are used as inputs. For analysis of variance of three test groups, Kruskal Wallis test was used. For pairwise comparisons, Mann Whitney rank sum test was applied with Bonferroni correction, where p values smaller than 0.05 were assumed to show a difference trend and p values smaller than 0.05/3 showed a statistically significant difference. These tests were carried out to assess regional FA and MD differences of the three groups. All test were carried out on both DTI-81 and MNI regions, which makes 57 regions in total.

Mann Whitney rank sum test was also used to analyze neuropsychological test

score differences between groups. All tests, except UPDRS, were compared in between pairwise combinations of three test groups. UPDRS scores were compared only in between PD-MCI and PD-CI groups, since this test was not applied on HC's.

In order to identify the associations between neuropsychological test scores and DWI derived parameters, Spearman's rank correlation coefficient was calculated. Spearman's rank correlation test gives information on type of relation and strength of association between two test groups of ordinal scale [65]. Thresholded p values show a relation, two variables are either positively correlated, that means the variables tend to increase or decrease together, or negatively correlated, meaning that the variables decrease or increase oppositely. First, the test was applied in between mean FA value of each region, and each neuropsychological test score of all subjects regardless of their disease status (The same test was repeated for MD values as well.) Secondly, FA or MD values of each region was correlated to each test score for PD-MCI, PD-CI and HC groups separately. A p value of less than 0.05 was assumed to indicate a statistically significantly correlation.

3. RESULTS

3.1 Demographic Assessments

Out of the 77 subjects, 53 were male (M) and 24 were female (F). For all groups, the number of male subjects was higher than the number of female subjects. The M/F ratio was 3 for PD-MCI, 1.7 for PD-CI and 2 for HC's. The mean age was 63.28±8.46 for PD-MCI, 60.64±8.87 for PD-CI and 58.67±7.05 for HC's. Mean education level was, 8.37±3.67 for PD-MCI, 10.15±3.98 years for PD-CI and 10.78±3.85 for HC's (see Table 3.1). Patients included in the study were chosen from similar education levels as much as possible. Table 3.2 shows the ACE-R, GDS, STROOP, BJLOT, SDMT and UPDRS scores of all subjects.

Table 3.1: Demographic information summary.

	GENDER	NUMBER	AGE (Mean ± Std)	EDUCATION (Mean ± Std)
PD-MCI	M	24	65.21 ± 8.24	9.0 ± 3.76
	F	8	57.5 ± 6.59	6.5 ± 2.77
Total		32	63.28 ± 8.46	8.37 ± 3.67
PD-CI	M	17	58.64 ± 8.21	10.18 ± 4.00
	F	10	63.3 ± 9.61	10.1 ± 4.17
Total		27	60.64 ± 8.87	10.15 ± 3.98
HC	M	12	59.75 ± 6.91	11.28 ± 3.23
	F	6	56.5 ± 7.45	9.16 ± 3.92
Total		18	58.67 ± 7.05	10.78 ± 3.55
Total		77	61.18 ± 8.42	9.55 ± 3.85

Table 3.3, 3.4 and 3.5 show the pairwise group comparison results of neuropsychological test scores. All comparisons showed statistically significant differences of ACE-R test scores (for PD-MCI/PD-CI $p<0.001$, for PD-MCI/PD-HC $p<0.001$, for PD-CI/HC $p=0.01$). A difference trend was found in between line orientation test scores of PD-MCI/PD-CI groups ($p=0.03$), while the same test scores differed significantly in between PD-MCI/HC groups ($p=0.01$). SDMT scores significantly differed

Table 3.2: Neuropsychological test scores.

#	STATUS	ACE-R	GDS	STROOP	BJLOT	SDMT	UPDRS	#	STATUS	ACER	GDS	STROOP	BJLOT	SDMT	UPDRS
1	PD-MCI	63	5	203	20	7	47	40	PD-N	91	2	60	14	35	55
2	PD-MCI	77	3	130	25	20	31	41	PD-N	89	4	39	22	29	36
3	PD-MCI	81	1	81	29	23	63	42	PD-N	88	8	46	22	20	38
4	PD-MCI	82	1	47	25	36	22	43	PD-N	87	2	48	25	26	80
5	PD-MCI	83	5	97	27	27	32	44	PD-N	85	6	88	30	28	47
6	PD-MCI	72	12	46	26	34	56	45	PD-N	88	4	45	26	31	31
7	PD-MCI	72	10	60	21	20	79	46	PD-N	92	2	67	26	44	39
8	PD-MCI	71	9	72	18	14	74	47	PD-N	84	1	46	26	17	30
9	PD-MCI	80	9	54	26	38	70	48	PD-N	86	1	65	13	9	29
10	PD-MCI	82	11	23	25	35	33	49	PD-N	91	3	15	24	35	23
11	PD-MCI	71	7	86	19	17	55	50	PD-N	84	11	79	23	30	46
12	PD-MCI	67	2	12	18	18	27	51	PD-N	85	11	49	22	23	87
13	PD-MCI	79	4	33	13	22	66	52	PD-N	85	9	81	24	31	24
14	PD-MCI	72	10	67	19	20	43	53	PD-N	92	0	28	28	39	45
15	PD-MCI	81	11	68	25	28	71	54	PD-N	95	11	37	18	29	30
16	PD-MCI	74	6	101	8	8	65	55	PD-N	93	0	43	26	42	15
17	PD-MCI	82	5	65	24	35	46	56	PD-N	93	2	60	25	24	31
18	PD-MCI	72	12	136	8	11	102	57	PD-N	88	8	63	26	35	54
19	PD-MCI	81	3	57	25	17	48	58	PD-N	93	3	59	25	29	29
20	PD-MCI	83	9	96	23	21	55	59	PD-N	93	7	85	25	32	52
21	PD-MCI	77	3	95	19	16	84	60	HC	91	2	33	27	31	
22	PD-MCI	83	7	166	23	12	22	61	HC	100	9	33	28	51	
23	PD-MCI	82	1	79	17	16	64	62	HC	96	7	27	29	67	
24	PD-MCI	83	6	114	26	12	88	63	HC	87	3	68	22	22	
25	PD-MCI	68	2	14	22	20	13	64	HC	95	0	33	24	20	
26	PD-MCI	76	4	77	14	8	34	65	HC	84	6	56	24	43	
27	PD-MCI	72	3	23	21	27	51	66	HC	94	5	78	23	38	
28	PD-MCI	80	3	26	24	38	17	67	HC	84	1	54	23	20	
29	PD-MCI	68	2	55	24	21	49	68	HC	100	3	43	24	51	
30	PD-MCI	66	11	55	27	16	66	69	HC	96	11	76	20	36	
31	PD-MCI	77	8	48	15	17	68	70	HC	95	1	52	26	34	
32	PD-MCI	81	12	64	26	35	53	71	HC	97	3	38	27	50	
33	PD-N	89	11	69	24	19	57	72	HC	89	12	43	23	40	
34	PD-N	90	5	65	26	26	70	73	HC	96	0	39	29	50	
35	PD-N	90	10	47	26	24	45	74	HC	99	7	30	30	59	
36	PD-N	98	11	27	27	53	53	75	HC	97	5	50	25	39	
37	PD-N	90	5	57	27	50	52	76	HC	85	5	61	21	16	
38	PD-N	97	10	30	25	41	54	77	HC	96	0	21	28	55	
39	PD-N	84	8	39	24	40	47								

for PD-MCI/PD-CI ($p=0.001$) and for PD-MCI/PD-HC comparisons ($p<0.001$), and showed a difference trend for PD-CI/HC comparison ($p=0.04$).

Table 3.3: Comparison of neuropsychological test scores between PD-MCI and PD-CI groups.

	PD-MCI	PD-CI	p
Test Name	Mean ± Std	Mean ± Std	
ACE-R	76.19 ± 5.94	89.63 ± 3.93	<0.001**
GDS	6.16 ± 3.71	5.74 ± 3.88	0.61
STROOP	73.44 ± 42.80	53.22 ± 18.56	0.05
BJLOT	21.31 ± 5.34	24.04 ± 3.79	0.03*
SDMT	21.53 ± 9.26	31.15 ± 10.01	0.001**
UPDRS	52.94 ± 21.75	44.41 ± 14.56	0.09

*trend, **p<0.05/3

Table 3.4: Comparison of neuropsychological test scores between PD-MCI and HC groups.

	PD-MCI	HC	p
Test Name	Mean ± Std	Mean ± Std	
ACE-R	76.19 ± 5.94	93.39 ± 5.37	<0.001**
GDS	6.16 ± 3.71	4.44 ± 3.70	0.13
STROOP	73.44 ± 42.80	46.39 ± 16.67	0.01**
BJLOT	21.31 ± 5.34	25.17 ± 2.96	0.01**
SDMT	21.53 ± 9.26	40.11 ± 14.56	<0.001**

*trend, **p<0.05/3

Table 3.5: Comparison of neuropsychological test scores between PD-CI and HC groups.

	PD-CI	HC	p
Test Name	Mean ± Std	Mean ± Std	
ACE-R	89.63 ± 3.93	93.39 ± 5.37	0.01**
GDS	5.74 ± 3.88	4.44 ± 3.70	0.29
STROOP	53.22 ± 18.56	46.39 ± 16.67	0.19
BJLOT	24.04 ± 3.79	25.17 ± 2.96	0.58
SDMT	31.15 ± 10.01	40.11 ± 14.56	0.04*

*trend, **p<0.05/3

3.2 Neuropsychological Test Scores and DWI Parameter Correlations

On Table 3.6 Spearman's rank correlation test results of all subjects regional mean FA value versus neuropsychological test scores are reported. ACE-R test scores

showed a positive correlation with FA values of all subjects at body of corpus callosum (p=0.02 r=0.26), splenium of corpus callosum (p=0.01, r=0.31), left cerebral peduncle (p=0.05, r=0.23), left posterior limb of internal capsule (p=0.05, r=0.23), bilateral posterior thalamic radiation (right: p=0.04, r=0.24, left: p= 0.01, r=0.29), right sagittal stratum (p=0.02, r= 0.26), left fornix (p=0.01, r=0.28), bilateral tapetum (right: p=0.003, r=0.33, left: p=0.04, r=0.23), and parietal lobe (p=0.016, r=0.27). BJLOT scores were positively correlated to mean FA values at bilateral retrolenticular internal capsule (right: p=0.3, r=0.25, left: p=0.01, r=0.28). Another positive correlation was seen in between FA values and SDMT scores at splenium of corpus callosum (p=0.05, r=0.23), left retrolenticular internal capsule (p=0.01, r=0.31), bilateral sagittal stratum (right: p=0.01, r=0.3, left: p=0.02, r=0.26) and tapetum (p=0.04, r=0.23). GDS test scores were found to be negatively correlated to mean FA value at right inferior cerebellar peduncle (p=0.001, r=-0.37). Similarly, STROOP test showed a negative correlation to FA at right fornix (p=0.2, r=-0.26).

All subjects' mean MD values were found to be negatively correlated to neuropsychological test scores. Correlation coefficients are listed on Table 3.7. ACE-R test scores showed a negative correlation to mean MD values at left cerebral peduncle (p=0.03, r=-0.25), right anterior corona radiata (p=0.001, r=-0.30), right superior corona radiata (p=0.03, r=-0.25), bilateral sagittal stratum (right: p=0.002, r=-0.34, left: p=0.01, r=-0.3), left external capsule (p=0.02, r=-0.27), right tapetum (p=0.02, r=-0.26), parietal lobe (p=0.05, r=-0.23), putamen (p=0.01, r=-0.28) and temporal lobe (p=0.03, r=-0.24). Negative correlations were identified in between MD values and GDS scores at right superior cerebellar peduncle (p=0.04, r=-0.24) and MD values and SDMT scores at right superior cerebellar peduncle (p=0.03, r=-0.25), left retrolenticular internal capsule (p=0.04, r=-0.24), and right sagittal stratum (p=0.05, r=-0.23).

Table 3.6: Spearman's correlation coefficients between regional mean FA values and neuropsychological test scores for PD-MCI, PD-CI and HC groups.

FA										
Region	ACE-R		GDS		STROOP		BJLOT		SDMT	
	r	p	r	p	r	p	r	p	r	p
Middle Cerebellar Peduncle	0.09	0.43	-0.16	0.18	-0.21	0.06	-0.06	0.63	-0.01	0.96

Pontine Crossing Tract	-0.08	0.50	0.09	0.42	-0.01	0.92	-0.08	0.47	-0.03	0.80
Genu of Corpus Callosum	0.13	0.25	0.09	0.42	-0.09	0.42	0.05	0.64	0.02	0.84
Body of Corpus Callosum	0.26	0.02*	-0.01	0.90	-0.13	0.25	0.12	0.30	0.12	0.31
Splenium of Corpus Callosum	0.31	0.01*	0.04	0.75	0.01	0.94	0.15	0.21	0.23	0.05*
Fornix	0.18	0.12	-0.11	0.35	-0.17	0.13	0.06	0.60	0.14	0.22
Corticospinal Tract R	0.02	0.88	-0.10	0.40	-0.09	0.45	-0.05	0.65	0.05	0.68
Corticospinal Tract L	0.15	0.18	-0.03	0.82	-0.12	0.29	-0.03	0.81	0.18	0.12
Medial Lemniscus R	0.08	0.49	-0.07	0.53	-0.09	0.43	-0.10	0.36	0.01	0.92
Medial Lemniscus L	0.13	0.24	0.15	0.20	-0.11	0.35	-0.07	0.55	0.09	0.42
Inferior Cerebellar Peduncle R	-0.10	0.38	-0.37	0.001*	0.02	0.85	-0.13	0.28	-0.14	0.24
Inferior Cerebellar Peduncle L	0.13	0.26	-0.08	0.50	-0.13	0.26	-0.04	0.75	0.15	0.18
Superior Cerebellar Peduncle R	0.19	0.11	0.20	0.08	-0.04	0.73	0.13	0.24	0.22	0.06
Superior Cerebellar Peduncle L	0.05	0.66	-0.06	0.58	0.01	0.97	-0.04	0.70	-0.08	0.51
Cerebral Peduncle R	0.10	0.37	-0.10	0.40	-0.02	0.85	-0.02	0.88	0.09	0.42
Cerebral Peduncle L	0.23	0.05*	0.03	0.81	0.04	0.75	-0.03	0.80	0.16	0.17
Anterior Limb of Internal Capsule R	0.09	0.45	-0.06	0.61	-0.01	0.91	-0.11	0.35	0.12	0.29
Anterior Limb of Internal Capsule L	0.03	0.81	-0.07	0.53	-0.08	0.47	-0.10	0.36	0.04	0.70
Posterior Limb of Internal Capsule R	0.18	0.12	0.10	0.38	0.01	0.91	0.00	0.97	0.10	0.39
Posterior Limb of Internal Capsule L	0.23	0.05*	-0.06	0.58	0.05	0.65	-0.03	0.80	0.01	0.92
Retrolenticular Internal Capsule R	0.02	0.84	0.18	0.12	0.07	0.54	0.25	0.03*	0.08	0.47
Retrolenticular Internal Capsule L	0.22	0.05*	0.11	0.35	-0.01	0.94	0.28	0.01*	0.31	0.01*
Anterior Corona Radiata R	0.12	0.28	0.01	0.93	-0.07	0.55	0.05	0.69	0.12	0.32
Anterior Corona Radiata L	0.07	0.55	0.09	0.42	0.002	0.99	-0.04	0.70	-0.03	0.78
Superior Corona Radiata R	0.13	0.25	0.03	0.76	0.03	0.77	-0.03	0.78	0.02	0.86
Superior Corona Radiata L	0.17	0.14	-0.06	0.58	0.09	0.44	0.04	0.73	-0.07	0.54
Posterior Corona Radiata R	0.02	0.84	0.20	0.07	0.18	0.11	0.16	0.15	0.04	0.75
Posterior Corona Radiata L	0.05	0.69	0.22	0.06	0.23	0.04*	0.16	0.16	0.01	0.96
Posterior Thalamic Radiation R	0.24	0.04*	-0.03	0.78	-0.05	0.67	0.03	0.80	0.15	0.18
Posterior Thalamic Radiation L	0.29	0.01*	0.14	0.22	-0.04	0.71	0.08	0.50	0.21	0.07
Sagittal Stratum R	0.26	0.02*	0.16	0.16	-0.17	0.13	0.21	0.07	0.30	0.01*
Sagittal Stratum L	0.22	0.06	0.20	0.09	-0.13	0.27	0.22	0.05	0.26	0.02*
External Capsule R	0.05	0.69	-0.02	0.83	-0.18	0.11	0.08	0.47	0.06	0.62
External Capsule L	0.11	0.36	-0.06	0.63	-0.02	0.86	0.14	0.23	-0.03	0.83
Cingulum (Cing.Gyrus) R	0.07	0.52	-0.13	0.27	-0.07	0.56	0.06	0.58	0.08	0.47
Cingulum (Cing.Gyrus) L	-0.04	0.74	-0.15	0.18	0.07	0.56	0.05	0.64	-0.20	0.09
Cingulum (Hippocampal) R	-0.03	0.79	0.18	0.11	0.05	0.69	-0.09	0.43	-0.03	0.82
Cingulum (Hippocampal) L	0.11	0.36	0.01	0.95	-0.20	0.08	-0.03	0.79	0.08	0.50
Fornix R	0.17	0.14	0.08	0.51	-0.26	0.02*	0.07	0.52	0.14	0.23
Fornix L	0.28	0.01*	0.06	0.59	-0.05	0.66	0.07	0.52	0.12	0.30
Superior Longitudinal Fasciculus R	0.10	0.38	0.09	0.41	-0.10	0.39	0.07	0.54	0.08	0.46
Superior Longitudinal Fasciculus L	0.18	0.12	-0.01	0.94	-0.09	0.45	0.17	0.15	0.09	0.42
Superior Fronto Occipital Fasciculus R	0.19	0.10	-0.10	0.36	-0.10	0.41	-0.04	0.72	0.18	0.11
Superior Fronto Occipital Fasciculus L	-0.01	0.90	-0.11	0.34	-0.09	0.42	-0.04	0.75	-0.06	0.60
Uncinate Fasciculus R	0.09	0.46	0.06	0.61	-0.10	0.40	-0.02	0.88	0.04	0.70
Uncinate Fasciculus L	0.05	0.65	0.11	0.34	0.14	0.21	-0.05	0.65	-0.05	0.68
Tapetum R	0.33	0.003*	-0.01	0.93	-0.12	0.31	0.05	0.66	0.23	0.04*
Tapetum L	0.23	0.04*	-0.03	0.82	0.12	0.29	-0.04	0.75	0.10	0.38
Caudate	0.04	0.73	0.05	0.68	0.03	0.81	-0.08	0.47	-0.01	0.92
Cerebellum	-0.13	0.26	-0.02	0.83	0.05	0.65	-0.15	0.20	-0.09	0.41
Frontal Lobe	0.21	0.07	-0.04	0.71	-0.03	0.80	-0.05	0.66	0.06	0.59
Insula	0.12	0.30	0.03	0.82	-0.07	0.57	0.10	0.41	0.17	0.15
Occipital Lobe	0.004	0.97	0.20	0.08	0.01	0.95	0.12	0.29	-0.02	0.88
Parietal Lobe	0.27	0.016*	0.14	0.22	0.01	0.92	0.17	0.13	0.12	0.30
Putamen	0.03	0.77	-0.01	0.95	-0.11	0.33	0.04	0.74	0.15	0.21
Temporal Lobe	-0.004	0.97	0.13	0.24	0.01	0.91	-0.06	0.61	0.02	0.86
Thalamus	0.12	0.30	0.02	0.89	-0.03	0.76	-0.04	0.72	0.01	0.96

Table 3.7: Spearman's correlation coefficients between regional mean MD values and neuropsychological test scores for PD-MCI, PD-CI and HC groups.

MD										
Region	ACE-R		GDS		STROOP		BJLOT		SDMT	
	r	p	r	p	r	p	r	p	r	p
Middle Cerebellar Peduncle	-0.05	0.65	0.11	0.35	0.17	0.14	0.16	0.16	0.04	0.76
Pontine Crossing Tract	-0.12	0.32	0.04	0.75	0.04	0.76	0.08	0.49	0.01	0.90
Genu of Corpus Callosum	-0.03	0.77	-0.07	0.54	0.02	0.88	0.01	0.94	0.09	0.44
Body of Corpus Callosum	-0.15	0.18	-0.02	0.83	0.10	0.41	0.03	0.82	-0.13	0.27
Splenium of Corpus Callosum	-0.22	0.05	0.01	0.95	0.02	0.85	0.01	0.95	-0.13	0.27
Fornix	-0.19	0.10	0.05	0.64	0.20	0.09	-0.05	0.64	-0.14	0.23
Corticospinal Tract R	-0.16	0.17	0.12	0.30	0.16	0.18	0.06	0.63	-0.10	0.38
Corticospinal Tract L	-0.22	0.05	0.06	0.62	0.16	0.16	0.02	0.89	-0.21	0.06
Medial Lemniscus R	0.02	0.87	0.02	0.83	0.03	0.78	-0.02	0.89	0.13	0.27
Medial Lemniscus L	0.001	0.99	-0.06	0.59	0.07	0.52	0.12	0.30	0.01	0.90
Inferior Cerebellar Peduncle R	-0.14	0.22	0.22	0.05	0.004	0.98	0.10	0.36	0.10	0.38
Inferior Cerebellar Peduncle L	-0.09	0.41	0.02	0.83	0.15	0.20	0.06	0.63	-0.19	0.10
Superior Cerebellar Peduncle R	-0.15	0.19	-0.24	0.04*	0.02	0.88	-0.07	0.52	-0.25	0.03*
Superior Cerebellar Peduncle L	0.03	0.77	0.12	0.29	-0.06	0.58	0.15	0.18	0.19	0.10
Cerebral Peduncle R	-0.21	0.07	0.07	0.54	0.08	0.48	0.11	0.35	-0.15	0.20
Cerebral Peduncle L	-0.25	0.03*	-0.06	0.59	0.03	0.78	0.08	0.47	-0.20	0.08
Anterior Limb of Internal Capsule R	-0.16	0.15	0.05	0.66	0.03	0.80	0.14	0.23	-0.16	0.16
Anterior Limb of Internal Capsule L	-0.08	0.49	0.10	0.39	0.17	0.14	0.06	0.60	-0.08	0.46
Posterior Limb of Internal Capsule R	-0.08	0.47	-0.04	0.73	-0.20	0.08	0.07	0.57	-0.01	0.93
Posterior Limb of Internal Capsule L	-0.25	0.03*	0.001	0.99	-0.05	0.67	-0.01	0.95	-0.11	0.34
Retrolenticular Internal Capsule R	-0.10	0.39	-0.09	0.46	0.02	0.86	-0.18	0.12	-0.10	0.38
Retrolenticular Internal Capsule L	-0.21	0.07	0.01	0.96	0.05	0.67	-0.21	0.06	-0.24	0.04*
Anterior Corona Radiata R	-0.30	0.001*	0.06	0.58	0.06	0.58	-0.01	0.94	-0.20	0.08
Anterior Corona Radiata L	-0.20	0.08	-0.05	0.65	0.11	0.36	0.003	0.98	-0.14	0.22
Superior Corona Radiata R	-0.25	0.03*	0.04	0.71	0.03	0.79	0.07	0.57	-0.17	0.13
Superior Corona Radiata L	-0.20	0.09	0.08	0.50	0.03	0.80	0.004915	0.97	-0.13	0.26
Posterior Corona Radiata R	-0.20	0.08	-0.09	0.42	-0.00204	0.99	-0.01	0.91	-0.16	0.17
Posterior Corona Radiata L	-0.15	0.19	-0.03	0.82	-0.05	0.66	0.03	0.83	-0.11	0.35
Posterior Thalamic Radiation R	-0.25	0.03*	-0.05	0.66	0.03	0.80	-0.004	0.97	-0.15	0.21
Posterior Thalamic Radiation L	-0.22	0.05	-0.10	0.39	0.01	0.90	0.03	0.82	-0.11	0.36
Sagittal Stratum R	-0.34	0.002*	-0.09	0.42	0.10	0.37	-0.14	0.21	-0.23	0.05*
Sagittal Stratum L	-0.30	0.01*	-0.05	0.67	0.09	0.44	-0.13	0.27	-0.21	0.07
External Capsule R	-0.11	0.36	-0.01	0.96	0.13	0.26	0.02	0.87	-0.05	0.68
External Capsule L	-0.27	0.02*	0.04	0.72	0.18	0.12	-0.22	0.06	-0.17	0.13
Cingulum (Cing.Gyrus) R	-0.23	0.04*	0.17	0.13	0.08	0.51	-0.06	0.62	-0.11	0.33
Cingulum (Cing.Gyrus) L	-0.09	0.43	0.04	0.76	-0.01	0.92	-0.08	0.48	0.02	0.89
Cingulum (Hippocampal) R	-0.07	0.53	-0.06	0.58	0.12	0.31	0.08	0.51	-0.11	0.34
Cingulum (Hippocampal) L	-0.07	0.55	-0.02	0.87	0.22	0.05	0.04	0.70	-0.03	0.82
Fornix R	-0.17	0.14	-0.14	0.21	0.15	0.20	-0.10	0.41	-0.14	0.23
Fornix L	-0.20	0.09	-0.06	0.58	-0.01	0.96	0.05	0.67	-0.06	0.58
Superior Longitudinal Fasciculus R	-0.06	0.62	-0.09	0.42	0.14	0.24	0.03	0.82	-0.03	0.82
Superior Longitudinal Fasciculus L	-0.19	0.10	-0.04	0.76	0.13	0.24	-0.005	0.97	-0.13	0.26
Superior Fronto Occipital Fasciculus R	-0.19	0.10	0.11	0.34	0.06	0.61	0.11	0.35	-0.17	0.14
Superior Fronto Occipital Fasciculus L	-0.10	0.39	0.12	0.31	0.14	0.23	0.08	0.48	-0.04	0.70
Uncinate Fasciculus R	-0.07	0.55	-0.03	0.83	0.10	0.39	0.06	0.58	-0.06	0.59
Uncinate Fasciculus L	-0.03	0.81	0.06	0.59	0.07	0.55	0.10	0.39	-0.01	0.92
Tapetum R	-0.26	0.02*	0.03	0.77	0.12	0.28	-0.01	0.93	-0.18	0.11
Tapetum L	-0.12	0.30	0.05	0.69	-0.09	0.42	0.12	0.29	-0.01	0.91
Caudate	-0.05	0.68	0.01	0.96	0.04	0.74	0.14	0.22	0.02	0.84
Cerebellum	-0.03	0.81	-0.01	0.92	0.06	0.60	0.11	0.36	0.04	0.74
Frontal Lobe	-0.19	0.10	0.09	0.43	0.19	0.10	0.01	0.92	-0.07	0.55
Insula	-0.22	0.06	0.05	0.66	0.15	0.20	-0.04	0.70	-0.12	0.28
Occipital Lobe	-0.15	0.19	-0.13	0.27	0.12	0.30	-0.11	0.34	-0.07	0.55
Parietal Lobe	-0.23	0.05*	-0.01	0.92	0.17	0.15	-0.06	0.61	-0.12	0.32
Putamen	-0.28	0.01*	-0.04	0.76	0.14	0.23	-0.07	0.55	-0.21	0.06

Temporal Lobe	-0.24	0.03*	-0.01	0.90	0.21	0.06	-0.03	0.82	-0.14	0.23
Thalamus	-0.13	0.26	0.04	0.72	0.09	0.45	0.08	0.48	-0.03	0.80

The correlation coefficients of mean FA and mean MD values to neuropsychological test scores for PD-MCI, PD-CI and HC groups are presented at tables 3.8 to 3.17.

For PD-MCI group, ACE-R test scores showed negative correlation with mean FA (p=0.04, r=-0.36) and positive correlation with mean MD (p=0.02, r=0.41) at cerebral peduncle. Similarly, for mean FA values, a negative correlation was found at right fornix (p=0.01, r=-0.45) and for MD values, a positive correlation was found (p=0.02, r=0.41). Also, ACE-R scores were negatively correlated to mean FA values at middle cerebellar peduncle (p=0.02, r=-0.40), right retrolenticular capsule (p=0.045, r=-0.36), left anterior corona radiata (p=0.02, r=-0.4), and left external capsule (p=0.048, r=-0.35) and positive correlation was found at left cingulum (cingulate gyrus) (p=0.02, r=0.41), right cingulum (hippocampal) (p=0.03, r=0.38) and left superior longitudinal fasciculus (p=0.03, r=0.39). GDS test scores showed a positive correlation to mean FA values at occipital lobe (p=0.016, r=0.42) and negative correlation to mean MD values were observed at the same region (p=0.04, r=-0.36). Also for mean FA values, positive correlations with GDS scores were found at left posterior thalamic radiation (p=0.03, r=0.39), left sagittal stratum (p=0.016, r=0.42) and parietal lobe (p=0.02, r=0.41). STROOP test scores showed positive correlation to FA values at left posterior corona radiata (p=0.01, r=0.43) and negative correlation to MD values at right posterior limb of internal capsule (p=0.048, r=-0.35). BJLOT scores were negatively correlated to mean FA values (p=0.03, r=-0.39) and positively correlated to mean MD values (p=0.004, r=0.49) at middle cerebellar peduncle. Likewise, a negative correlation to mean FA was found for BJLOT at bilateral cerebral peduncle (right: p=0.01, r=-0.44, left: p=0.04, r=-0.37) and negative correlation with mean MD value was found at the same region (right: p=0.003, r=0.51, left: p=0.01, r=0.46). For BJLOT scores, a negative correlation to FA value was also found at bilateral medial lemniscus (right: p=0.01, r=-0.44, left: p=0.02, r=-0.41), and a positive correlation to mean MD values existed

at the same region (left: p=0.01, r=0.44). BJLOT scores were negatively correlated to mean FA values at right uncinate fasciculus (p=0.01, r=-0.43). Positive correlation to mean MD was found at right inferior cerebellar peduncle (p=0.01, r=-0.43), right anterior limb of internal capsule (p=0.04, r=0.36), frontal lobe (p=0.045, r=0.36), and temporal lobe (p=0.04, r=0.36). SDMT scores were negatively correlated to mean FA at left superior corona radiata (p=0.004, r=-0.49), left external capsule (p=0.049, r=-0.35) and positively correlated to mean MD values at right medial lemniscus (p=0.01, r=0.44) and right inferior cerebellar peduncle (p=0.01, r=0.43).

For PD-CI group, correlations between mean FA values and test scores showed both positive and negative directions while correlations with mean MD values were only negatively correlated. Mean FA values were positively correlated with ACE-R scores at splenium of corpus callosum (p=0.01, r=0.5), and with GDS scores at sagittal stratum (p=0.02, r=0.44), and right uncinate fasciculus (p=0.03, r=0.43), while they were negatively correlated with GDS scores at inferior cerebellar peduncle (p=0.03, r=-0.41) and right superior fronto occipital fasciculus (p=0.04, r=-0.40). For STROOP test scores, a positive correlation with mean FA values was found at left superior cerebellar peduncle (p=0.04, r=0.4), right retrolenticular internal capsule (p=0.01, r=0.52), left uncinate fasciculus (p=0.002, r=0.57), and left tapetum (p=0.001, r=0.58). STROOP test scores were also found to be negatively correlated to mean MD values at splenium of corpus callosum (p=0.001, r=-0.59) and left tapetum (p=0.0005, r=-0.63). For BJLOT scores, a positive correlation with mean FA values (p=0.01, r=0.51) and a negative correlation with mean MD values (p=0.02, r=-0.45) was found at right superior cerebellar peduncle. Additionally, a positive correlation between mean FA values and BJLOT scores was found at right posterior corona radiata (p=0.03, r=0.41).

For HC group, mean FA values were found to be correlated with ACE-R scores at superior cerebral peduncle (p=0.03, r=0.51), left superior corona radiata (p=0.03, r=0.52), left external capsule (p=0.05, r=0.47), and superior longitudinal fascicle (p=0.01, r=0.62). GDS scores showed positive correlation with mean FA values at right posterior corona radiata (p=0.05, r=0.47), and hippocampal cingulum (p=0.01, r=0.59). Also, GDS scores had negative correlations at middle cerebellar peduncle

(p=0.05, r=-0.48), left cingulum (cingulate gyrus) (p=0.04, r=-0.48), and right inferior cerebral peduncle (p=0.03, r=-0.52). A positive correlation of GDS scores with FA was found at right posterior corona radiata (p=0.05, r=0.47). Additionally mean MD values were positively correlated with GDS scores at right inferior cerebral peduncle (p=0.016, r=0.56). While SDMT scores were positively correlated to mean FA at right sagittal stratum (p=0.04, r=0.49), a negative correlation was found at cerebellum (p=0.03, r=-0.51).

Table 3.8: Spearman's correlation between FA values and ACE-R, GDS, STROOP test scores for PD-MCI group.

FA						
Region	ACE-R		GDS		STROOP	
	r	p	r	p	r	p
Middle Cerebellar Peduncle	-0.40	0.02*	0.11	0.54	-0.17	0.34
Pontine Crossing Tract	-0.14	0.45	0.10	0.60	-0.12	0.53
Genu of Corpus Callosum	-0.08	0.64	0.07	0.70	-0.01	0.98
Body of Corpus Callosum	-0.07	0.71	0.02	0.92	-0.23	0.21
Splenium of Corpus Callosum	0.14	0.46	-0.13	0.46	-0.08	0.65
Fornix	-0.03	0.87	-0.08	0.66	-0.07	0.70
Corticospinal Tract R	-0.26	0.16	-0.03	0.86	-0.06	0.73
Corticospinal Tract L	-0.23	0.21	0.10	0.59	-0.01	0.95
Medial Lemniscus R	-0.22	0.23	0.15	0.41	-0.05	0.78
Medial Lemniscus L	-0.32	0.07	0.27	0.13	-0.10	0.59
Inferior Cerebellar Peduncle R	-0.12	0.53	-0.26	0.15	-0.04	0.83
Inferior Cerebellar Peduncle L	0.02	0.90	0.10	0.60	-0.13	0.50
Superior Cerebellar Peduncle R	-0.10	0.60	0.29	0.10	0.01	0.96
Superior Cerebellar Peduncle L	-0.13	0.49	-0.15	0.42	0.01	0.97
Cerebral Peduncle R	-0.34	0.05	-0.22	0.24	0.01	0.97
Cerebral Peduncle L	-0.36	0.04*	0.11	0.53	0.15	0.40
Anterior Limb of Internal Capsule R	0.07	0.69	-0.14	0.46	0.03	0.87
Anterior Limb of Internal Capsule L	-0.25	0.17	-0.07	0.69	-0.22	0.23
Posterior Limb of Internal Capsule R	0.05	0.81	0.18	0.32	0.25	0.16
Posterior Limb of Internal Capsule L	-0.01	0.95	0.04	0.82	0.15	0.40
Retrolenticular Internal Capsule R	-0.36	0.045*	0.26	0.14	-0.03	0.88
Retrolenticular Internal Capsule L	-0.03	0.89	0.21	0.24	-0.0033	0.99
Anterior Corona Radiata R	-0.23	0.21	0.19	0.29	0.02	0.90
Anterior Corona Radiata L	-0.40	0.02*	0.27	0.13	0.02	0.91
Superior Corona Radiata R	-0.21	0.26	-0.01	0.96	0.18	0.34
Superior Corona Radiata L	-0.17	0.34	0.04	0.85	0.30	0.09
Posterior Corona Radiata R	0.02	0.90	0.32	0.07	0.31	0.09
Posterior Corona Radiata L	0.11	0.55	0.26	0.15	0.43	0.01*
Posterior Thalamic Radiation R	-0.02	0.92	0.23	0.20	-0.05	0.77
Posterior Thalamic Radiation L	0.05	0.80	0.39	0.03*	-0.02	0.90
Sagittal Stratum R	-0.31	0.08	0.16	0.38	-0.15	0.43
Sagittal Stratum L	-0.16	0.39	0.42	0.016*	-0.24	0.19
External Capsule R	-0.22	0.22	0.05	0.81	-0.30	0.09
External Capsule L	-0.35	0.048*	0.17	0.35	0.11	0.54
Cingulum (Cing.Gyrus) R	0.02	0.92	-0.02	0.93	0.02	0.91
Cingulum (Cing.Gyrus) L	-0.16	0.39	0.03	0.89	0.17	0.36
Cingulum (Hippocampal) R	-0.31	0.08	0.09	0.64	-0.07	0.68
Cingulum (Hippocampal) L	-0.16	0.38	0.19	0.30	-0.23	0.21
Fornix R	-0.45	0.01*	0.03	0.89	-0.20	0.27
Fornix L	0.002	0.99	0.08	0.64	0.05	0.79
Superior Longitudinal Fasciculus R	-0.28	0.12	0.25	0.17	0.01	0.97
Superior Longitudinal Fasciculus L	-0.32	0.07	0.25	0.17	0.14	0.45
Superior Fronto Occipital Fasciculus R	0.10	0.60	0.06	0.73	-0.05	0.78
Superior Fronto Occipital Fasciculus L	0.02	0.90	-0.12	0.51	-0.20	0.27
Uncinate Fasciculus R	-0.28	0.12	-0.11	0.56	-0.19	0.29
Uncinate Fasciculus L	-0.30	0.09	0.14	0.44	-0.08	0.64
Tapetum R	0.18	0.31	-0.03	0.86	-0.16	0.39
Tapetum L	0.18	0.33	-0.02	0.91	-0.05	0.80
Caudate	0.03	0.87	-0.01	0.97	0.0004	1.00
Cerebellum	-0.14	0.43	0.07	0.70	0.03	0.88
Frontal Lobe	-0.17	0.34	0.22	0.23	0.06	0.76
Insula	-0.12	0.53	0.13	0.49	0.03	0.87
Occipital Lobe	-0.03	0.87	0.42	0.016*	0.02	0.92
Parietal Lobe	-0.03	0.89	0.41	0.02*	0.29	0.11
Putamen	-0.23	0.21	-0.10	0.59	-0.15	0.40

Temporal Lobe	-0.20	0.27	0.17	0.35	-0.14	0.45
Thalamus	0.05	0.79	0.03	0.86	0.15	0.42

Table 3.9: Spearman's correlation between regional mean FA values and BJLOT, SDMT, UPDRS test scores for PD-MCI group.

FA						
Region	BJLOT		SDMT		UPDRS	
	r	p	r	p	r	p
Middle Cerebellar Peduncle	-0.39	0.03*	-0.09	0.62	-0.01	0.94
Pontine Crossing Tract	-0.19	0.30	-0.21	0.25	-0.02	0.90
Genu of Corpus Callosum	-0.13	0.48	-0.21	0.26	0.12	0.51
Body of Corpus Callosum	-0.01	0.96	0.06	0.74	0.02	0.91
Splenium of Corpus Callosum	0.19	0.30	0.19	0.29	-0.13	0.47
Fornix	-0.20	0.26	0.12	0.50	-0.27	0.14
Corticospinal Tract R	-0.26	0.15	-0.12	0.53	-0.01	0.94
Corticospinal Tract L	-0.27	0.14	-0.08	0.68	0.03	0.87
Medial Lemniscus R	-0.44	0.01*	-0.32	0.07	0.14	0.44
Medial Lemniscus L	-0.41	0.02*	-0.10	0.57	0.21	0.24
Inferior Cerebellar Peduncle R	-0.24	0.19	-0.19	0.29	0.02	0.91
Inferior Cerebellar Peduncle L	-0.10	0.57	0.20	0.28	-0.08	0.66
Superior Cerebellar Peduncle R	-0.13	0.48	0.05	0.77	0.16	0.39
Superior Cerebellar Peduncle L	-0.32	0.07	-0.24	0.19	-0.02	0.90
Cerebral Peduncle R	-0.44	0.01*	-0.22	0.23	0.02	0.90
Cerebral Peduncle L	-0.37	0.04*	-0.29	0.10	-0.04	0.83
Anterior Limb of Internal Capsule R	-0.31	0.09	0.03	0.86	-0.28	0.12
Anterior Limb of Internal Capsule L	-0.35	0.05	0.03	0.88	-0.27	0.13
Posterior Limb of Internal Capsule R	-0.05	0.80	-0.07	0.72	-0.24	0.19
Posterior Limb of Internal Capsule L	-0.22	0.23	-0.27	0.13	-0.21	0.25
Retrolenticular Internal Capsule R	0.28	0.12	0.07	0.71	0.26	0.16
Retrolenticular Internal Capsule L	0.15	0.40	0.08	0.68	0.14	0.44
Anterior Corona Radiata R	-0.09	0.62	-0.08	0.66	0.04	0.81
Anterior Corona Radiata L	-0.33	0.07	-0.21	0.26	0.11	0.56
Superior Corona Radiata R	-0.33	0.06	-0.29	0.11	-0.11	0.55
Superior Corona Radiata L	-0.25	0.17	-0.49	0.004*	-0.02	0.92
Posterior Corona Radiata R	0.09	0.64	-0.20	0.28	0.05	0.79
Posterior Corona Radiata L	0.07	0.70	-0.29	0.11	0.20	0.27
Posterior Thalamic Radiation R	0.04	0.84	0.04	0.83	-0.005	0.98
Posterior Thalamic Radiation L	-0.06	0.74	0.04	0.83	0.04	0.84
Sagittal Stratum R	-0.15	0.42	-0.03	0.86	-0.01	0.94
Sagittal Stratum L	0.01	0.96	0.11	0.53	0.17	0.35
External Capsule R	-0.05	0.79	0.10	0.57	-0.002	0.99
External Capsule L	-0.16	0.38	-0.35	0.049*	-0.02	0.92
Cingulum (Cing.Gyrus) R	0.09	0.61	0.06	0.76	-0.27	0.13
Cingulum (Cing.Gyrus) L	0.01	0.96	-0.22	0.22	-0.26	0.15
Cingulum (Hippocampal) R	-0.28	0.12	-0.14	0.46	-0.03	0.88
Cingulum (Hippocampal) L	-0.24	0.18	0.002	0.99	-0.24	0.18
Fornix R	-0.24	0.18	-0.08	0.66	0.08	0.67
Fornix L	-0.10	0.59	-0.04	0.83	0.21	0.25
Superior Longitudinal Fasciculus R	-0.09	0.64	-0.12	0.51	-0.06	0.76
Superior Longitudinal Fasciculus L	-0.04	0.84	-0.16	0.38	-0.05	0.77
Superior Fronto Occipital Fasciculus R	-0.12	0.52	0.17	0.35	-0.18	0.31
Superior Fronto Occipital Fasciculus L	-0.06	0.73	0.14	0.45	-0.40	0.02*
Uncinate Fasciculus R	-0.43	0.01*	-0.14	0.46	0.15	0.42
Uncinate Fasciculus L	-0.30	0.10	-0.15	0.41	0.07	0.70
Tapetum R	-0.13	0.49	0.21	0.25	-0.06	0.75
Tapetum L	-0.01	0.97	0.23	0.20	-0.15	0.40
Caudate	-0.22	0.22	-0.01	0.94	-0.08	0.66
Cerebellum	-0.21	0.24	-0.10	0.60	-0.17	0.35
Frontal Lobe	-0.31	0.09	-0.07	0.69	-0.23	0.21

Insula	-0.28	0.12	-0.09	0.64	0.24	0.18
Occipital Lobe	0.06	0.76	0.04	0.83	-0.06	0.74
Parietal Lobe	0.05	0.78	-0.12	0.50	0.03	0.85
Putamen	-0.23	0.21	0.04	0.83	0.04	0.84
Temporal Lobe	-0.32	0.08	-0.03	0.88	-0.27	0.13
Thalamus	-0.20	0.27	-0.09	0.63	-0.28	0.12

Table 3.10: Spearman's correlation between regional mean MD values and ACE-R, GDS, STROOP test scores for PD-MCI group.

MD						
Region	ACE-R		GDS		STROOP	
	r	p	r	p	r	p
Middle Cerebellar Peduncle	0.33	0.07	-0.04	0.82	0.22	0.23
Pontine Crossing Tract	0.33	0.06	-0.01	0.97	-0.04	0.82
Genu of Corpus Callosum	-0.02	0.93	-0.03	0.85	-0.05	0.81
Body of Corpus Callosum	0.09	0.62	-0.02	0.90	0.18	0.34
Splenium of Corpus Callosum	0.12	0.50	0.10	0.60	0.25	0.17
Fornix	-0.03	0.85	0.07	0.68	0.13	0.48
Corticospinal Tract R	0.20	0.28	-0.03	0.85	0.09	0.62
Corticospinal Tract L	0.20	0.26	-0.09	0.62	0.13	0.46
Medial Lemniscus R	0.28	0.13	-0.11	0.54	-0.11	0.56
Medial Lemniscus L	0.29	0.10	-0.12	0.52	0.18	0.32
Inferior Cerebellar Peduncle R	0.31	0.09	0.11	0.54	-0.06	0.73
Inferior Cerebellar Peduncle L	0.11	0.54	0.03	0.87	0.27	0.14
Superior Cerebellar Peduncle R	-0.01	0.95	-0.33	0.07	0.02	0.93
Superior Cerebellar Peduncle L	0.004	0.98	0.32	0.07	-0.07	0.70
Cerebral Peduncle R	0.32	0.07	0.07	0.70	-0.003	0.99
Cerebral Peduncle L	0.41	0.02*	-0.12	0.53	-0.06	0.73
Anterior Limb of Internal Capsule R	-0.04	0.84	-0.09	0.63	-0.08	0.67
Anterior Limb of Internal Capsule L	0.27	0.13	-0.07	0.70	0.20	0.28
Posterior Limb of Internal Capsule R	0.09	0.64	-0.11	0.54	-0.35	0.048*
Posterior Limb of Internal Capsule L	-0.01	0.96	-0.15	0.40	-0.18	0.32
Retrolenticular Internal Capsule R	0.29	0.11	-0.20	0.27	0.01	0.95
Retrolenticular Internal Capsule L	-0.10	0.60	-0.04	0.84	0.08	0.65
Anterior Corona Radiata R	-0.29	0.11	-0.03	0.86	-0.11	0.56
Anterior Corona Radiata L	0.19	0.30	-0.22	0.23	0.11	0.55
Superior Corona Radiata R	-0.04	0.82	-0.04	0.83	-0.10	0.59
Superior Corona Radiata L	0.06	0.76	-0.06	0.75	-0.07	0.72
Posterior Corona Radiata R	-0.14	0.44	-0.23	0.21	-0.02	0.91
Posterior Corona Radiata L	-0.02	0.90	-0.09	0.61	-0.09	0.64
Posterior Thalamic Radiation R	-0.0004	1.00	-0.17	0.35	0.03	0.88
Posterior Thalamic Radiation L	0.03	0.86	-0.25	0.17	0.14	0.44
Sagittal Stratum R	0.05	0.80	-0.19	0.30	0.05	0.79
Sagittal Stratum L	0.05	0.78	-0.25	0.17	0.13	0.46
External Capsule R	0.16	0.37	-0.16	0.38	0.02	0.90
External Capsule L	0.22	0.23	-0.31	0.08	-0.16	0.40
Cingulum (Cing.Gyrus) R	0.07	0.69	0.15	0.40	-0.04	0.84
Cingulum (Cing.Gyrus) L	0.41	0.02*	-0.10	0.58	-0.04	0.83
Cingulum (Hippocampal) R	0.38	0.03*	-0.16	0.38	0.19	0.30
Cingulum (Hippocampal) L	0.28	0.12	-0.28	0.12	0.24	0.19
Fornix R	0.41	0.02*	-0.25	0.17	0.04	0.82
Fornix L	-0.05	0.80	-0.04	0.83	-0.21	0.25
Superior Longitudinal Fasciculus R	0.30	0.10	-0.27	0.13	-0.04	0.81
Superior Longitudinal Fasciculus L	0.39	0.03*	-0.25	0.16	0.03	0.88
Superior Fronto Occipital Fasciculus R	-0.13	0.47	-0.01	0.94	0.02	0.91
Superior Fronto Occipital Fasciculus L	0.17	0.36	0.02	0.92	0.13	0.46
Uncinate Fasciculus R	0.10	0.57	-0.06	0.74	0.16	0.37
Uncinate Fasciculus L	0.30	0.10	-0.10	0.58	0.17	0.35
Tapetum R	-0.12	0.53	0.06	0.73	0.11	0.55

Tapetum L	-0.02	0.90	0.07	0.69	0.09	0.61
Caudate	-0.05	0.80	-0.01	0.97	0.04	0.84
Cerebellum	0.29	0.11	-0.19	0.29	-0.0014	0.99
Frontal Lobe	0.22	0.22	-0.06	0.75	0.01	0.97
Insula	0.17	0.35	0.03	0.88	0.01	0.96
Occipital Lobe	0.14	0.45	-0.36	0.04*	0.05	0.79
Parietal Lobe	0.08	0.68	-0.20	0.27	-0.02	0.93
Putamen	0.16	0.39	-0.31	0.08	-0.09	0.63
Temporal Lobe	0.22	0.23	-0.27	0.14	0.13	0.49
Thalamus	0.01	0.94	-0.02	0.90	-0.05	0.79

Table 3.11: Spearman's correlation between regional mean MD values and BJLOT, SDMT, UPDRS test scores for PD-MCI group.

MD						
Region	BJLOT		SDMT		UPDRS	
	r	p	r	p	r	p
Middle Cerebellar Peduncle	0.49	0.004*	0.06	0.75	0.07	0.71
Pontine Crossing Tract	0.31	0.09	0.34	0.06	-0.03	0.87
Genu of Corpus Callosum	0.12	0.50	0.23	0.21	-0.06	0.74
Body of Corpus Callosum	0.22	0.24	-0.05	0.77	-0.10	0.57
Splenium of Corpus Callosum	0.18	0.32	-0.07	0.72	0.05	0.80
Fornix	0.21	0.26	-0.14	0.44	0.22	0.23
Corticospinal Tract R	0.28	0.12	0.01	0.97	0.0002	1.00
Corticospinal Tract L	0.28	0.12	-0.04	0.83	0.05	0.77
Medial Lemniscus R	0.34	0.06	0.44	0.01*	-0.20	0.28
Medial Lemniscus L	0.44	0.01*	-0.01	0.97	0.06	0.73
Inferior Cerebellar Peduncle R	0.44	0.01*	0.43	0.01*	-0.06	0.73
Inferior Cerebellar Peduncle L	0.24	0.19	-0.21	0.25	0.16	0.38
Superior Cerebellar Peduncle R	0.12	0.52	-0.19	0.31	-0.15	0.41
Superior Cerebellar Peduncle L	0.34	0.05	0.28	0.12	0.01	0.97
Cerebral Peduncle R	0.51	0.003*	0.29	0.11	-0.12	0.50
Cerebral Peduncle L	0.46	0.01*	0.26	0.15	-0.13	0.46
Anterior Limb of Internal Capsule R	0.36	0.04*	-0.002	0.99	0.10	0.60
Anterior Limb of Internal Capsule L	0.26	0.14	-0.02	0.90	0.04	0.82
Posterior Limb of Internal Capsule R	0.19	0.29	0.22	0.23	0.003	0.98
Posterior Limb of Internal Capsule L	0.18	0.31	0.21	0.25	-0.06	0.75
Retrolenticular Internal Capsule R	-0.19	0.30	0.002	0.99	-0.11	0.55
Retrolenticular Internal Capsule L	-0.22	0.22	-0.23	0.20	0.13	0.47
Anterior Corona Radiata R	0.19	0.29	0.07	0.71	0.04	0.83
Anterior Corona Radiata L	0.18	0.31	0.09	0.64	-0.12	0.50
Superior Corona Radiata R	0.31	0.09	0.12	0.50	0.11	0.53
Superior Corona Radiata L	0.16	0.39	0.12	0.52	-0.03	0.89
Posterior Corona Radiata R	0.03	0.88	-0.07	0.71	0.07	0.72
Posterior Corona Radiata L	0.05	0.77	0.03	0.88	0.10	0.59
Posterior Thalamic Radiation R	0.13	0.47	-0.06	0.73	0.08	0.67
Posterior Thalamic Radiation L	0.05	0.79	-0.13	0.49	-0.04	0.83
Sagittal Stratum R	0.13	0.46	0.02	0.91	0.04	0.81
Sagittal Stratum L	0.06	0.76	-0.06	0.74	-0.10	0.58
External Capsule R	0.27	0.13	0.25	0.17	-0.15	0.41
External Capsule L	0.19	0.30	0.32	0.08	0.05	0.79
Cingulum (Cing.Gyrus) R	0.02	0.91	0.08	0.66	0.20	0.27
Cingulum (Cing.Gyrus) L	-0.06	0.74	0.13	0.48	0.14	0.44
Cingulum (Hippocampal) R	0.35	0.05	0.15	0.42	0.01	0.97
Cingulum (Hippocampal) L	0.28	0.12	0.18	0.31	0.01	0.96
Fornix R	0.15	0.41	0.13	0.46	-0.10	0.57
Fornix L	0.24	0.19	0.14	0.46	-0.29	0.11
Superior Longitudinal Fasciculus R	0.20	0.28	0.27	0.14	0.005	0.98
Superior Longitudinal Fasciculus L	0.15	0.41	0.20	0.27	0.09	0.62
Superior Fronto Occipital Fasciculus R	0.29	0.11	-0.02	0.93	0.06	0.73

Superior Fronto Occipital Fasciculus L	0.28	0.12	-0.03	0.89	0.17	0.35
Uncinate Fasciculus R	0.26	0.15	0.04	0.82	-0.06	0.76
Uncinate Fasciculus L	0.25	0.17	0.04	0.81	-0.07	0.70
Tapetum R	0.20	0.28	-0.13	0.49	0.09	0.62
Tapetum L	0.11	0.55	-0.16	0.37	0.16	0.38
Caudate	0.26	0.15	-0.03	0.87	0.18	0.33
Cerebellum	0.30	0.09	0.19	0.29	0.19	0.30
Frontal Lobe	0.36	0.045*	0.20	0.28	0.28	0.12
Insula	0.31	0.08	0.12	0.50	-0.01	0.98
Occipital Lobe	0.10	0.60	0.05	0.78	0.12	0.52
Parietal Lobe	0.20	0.28	0.10	0.59	0.20	0.27
Putamen	0.33	0.07	0.27	0.14	-0.34	0.06
Temporal Lobe	0.36	0.04*	0.13	0.49	0.12	0.53
Thalamus	0.23	0.20	0.02	0.90	0.27	0.13

Table 3.12: Spearman's correlation between regional mean FA values and ACE-R, GDS, STROOP test scores for PD-CI group.

FA						
Region	ACE-R		GDS		STROOP	
	r	p	r	p	r	p
Middle Cerebellar Peduncle	0.14	0.48	-0.16	0.42	-0.25	0.21
Pontine Crossing Tract	-0.20	0.33	0.19	0.33	0.20	0.33
Genu of Corpus Callosum	-0.02	0.94	0.23	0.25	-0.04	0.83
Body of Corpus Callosum	-0.002	0.99	0.001	1.00	0.24	0.23
Splenium of Corpus Callosum	0.50	0.01*	0.17	0.40	0.21	0.30
Fornix	0.04	0.86	-0.16	0.42	0.02	0.92
Corticospinal Tract R	0.12	0.56	-0.22	0.27	-0.11	0.60
Corticospinal Tract L	0.19	0.35	-0.22	0.27	-0.15	0.46
Medial Lemniscus R	0.11	0.59	-0.19	0.33	0.08	0.71
Medial Lemniscus L	0.16	0.44	0.14	0.47	0.07	0.74
Inferior Cerebellar Peduncle R	0.01	0.96	-0.41	0.03*	-0.08	0.70
Inferior Cerebellar Peduncle L	0.19	0.33	-0.08	0.68	-0.31	0.12
Superior Cerebellar Peduncle R	0.29	0.14	0.13	0.51	0.12	0.56
Superior Cerebellar Peduncle L	-0.14	0.49	0.02	0.94	0.40	0.04*
Cerebral Peduncle R	0.05	0.79	0.02	0.91	0.15	0.46
Cerebral Peduncle L	0.11	0.60	0.08	0.70	0.27	0.18
Anterior Limb of Internal Capsule R	0.12	0.55	-0.13	0.51	0.11	0.60
Anterior Limb of Internal Capsule L	0.20	0.33	-0.23	0.26	0.28	0.15
Posterior Limb of Internal Capsule R	-0.05	0.79	0.05	0.82	-0.10	0.63
Posterior Limb of Internal Capsule L	0.29	0.14	-0.19	0.34	0.19	0.33
Retrolenticular Internal Capsule R	-0.26	0.20	0.19	0.34	0.52	0.01*
Retrolenticular Internal Capsule L	0.30	0.13	-0.04	0.83	0.17	0.39
Anterior Corona Radiata R	0.18	0.38	-0.19	0.36	-0.07	0.72
Anterior Corona Radiata L	-0.01	0.95	0.01	0.95	0.06	0.75
Superior Corona Radiata R	0.31	0.12	0.02	0.91	-0.10	0.61
Superior Corona Radiata L	0.01	0.94	-0.11	0.60	0.09	0.67
Posterior Corona Radiata R	0.19	0.35	-0.06	0.76	0.11	0.59
Posterior Corona Radiata L	-0.02	0.93	0.16	0.43	0.03	0.89
Posterior Thalamic Radiation R	-0.03	0.89	-0.22	0.28	0.29	0.14
Posterior Thalamic Radiation L	0.38	0.05	-0.01	0.96	0.13	0.53
Sagittal Stratum R	-0.03	0.86	0.44	0.02*	0.18	0.36
Sagittal Stratum L	0.20	0.31	0.11	0.58	0.25	0.21
External Capsule R	-0.13	0.50	-0.10	0.62	-0.03	0.86
External Capsule L	-0.14	0.49	-0.18	0.36	0.14	0.48
Cingulum (Cing.Gyrus) R	0.18	0.37	-0.24	0.22	-0.29	0.15
Cingulum (Cing.Gyrus) L	-0.06	0.75	-0.31	0.12	-0.11	0.58
Cingulum (Hippocampal) R	0.07	0.71	0.14	0.49	0.18	0.38
Cingulum (Hippocampal) L	0.04	0.85	-0.17	0.41	-0.06	0.76
Fornix R	-0.11	0.60	0.25	0.20	-0.21	0.30

Fornix L	0.06	0.78	0.30	0.12	0.15	0.47
Superior Longitudinal Fasciculus R	0.32	0.11	0.08	0.68	-0.21	0.29
Superior Longitudinal Fasciculus L	0.29	0.15	-0.14	0.48	-0.28	0.15
Superior Fronto Occipital Fasciculus R	0.22	0.26	-0.40	0.04*	-0.12	0.54
Superior Fronto Occipital Fasciculus L	0.02	0.90	-0.21	0.30	0.15	0.46
Uncinate Fasciculus R	0.19	0.35	0.43	0.03*	0.11	0.60
Uncinate Fasciculus L	0.05	0.80	0.29	0.14	0.57	0.002*
Tapetum R	-0.13	0.52	0.16	0.41	0.18	0.38
Tapetum L	-0.19	0.35	-0.04	0.86	0.58	0.001*
Caudate	-0.06	0.77	0.02	0.92	0.08	0.68
Cerebellum	-0.09	0.66	-0.02	0.93	-0.23	0.26
Frontal Lobe	0.10	0.62	-0.18	0.36	0.02	0.93
Insula	-0.23	0.24	0.11	0.58	-0.10	0.63
Occipital Lobe	-0.07	0.74	0.11	0.57	-0.07	0.73
Parietal Lobe	-0.17	0.39	0.11	0.58	-0.02	0.93
Putamen	0.02	0.93	0.08	0.67	0.01	0.97
Temporal Lobe	-0.19	0.35	0.21	0.28	0.23	0.26
Thalamus	-0.04	0.85	-0.002	0.99	-0.08	0.68

Table 3.13: Spearman's correlation between regional mean FA values and BJLOT, SDMT, UPDRS test scores for PD-CI group.

FA						
Region	BJLOT		SDMT		UPDRS	
	r	p	r	p	r	p
Middle Cerebellar Peduncle	0.09	0.64	-0.20	0.31	0.04	0.86
Pontine Crossing Tract	-0.09	0.66	-0.05	0.82	0.003	0.99
Genu of Corpus Callosum	0.04	0.83	-0.01	0.97	-0.13	0.50
Body of Corpus Callosum	0.22	0.27	-0.14	0.48	-0.12	0.54
Splenium of Corpus Callosum	0.18	0.36	0.09	0.67	0.21	0.28
Fornix	0.16	0.44	-0.05	0.79	0.06	0.78
Corticospinal Tract R	0.17	0.38	0.05	0.82	0.13	0.52
Corticospinal Tract L	0.11	0.60	0.02	0.93	0.09	0.67
Medial Lemniscus R	-0.002	0.99	0.06	0.77	-0.24	0.24
Medial Lemniscus L	0.13	0.52	0.03	0.90	0.06	0.78
Inferior Cerebellar Peduncle R	0.09	0.65	0.20	0.31	-0.09	0.67
Inferior Cerebellar Peduncle L	0.11	0.58	0.14	0.49	-0.10	0.64
Superior Cerebellar Peduncle R	0.51	0.01*	0.22	0.26	0.20	0.31
Superior Cerebellar Peduncle L	0.16	0.43	-0.30	0.12	-0.22	0.27
Cerebral Peduncle R	0.20	0.32	0.04	0.85	0.07	0.72
Cerebral Peduncle L	0.04	0.83	0.13	0.50	-0.22	0.27
Anterior Limb of Internal Capsule R	0.09	0.67	0.20	0.31	0.02	0.92
Anterior Limb of Internal Capsule L	0.19	0.34	0.004	0.99	-0.17	0.40
Posterior Limb of Internal Capsule R	0.02	0.94	-0.14	0.49	0.32	0.10
Posterior Limb of Internal Capsule L	-0.05	0.81	0.02	0.94	-0.17	0.38
Retrolenticular Internal Capsule R	0.10	0.61	-0.18	0.36	0.12	0.55
Retrolenticular Internal Capsule L	0.32	0.10	0.44	0.02*	0.04	0.85
Anterior Corona Radiata R	0.27	0.17	0.14	0.48	0.05	0.81
Anterior Corona Radiata L	0.22	0.27	-0.09	0.65	-0.05	0.82
Superior Corona Radiata R	0.32	0.11	0.15	0.45	0.28	0.16
Superior Corona Radiata L	0.19	0.33	-0.02	0.94	0.09	0.67
Posterior Corona Radiata R	0.41	0.03*	0.13	0.52	0.35	0.07
Posterior Corona Radiata L	0.17	0.39	0.11	0.58	0.55	0.003*
Posterior Thalamic Radiation R	-0.10	0.61	0.03	0.88	-0.17	0.41
Posterior Thalamic Radiation L	0.10	0.62	0.09	0.67	-0.24	0.22
Sagittal Stratum R	0.20	0.31	0.25	0.21	0.003	0.99
Sagittal Stratum L	0.24	0.22	0.12	0.54	-0.13	0.51
External Capsule R	0.10	0.62	-0.20	0.32	-0.01	0.95
External Capsule L	0.33	0.09	-0.17	0.40	-0.08	0.70
Cingulum (Cing.Gyrus) R	0.05	0.79	0.03	0.87	0.34	0.08

Cingulum (Cing.Gyrus) L	0.12	0.56	-0.27	0.18	0.28	0.16
Cingulum (Hippocampal) R	0.08	0.68	-0.10	0.62	-0.05	0.79
Cingulum (Hippocampal) L	-0.06	0.76	-0.12	0.54	-0.30	0.13
Fornix R	-0.07	0.72	-0.18	0.36	-0.19	0.34
Fornix L	-0.13	0.53	-0.05	0.82	-0.05	0.82
Superior Longitudinal Fasciculus R	0.37	0.06	0.09	0.65	0.10	0.62
Superior Longitudinal Fasciculus L	0.16	0.42	0.05	0.82	0.04	0.84
Superior Fronto Occipital Fasciculus R	0.01	0.96	0.12	0.55	0.04	0.84
Superior Fronto Occipital Fasciculus L	0.08	0.69	-0.33	0.09	-0.07	0.73
Uncinate Fasciculus R	0.24	0.23	-0.04	0.85	0.19	0.35
Uncinate Fasciculus L	0.05	0.82	-0.13	0.52	-0.02	0.92
Tapetum R	0.04	0.84	-0.05	0.82	-0.09	0.66
Tapetum L	-0.10	0.60	-0.20	0.31	-0.24	0.22
Caudate	0.24	0.23	-0.04	0.83	-0.004	0.98
Cerebellum	-0.003	0.99	0.10	0.62	0.04	0.85
Frontal Lobe	0.20	0.32	-0.10	0.62	0.04	0.85
Insula	0.12	0.56	0.24	0.23	0.12	0.55
Occipital Lobe	0.25	0.21	-0.20	0.31	0.41	0.03*
Parietal Lobe	0.13	0.51	-0.21	0.29	0.27	0.17
Putamen	0.32	0.11	0.15	0.45	0.22	0.27
Temporal Lobe	0.20	0.32	-0.19	0.33	0.12	0.55
Thalamus	0.05	0.82	-0.17	0.39	0.05	0.80

Table 3.14: Spearman's correlation between regional mean MD values and ACE-R, GDS, STROOP test scores for PD-CI group.

MD						
Region	ACE-R		GDS		STROOP	
	r	p	r	p	r	p
Middle Cerebellar Peduncle	0.01	0.96	-0.01	0.96	0.16	0.42
Pontine Crossing Tract	-0.11	0.59	0.04	0.86	-0.14	0.47
Genu of Corpus Callosum	0.05	0.79	-0.19	0.33	0.04	0.83
Body of Corpus Callosum	-0.003	0.99	-0.11	0.59	-0.13	0.51
Splenium of Corpus Callosum	-0.18	0.37	-0.07	0.74	-0.59	0.001*
Fornix	-0.01	0.97	0.10	0.61	0.09	0.64
Corticospinal Tract R	-0.06	0.75	0.18	0.38	0.09	0.65
Corticospinal Tract L	-0.28	0.16	0.27	0.17	0.14	0.49
Medial Lemniscus R	0.16	0.42	0.14	0.47	-0.06	0.76
Medial Lemniscus L	0.03	0.88	0.04	0.86	-0.21	0.29
Inferior Cerebellar Peduncle R	0.12	0.55	0.03	0.86	-0.13	0.52
Inferior Cerebellar Peduncle L	-0.22	0.26	0.04	0.83	0.13	0.51
Superior Cerebellar Peduncle R	-0.28	0.16	-0.18	0.38	0.0003	1.00
Superior Cerebellar Peduncle L	0.17	0.40	-0.15	0.46	-0.27	0.18
Cerebral Peduncle R	-0.10	0.63	-0.16	0.43	-0.13	0.51
Cerebral Peduncle L	-0.31	0.12	-0.16	0.42	-0.16	0.42
Anterior Limb of Internal Capsule R	-0.03	0.87	0.17	0.39	-0.03	0.90
Anterior Limb of Internal Capsule L	-0.10	0.63	0.24	0.23	-0.12	0.56
Posterior Limb of Internal Capsule R	0.23	0.26	-0.06	0.75	-0.23	0.24
Posterior Limb of Internal Capsule L	-0.003	0.98	0.13	0.50	-0.26	0.18
Retrolenticular Internal Capsule R	0.30	0.13	-0.06	0.77	-0.35	0.07
Retrolenticular Internal Capsule L	-0.14	0.49	-0.02	0.92	-0.30	0.14
Anterior Corona Radiata R	-0.09	0.66	0.18	0.36	0.17	0.39
Anterior Corona Radiata L	-0.16	0.42	0.06	0.77	0.06	0.77
Superior Corona Radiata R	0.02	0.93	-0.02	0.93	-0.07	0.71
Superior Corona Radiata L	-0.003	0.98	0.14	0.48	-0.18	0.37
Posterior Corona Radiata R	-0.002	0.99	0.02	0.91	-0.13	0.51
Posterior Corona Radiata L	0.001	1.00	0.03	0.89	-0.21	0.29
Posterior Thalamic Radiation R	0.30	0.13	-0.06	0.78	-0.36	0.07
Posterior Thalamic Radiation L	0.04	0.86	0.06	0.78	-0.38	0.05
Sagittal Stratum R	-0.02	0.90	-0.12	0.56	-0.21	0.30

Sagittal Stratum L	-0.15	0.45	0.04	0.86	-0.20	0.31
External Capsule R	0.08	0.67	-0.02	0.91	0.09	0.65
External Capsule L	0.04	0.83	0.05	0.82	0.09	0.66
Cingulum (Cing.Gyrus) R	-0.10	0.62	0.01	0.98	0.07	0.74
Cingulum (Cing.Gyrus) L	-0.04	0.85	-0.16	0.43	-0.16	0.43
Cingulum (Hippocampal) R	-0.30	0.13	0.01	0.97	0.01	0.95
Cingulum (Hippocampal) L	-0.15	0.46	0.19	0.35	0.12	0.55
Fornix R	0.002	0.99	-0.28	0.16	0.14	0.50
Fornix L	0.09	0.66	-0.33	0.10	-0.09	0.65
Superior Longitudinal Fasciculus R	0.07	0.72	-0.14	0.48	0.23	0.25
Superior Longitudinal Fasciculus L	-0.18	0.36	-0.03	0.88	0.05	0.82
Superior Fronto Occipital Fasciculus R	-0.16	0.44	0.30	0.13	-0.02	0.91
Superior Fronto Occipital Fasciculus L	0.04	0.86	0.28	0.16	-0.19	0.35
Uncinate Fasciculus R	0.01	0.95	-0.24	0.22	0.003	0.98
Uncinate Fasciculus L	-0.25	0.21	0.10	0.62	-0.12	0.55
Tapetum R	0.20	0.32	-0.18	0.37	-0.21	0.29
Tapetum L	0.34	0.08	-0.03	0.86	-0.63	0.0005*
Caudate	0.12	0.55	0.07	0.71	-0.09	0.67
Cerebellum	0.17	0.40	0.02	0.90	0.18	0.36
Frontal Lobe	0.06	0.77	0.13	0.51	0.07	0.73
Insula	0.06	0.78	-0.05	0.79	0.07	0.74
Occipital Lobe	-0.02	0.91	-0.03	0.90	0.10	0.61
Parietal Lobe	0.06	0.75	0.06	0.76	0.07	0.72
Putamen	-0.002	0.99	-0.12	0.54	0.13	0.52
Temporal Lobe	-0.11	0.58	0.07	0.73	0.11	0.57
Thalamus	0.02	0.93	0.10	0.63	0.14	0.48

Table 3.15: Spearman's correlation between regional mean MD values and BJLOT, SDMT, UPDRS test scores for PD-CI group.

MD						
Region	BJLOT		SDMT		UPDRS	
	r	p	r	p	r	p
Middle Cerebellar Peduncle	-0.03	0.90	0.24	0.23	-0.002	0.99
Pontine Crossing Tract	0.11	0.60	0.13	0.53	0.13	0.51
Genu of Corpus Callosum	0.02	0.93	-0.01	0.96	0.21	0.29
Body of Corpus Callosum	-0.15	0.46	-0.07	0.74	0.29	0.14
Splenium of Corpus Callosum	-0.04	0.82	0.01	0.95	0.14	0.49
Fornix	-0.07	0.73	-0.001	1.00	-0.04	0.85
Corticospinal Tract R	0.09	0.65	0.18	0.36	-0.05	0.82
Corticospinal Tract L	-0.11	0.59	0.07	0.73	-0.06	0.76
Medial Lemniscus R	-0.10	0.61	0.14	0.47	0.37	0.06
Medial Lemniscus L	-0.14	0.48	0.0003	1.00	0.11	0.58
Inferior Cerebellar Peduncle R	0.04	0.82	0.09	0.67	0.13	0.50
Inferior Cerebellar Peduncle L	-0.30	0.13	-0.17	0.41	0.08	0.70
Superior Cerebellar Peduncle R	-0.45	0.02*	-0.31	0.12	-0.23	0.25
Superior Cerebellar Peduncle L	-0.04	0.83	0.20	0.31	0.21	0.30
Cerebral Peduncle R	0.15	0.44	-0.03	0.87	-0.09	0.64
Cerebral Peduncle L	0.08	0.69	-0.11	0.57	-0.01	0.95
Anterior Limb of Internal Capsule R	0.02	0.91	-0.18	0.37	0.10	0.63
Anterior Limb of Internal Capsule L	-0.04	0.83	-0.01	0.96	0.15	0.44
Posterior Limb of Internal Capsule R	-0.05	0.80	0.10	0.62	-0.04	0.83
Posterior Limb of Internal Capsule L	-0.06	0.76	-0.03	0.87	0.01	0.95
Retrolenticular Internal Capsule R	-0.07	0.72	0.11	0.59	-0.04	0.83
Retrolenticular Internal Capsule L	-0.20	0.32	-0.24	0.24	-0.03	0.87
Anterior Corona Radiata R	-0.16	0.43	-0.19	0.34	0.09	0.66
Anterior Corona Radiata L	-0.15	0.44	-0.11	0.59	0.15	0.45
Superior Corona Radiata R	-0.01	0.98	-0.09	0.65	0.11	0.58
Superior Corona Radiata L	-0.03	0.90	0.06	0.76	0.27	0.18
Posterior Corona Radiata R	-0.06	0.77	0.05	0.80	0.02	0.91

Posterior Corona Radiata L	0.05	0.80	-0.05	0.81	0.27	0.17
Posterior Thalamic Radiation R	0.04	0.85	0.18	0.38	0.13	0.50
Posterior Thalamic Radiation L	0.10	0.62	0.19	0.34	0.25	0.21
Sagittal Stratum R	-0.21	0.30	-0.05	0.80	0.16	0.43
Sagittal Stratum L	-0.21	0.29	-0.06	0.77	0.21	0.30
External Capsule R	-0.17	0.41	-0.14	0.48	0.04	0.83
External Capsule L	-0.34	0.09	-0.12	0.55	0.07	0.73
Cingulum (Cing.Gyrus) R	0.04	0.86	-0.08	0.68	-0.13	0.51
Cingulum (Cing.Gyrus) L	0.09	0.67	0.13	0.51	-0.06	0.78
Cingulum (Hippocampal) R	-0.14	0.47	-0.26	0.19	0.19	0.35
Cingulum (Hippocampal) L	0.01	0.98	-0.03	0.87	0.33	0.09
Fornix R	0.02	0.92	-0.002	0.99	0.07	0.72
Fornix L	0.26	0.20	-0.06	0.78	0.07	0.74
Superior Longitudinal Fasciculus R	-0.11	0.60	-0.03	0.90	0.01	0.98
Superior Longitudinal Fasciculus L	-0.07	0.73	-0.07	0.74	-0.02	0.93
Superior Fronto Occipital Fasciculus R	0.01	0.96	-0.21	0.30	0.03	0.87
Superior Fronto Occipital Fasciculus L	-0.01	0.97	0.22	0.27	0.06	0.77
Uncinate Fasciculus R	-0.01	0.96	-0.12	0.55	-0.10	0.60
Uncinate Fasciculus L	0.04	0.84	-0.17	0.40	0.13	0.51
Tapetum R	-0.01	0.96	0.05	0.79	0.10	0.62
Tapetum L	0.20	0.33	0.26	0.20	0.16	0.42
Caudate	-0.07	0.72	0.13	0.53	0.25	0.20
Cerebellum	-0.10	0.63	0.02	0.93	-0.02	0.94
Frontal Lobe	-0.09	0.64	0.04	0.83	0.01	0.96
Insula	0.002	0.99	0.05	0.79	0.23	0.26
Occipital Lobe	-0.16	0.43	0.04	0.84	-0.13	0.53
Parietal Lobe	0.02	0.94	0.08	0.70	-0.03	0.88
Putamen	-0.21	0.28	-0.28	0.16	0.05	0.81
Temporal Lobe	-0.15	0.46	0.03	0.88	0.09	0.64
Thalamus	0.04	0.84	0.09	0.65	0.11	0.57

Table 3.16: Spearman's correlation between regional mean FA values and ACE-R, GDS, STROOP, BJLOT, SDMT test scores for HC group.

FA										
Region	ACE-R		GDS		STROOP		BJLOT		SDMT	
	r	p	r	p	r	p	r	p	r	p
Middle Cerebellar Peduncle	-0.14	0.57	-0.48	0.05*	-0.04	0.88	0.15	0.56	-0.09	0.72
Pontine Crossing Tract	-0.16	0.52	0.20	0.42	-0.19	0.46	0.06	0.81	0.21	0.39
Genu of Corpus Callosum	0.31	0.21	0.07	0.78	-0.28	0.26	0.14	0.58	0.24	0.35
Body of Corpus Callosum	0.39	0.11	0.12	0.64	-0.14	0.58	-0.02	0.95	0.10	0.70
Splenium of Corpus Callosum	0.24	0.33	0.31	0.20	0.31	0.21	-0.19	0.45	0.06	0.81
Fornix	0.35	0.15	0.05	0.84	-0.45	0.06	0.34	0.17	0.36	0.14
Corticospinal Tract R	-0.18	0.48	-0.05	0.85	0.06	0.81	0.07	0.78	0.10	0.70
Corticospinal Tract L	0.002	0.99	0.15	0.56	0.08	0.76	0.04	0.88	0.22	0.38
Medial Lemniscus R	0.004	0.99	-0.27	0.28	-0.19	0.45	0.31	0.21	0.25	0.32
Medial Lemniscus L	0.02	0.92	0.05	0.85	-0.07	0.79	0.07	0.80	0.12	0.63
Inferior Cerebellar Peduncle R	-0.34	0.17	-0.52	0.03*	0.29	0.24	-0.29	0.24	-0.31	0.22
Inferior Cerebellar Peduncle L	-0.37	0.14	-0.27	0.28	0.30	0.22	-0.34	0.16	-0.21	0.39
Superior Cerebellar Peduncle R	0.51	0.03*	0.21	0.39	-0.14	0.57	0.19	0.46	0.26	0.30
Superior Cerebellar Peduncle L	0.24	0.34	0.13	0.62	-0.23	0.37	0.07	0.79	0.002	0.99
Cerebral Peduncle R	-0.06	0.83	0.16	0.53	-0.13	0.60	0.25	0.31	0.16	0.53
Cerebral Peduncle L	0.18	0.48	0.19	0.44	-0.02	0.93	0.09	0.73	0.11	0.66
Anterior Limb of Internal Capsule R	-0.05	0.84	0.36	0.14	0.16	0.53	-0.13	0.60	-0.02	0.94
Anterior Limb of Internal Capsule L	0.14	0.58	0.23	0.35	-0.14	0.57	-0.08	0.75	-0.04	0.89
Posterior Limb of Internal Capsule R	0.21	0.39	0.28	0.26	0.17	0.49	-0.06	0.83	0.05	0.84
Posterior Limb of Internal Capsule L	0.31	0.21	0.24	0.34	-0.07	0.79	0.08	0.74	-0.003	0.99
Retrolenticular Internal Capsule R	0.38	0.12	0.15	0.54	-0.27	0.27	0.26	0.29	0.20	0.43
Retrolenticular Internal Capsule L	0.46	0.05	0.21	0.41	-0.20	0.42	0.31	0.21	0.40	0.10
Anterior Corona Radiata R	0.30	0.23	0.20	0.43	0.17	0.51	-0.09	0.71	0.01	0.96
Anterior Corona Radiata L	0.26	0.30	0.05	0.86	0.14	0.57	-0.11	0.65	-0.21	0.39
Superior Corona Radiata R	0.23	0.35	0.17	0.50	0.16	0.52	-0.03	0.90	-0.02	0.93
Superior Corona Radiata L	0.52	0.03*	-0.03	0.92	-0.17	0.49	0.24	0.33	0.15	0.56
Posterior Corona Radiata R	0.45	0.06	0.47	0.05*	0.03	0.90	0.14	0.58	0.38	0.12
Posterior Corona Radiata L	0.40	0.10	0.29	0.24	0.001	1.00	0.27	0.28	0.36	0.14
Posterior Thalamic Radiation R	-0.002	0.99	-0.01	0.96	0.24	0.33	-0.10	0.69	-0.10	0.71
Posterior Thalamic Radiation L	0.29	0.24	0.15	0.54	0.08	0.75	0.02	0.93	0.10	0.70
Sagittal Stratum R	0.27	0.27	0.02	0.94	-0.44	0.07	0.46	0.05	0.49	0.04*
Sagittal Stratum L	0.36	0.14	0.07	0.78	-0.34	0.17	0.41	0.09	0.46	0.05
External Capsule R	0.40	0.10	0.07	0.78	-0.31	0.21	0.29	0.24	0.30	0.23
External Capsule L	0.47	0.05*	-0.09	0.74	-0.18	0.47	0.27	0.27	0.17	0.50
Cingulum (Cing.Gyrus) R	0.05	0.84	-0.10	0.68	-0.05	0.84	0.001	1.00	0.004	0.99
Cingulum (Cing.Gyrus) L	-0.01	0.97	-0.48	0.04*	-0.21	0.40	0.24	0.33	-0.05	0.85
Cingulum (Hippocampal) R	-0.16	0.53	0.59	0.01*	0.19	0.44	-0.08	0.76	0.14	0.58
Cingulum (Hippocampal) L	0.33	0.17	0.07	0.79	-0.37	0.13	0.40	0.10	0.22	0.38
Fornix R	0.23	0.36	0.29	0.25	-0.27	0.28	0.32	0.19	0.33	0.18
Fornix L	0.27	0.28	-0.11	0.67	-0.30	0.22	0.28	0.26	0.16	0.53
Superior Longitudinal Fasciculus R	0.06	0.83	-0.02	0.93	0.19	0.46	-0.01	0.96	-0.04	0.87
Superior Longitudinal Fasciculus L	0.62	0.01*	-0.17	0.51	-0.34	0.17	0.45	0.06	0.28	0.26
Superior Fronto Occipital Fasciculus R	0.17	0.49	0.11	0.65	0.23	0.37	-0.14	0.59	-0.08	0.76
Superior Fronto Occipital Fasciculus L	0.24	0.35	-0.02	0.92	-0.08	0.75	0.001	1.00	-0.05	0.84
Uncinate Fasciculus R	0.14	0.58	-0.15	0.54	-0.28	0.25	0.23	0.35	0.36	0.14
Uncinate Fasciculus L	0.12	0.65	-0.16	0.52	0.01	0.96	-0.04	0.87	-0.17	0.51
Tapetum R	0.23	0.36	0.06	0.80	-0.21	0.41	0.05	0.85	0.12	0.64
Tapetum L	0.01	0.96	0.17	0.51	0.24	0.33	-0.44	0.07	-0.20	0.43
Caudate	0.07	0.78	0.27	0.27	0.12	0.63	-0.20	0.44	-0.10	0.70
Cerebellum	-0.24	0.35	-0.29	0.25	0.45	0.06	-0.39	0.11	-0.51	0.03*
Frontal Lobe	-0.05	0.84	-0.11	0.67	0.23	0.37	-0.29	0.24	-0.27	0.28
Insula	-0.13	0.62	-0.08	0.74	-0.12	0.63	0.29	0.24	0.11	0.67
Occipital Lobe	0.19	0.45	-0.001	1.00	0.12	0.63	-0.07	0.80	-0.03	0.90
Parietal Lobe	0.23	0.37	0.15	0.55	-0.02	0.94	-0.001	1.00	0.07	0.78
Putamen	0.18	0.46	0.24	0.34	-0.16	0.52	0.23	0.36	0.28	0.27

Temporal Lobe	-0.23	0.36	0.03	0.92	0.39	0.11	-0.24	0.34	-0.25	0.32
Thalamus	0.20	0.43	0.22	0.39	-0.05	0.85	-0.02	0.93	-0.03	0.91

Table 3.17: Spearman's correlation between MD values and ACE-R, GDS, STROOP, BJLOT, SDMT test scores for HC group.

MD										
Region	ACE-R		GDS		STROOP		BJLOT		SDMT	
	r	p	r	p	r	p	r	p	r	p
Middle Cerebellar Peduncle	0.14	0.57	0.41	0.09	-0.11	0.66	-0.001	1.00	0.07	0.77
Pontine Crossing Tract	0.05	0.84	-0.07	0.79	0.16	0.54	-0.05	0.85	-0.08	0.76
Genu of Corpus Callosum	-0.08	0.74	-0.02	0.94	0.11	0.66	0.02	0.93	0.02	0.93
Body of Corpus Callosum	-0.11	0.67	-0.13	0.61	-0.05	0.83	0.06	0.81	-0.03	0.89
Splenium of Corpus Callosum	0.04	0.87	-0.13	0.60	-0.17	0.51	0.11	0.65	0.14	0.57
Fornix	-0.46	0.06	0.03	0.91	0.41	0.09	-0.33	0.18	-0.26	0.30
Corticospinal Tract R	0.10	0.70	0.29	0.24	0.06	0.80	-0.13	0.61	-0.14	0.59
Corticospinal Tract L	-0.01	0.97	0.06	0.80	-0.06	0.80	-0.04	0.88	-0.23	0.36
Medial Lemniscus R	0.03	0.89	-0.09	0.72	0.27	0.27	-0.35	0.16	-0.09	0.73
Medial Lemniscus L	0.15	0.55	-0.28	0.26	0.03	0.90	0.11	0.66	0.25	0.32
Inferior Cerebellar Peduncle R	0.01	0.96	0.56	0.016*	-0.01	0.96	0.04	0.88	0.26	0.30
Inferior Cerebellar Peduncle L	0.19	0.44	-0.11	0.67	-0.40	0.10	0.36	0.14	0.11	0.66
Superior Cerebellar Peduncle R	-0.46	0.05	-0.24	0.35	-0.07	0.78	0.05	0.83	-0.10	0.70
Superior Cerebellar Peduncle L	-0.06	0.81	0.14	0.57	0.10	0.68	0.12	0.64	0.26	0.30
Cerebral Peduncle R	-0.03	0.91	0.05	0.86	-0.06	0.82	-0.15	0.55	-0.20	0.42
Cerebral Peduncle L	-0.13	0.61	-0.08	0.75	-0.13	0.61	-0.03	0.90	-0.21	0.39
Anterior Limb of Internal Capsule R	0.04	0.88	0.06	0.80	-0.13	0.60	0.08	0.75	0.04	0.86
Anterior Limb of Internal Capsule L	0.01	0.96	0.09	0.73	0.26	0.29	-0.12	0.64	0.06	0.81
Posterior Limb of Internal Capsule R	-0.06	0.80	-0.06	0.80	-0.26	0.29	0.18	0.47	-0.03	0.91
Posterior Limb of Internal Capsule L	-0.14	0.58	0.02	0.94	-0.08	0.75	0.06	0.82	0.02	0.93
Retrolenticular Internal Capsule R	-0.43	0.07	-0.08	0.75	0.30	0.23	-0.08	0.75	-0.15	0.56
Retrolenticular Internal Capsule L	-0.45	0.06	-0.02	0.93	0.23	0.37	-0.07	0.77	-0.19	0.44
Anterior Corona Radiata R	-0.19	0.45	0.0010	1.00	-0.17	0.49	0.09	0.71	0.02	0.95
Anterior Corona Radiata L	-0.19	0.45	-0.04	0.88	-0.04	0.89	0.02	0.93	0.003	0.99
Superior Corona Radiata R	-0.20	0.43	-0.02	0.92	-0.21	0.40	0.04	0.86	-0.01	0.98
Superior Corona Radiata L	-0.28	0.26	-0.03	0.90	-0.08	0.75	-0.10	0.68	-0.16	0.53
Posterior Corona Radiata R	-0.18	0.48	-0.20	0.42	-0.18	0.47	0.13	0.59	-0.08	0.75
Posterior Corona Radiata L	-0.13	0.61	-0.11	0.67	-0.16	0.51	0.03	0.91	-0.06	0.83
Posterior Thalamic Radiation R	-0.07	0.79	-0.03	0.92	0.02	0.92	0.08	0.75	0.14	0.57
Posterior Thalamic Radiation L	-0.18	0.48	-0.22	0.39	-0.12	0.65	0.23	0.37	0.02	0.93
Sagittal Stratum R	-0.20	0.43	-0.17	0.49	0.30	0.22	-0.25	0.32	-0.24	0.33
Sagittal Stratum L	-0.14	0.59	0.01	0.96	0.14	0.58	-0.12	0.64	-0.17	0.51
External Capsule R	0.14	0.57	0.21	0.41	-0.05	0.83	0.01	0.98	0.09	0.72
External Capsule L	-0.11	0.66	0.22	0.38	0.15	0.55	-0.23	0.35	-0.11	0.67
Cingulum (Cing.Gyrus) R	-0.15	0.55	0.24	0.34	0.05	0.84	-0.06	0.81	0.15	0.56
Cingulum (Cing.Gyrus) L	-0.07	0.79	0.43	0.08	-0.06	0.82	-0.18	0.48	0.21	0.40
Cingulum (Hippocampal) R	0.20	0.42	-0.21	0.40	-0.07	0.79	0.07	0.77	-0.13	0.60
Cingulum (Hippocampal) L	-0.34	0.17	0.07	0.79	0.54	0.02*	-0.44	0.07	-0.46	0.05
Fornix R	-0.28	0.25	-0.20	0.44	0.18	0.47	-0.25	0.31	-0.21	0.39
Fornix L	-0.19	0.46	0.09	0.71	0.24	0.34	-0.18	0.48	-0.01	0.96
Superior Longitudinal Fasciculus R	-0.01	0.98	0.11	0.67	-0.09	0.72	0.03	0.90	0.11	0.67
Superior Longitudinal Fasciculus L	-0.25	0.32	0.04	0.88	-0.22	0.38	0.02	0.93	-0.07	0.79
Superior Fronto Occipital Fasciculus R	0.07	0.79	-0.02	0.93	-0.12	0.62	0.16	0.53	0.11	0.67
Superior Fronto Occipital Fasciculus L	-0.20	0.41	0.01	0.96	0.17	0.50	-0.05	0.84	-0.02	0.94
Uncinate Fasciculus R	-0.05	0.83	0.33	0.18	0.04	0.89	-0.09	0.71	0.01	0.97
Uncinate Fasciculus L	-0.10	0.71	0.11	0.66	-0.06	0.80	0.09	0.71	0.13	0.61
Tapetum R	-0.15	0.55	0.05	0.84	0.18	0.48	-0.07	0.79	0.002	0.99
Tapetum L	0.003	0.99	-0.07	0.77	-0.15	0.56	0.35	0.15	0.22	0.37
Caudate	0.03	0.91	-0.09	0.72	-0.04	0.87	0.20	0.43	0.16	0.54
Cerebellum	-0.03	0.90	0.31	0.21	-0.25	0.33	0.22	0.37	0.23	0.35
Frontal Lobe	-0.07	0.79	0.01	0.97	0.12	0.65	-0.15	0.57	0.01	0.96

Insula	0.09	0.72	-0.09	0.73	0.12	0.63	-0.17	0.50	-0.02	0.93
Occipital Lobe	-0.16	0.53	-0.03	0.90	0.06	0.81	-0.13	0.59	0.05	0.83
Parietal Lobe	-0.10	0.69	-0.03	0.91	0.18	0.46	-0.26	0.30	-0.12	0.65
Putamen	0.13	0.61	0.13	0.61	-0.11	0.65	0.05	0.86	0.10	0.70
Temporal Lobe	0.05	0.85	-0.18	0.48	0.003	0.99	-0.11	0.66	-0.03	0.90
Thalamus	-0.13	0.61	0.06	0.82	0.05	0.85	-0.04	0.88	0.03	0.90

3.3 Region Based Results

Table 3.18 summarizes the data collected from MD and FA maps. Accordingly, the range of FA values was 0.2-0.57 for PD-MCI and PD-CI patients, while it varied between 0.2-0.6 for healthy controls. FA values were generally higher for HC group, lower for PD-CI and much lower for PD-MCI groups. Mean FA values differed in the range of orders of 0.001 to 0.01 between the groups. Mean and standard deviations did not significantly vary at frontal lobe (0.21 ± 0.01) and cerebellum (0.24 ± 0.02) between the groups.

On the other hand, MD values, which is represented in the order of 10^{-6}, ranged between 0.74-2.35 for PD-MCI group, 0.74 to 2.19 for PD-CI group, and 0.71-2.26 for HC group. On all regions, MD values were higher for PD-MCI group than HC group, and slightly higher than PD-CI group. Mean MD values differed in the range of orders of 0.001 to 0.01 between the groups. No regions showed exactly the same mean MD value and standard deviation for the groups of interest.

Table 3.19 shows the results of the Kruskal Wallis test where mean MD and FA values between all three groups were compared. For FA values, there was a statistically significant difference in between PD-MCI, PD-CI and HC groups at pontine crossing tract, body of corpus callosum, cerebral peduncle, right posterior thalamic radiation, right sagittal stratum, right fornix, bilateral tapteum and parietal lobe.

On the other hand, for MD values, number of regions that showed significant differences between the study groups, exceeded number of significantly differing regions of FA values. Similar to FA maps, pontine crossing tract, right posterior thalamic

radiation, right sagittal stratum, right tapetum and left cerebral peduncle showed statistically significant differences. Additionally, right cerebral peduncle, left posterior limb of internal capsule, left external capsule, left superior longitudinal fascicle, right superior corona radiata, insula, putamen and temporal lobe were observed to have statistically significantly different MD values.

Pairwise comparisons were made by Mann Whitney rank sum test with Bonferroni correction and Table 3.20 reports the regions showing difference trends ($p<.05$) and statistically significant differences ($p<.05/3$). For both FA and MD regions, most of the differences were found in between PD-MCI and HC groups. Mean FA values showed a significant reduction between PD-MCI and HC at body of corpus callosum ($p=0.005$), left cerebral peduncle ($p=0.002$), and right tapetum ($p=0.008$). Also, trends for differences of FA values between PD-MCI and HC were found at right posterior thalamic radiation ($p=0.02$), right sagittal stratum ($p=0.03$), right fornix ($p=0.03$), left tapetum ($p=0.04$) and parietal lobe ($p=0.02$). For PD-MCI and PD-CI comparison, no region showed statistically significant differences, but difference trends were observed at pontine crossing tract ($p=0.04$), right posterior thalamic radiation ($p=0.03$), right sagittal stratum ($p=0.017$), bilateral tapetum ($p=0.04$ for both sides), and parietal lobe ($p=0.02$). Another significant FA reduction was found at pontine crossing tract between PD-CI and HC groups ($p=0.002$). Additionally a difference trend was found between PD-CI and HC at left cerebral peduncle ($p=0.02$).

A significant increase of MD values was found between PD-MCI and HC groups at bilateral cerebral peduncle (right: $p=0.003$, left: $p=0.001$), left posterior limb of internal capsule ($p=0.014$), right posterior thalamic radiation ($p=0.007$), bilateral sagittal stratum (right: $p=0.005$, left: $p=0.007$), left external capsule ($p=0.003$), left superior longitudinal fasciculus ($p=0.007$), insula ($p=0.015$) and putamen ($p=0.03$). Moreover, difference trends between the same groups were found at pontine crossing tract ($p=0.02$), splenium of corpus callosum ($p=0.04$), right superior corona radiata, right tapetum and temporal lobe ($p=0.02$). Between PD-MCI and PD-CI groups, while a significant increase of MD was found at right sagittal stratum ($p=0.014$), a difference trend was found at right posterior thalamic radiation ($p=0.04$) and putamen ($p=0.048$).

The least number of different regions were noted in between PD-CI and HC groups. Only left superior longitudinal fasciculus (p=0.007) and bilateral cerebral peduncle (right: p=0.003, left: p=0.004) showed significant MD value differences and pontine crossing tract had a difference trend (p=0.03).

3.4 TBSS Results

As reported in section 2.4, TBSS analysis was carried out on FA and MD maps, permutation tests were applied for pairwise comparisons by using FSL's randomise tool. A sample image of filled version of t stats map of FA image is presented in Figure 3.1.

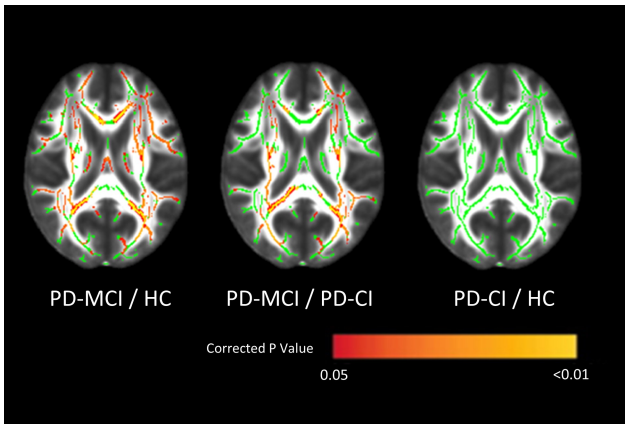

Figure 3.1: t statistics maps of pairwise comparisons after TBSS and permutation tests.

Table 3.21 summarizes the regions where statistically significant (p<.05) FA differences were found. Accordingly, it can be said that on each region assessed, statistically significant differences were observed between PD-MCI and HC groups, but no differences were found between PD-CI/HC groups. On the other hand, FA differences were observed between PD-MCI/PD-CI groups at corpus callosum, cerebral peduncle, internal capsule, external capsule, bilateral corona radiata, posterior thalamic radiation, sagittal stratum, cingulum, fornix and tapetum.

Table 3.18: Regional mean and standard deviations of mean FA and MD values for the study groups.

Region	FA			MD (10^-6)		
	MCI	CI	HC	MCI	CI	HC
	Mean±Std	Mean±Std	Mean±Std	Mean±Std	Mean±Std	Mean±Std
Middle Cerebellar Peduncle	0.42±0.04	0.42±0.04	0.45±0.05	1.1±0.19	1.1±0.18	1.04±0.19
Pontine Crossing Tract	0.43±0.04	0.41±0.04	0.44±0.03	0.74±0.05	0.74±0.05	0.71±0.03
Genu of Corpus Callosum	0.46±0.09	0.49±0.08	0.49±0.08	1.42±0.48	1.35±0.42	1.36±0.31
Body of Corpus Callosum	0.46±0.08	0.47±0.11	0.51±0.03	1.29±0.44	1.26±0.53	1.07±0.21
Splenium of Corpus Callosum	0.53±0.08	0.56±0.07	0.57±0.05	1.18±0.28	1.05±0.27	1.03±0.18
Fornix	0.28±0.09	0.31±0.08	0.31±0.07	2.33±0.37	2.19±0.32	2.26±0.29
Corticospinal Tract R	0.46±0.07	0.47±0.06	0.48±0.06	1.03±0.26	0.97±0.17	0.95±0.19
Corticospinal Tract L	0.43±0.08	0.44±0.06	0.47±0.06	1.13±0.31	1.02±0.17	1.03±0.22
Medial Lemniscus R	0.47±0.06	0.47±0.05	0.5±0.05	0.75±0.05	0.74±0.05	0.73±0.03
Medial Lemniscus L	0.46±0.06	0.47±0.06	0.49±0.05	0.76±0.05	0.76±0.05	0.75±0.03
Inferior Cerebellar Peduncle R	0.41±0.05	0.41±0.06	0.41±0.06	0.91±0.19	0.89±0.12	0.87±0.09
Inferior Cerebellar Peduncle L	0.39±0.06	0.39±0.06	0.41±0.05	1.02±0.22	0.99±0.16	0.94±0.12
Superior Cerebellar Peduncle R	0.52±0.07	0.53±0.06	0.54±0.07	1.27±0.2	1.29±0.23	1.25±0.23
Superior Cerebellar Peduncle L	0.54±0.07	0.53±0.05	0.57±0.07	1.19±0.21	1.23±0.23	1.15±0.19
Cerebral Peduncle R	0.57±0.06	0.57±0.05	0.6±0.04	0.96±0.14	0.92±0.1	0.82±0.08
Cerebral Peduncle L	0.55±0.05	0.55±0.04	0.59±0.04	0.96±0.11	0.93±0.08	0.85±0.08
Anterior Limb of Internal Capsule R	0.46±0.1	0.47±0.09	0.49±0.06	0.82±0.16	0.78±0.18	0.75±0.08
Anterior Limb of Internal Capsule L	0.42±0.1	0.43±0.09	0.44±0.06	0.85±0.15	0.83±0.2	0.79±0.13
Posterior Limb of Internal Capsule R	0.56±0.06	0.57±0.06	0.58±0.05	0.76±0.05	0.76±0.08	0.73±0.03
Posterior Limb of Internal Capsule L	0.55±0.05	0.56±0.05	0.57±0.05	0.79±0.05	0.78±0.08	0.75±0.04
Retrolenticular Internal Capsule R	0.5±0.06	0.51±0.04	0.52±0.04	1.01±0.21	0.97±0.19	0.92±0.14
Retrolenticular Internal Capsule L	0.49±0.05	0.5±0.05	0.51±0.04	0.97±0.2	0.94±0.17	0.9±0.1
Anterior Corona Radiata R	0.38±0.04	0.38±0.03	0.39±0.04	0.88±0.1	0.84±0.1	0.83±0.08
Anterior Corona Radiata L	0.36±0.04	0.37±0.03	0.37±0.04	0.9±0.1	0.87±0.14	0.85±0.09
Superior Corona Radiata R	0.42±0.04	0.43±0.03	0.43±0.03	0.84±0.12	0.82±0.14	0.77±0.06
Superior Corona Radiata L	0.41±0.04	0.42±0.03	0.42±0.03	0.85±0.1	0.85±0.17	0.79±0.07
Posterior Corona Radiata R	0.42±0.04	0.41±0.04	0.41±0.04	1.02±0.23	1±0.28	0.91±0.12
Posterior Corona Radiata L	0.4±0.04	0.39±0.03	0.39±0.04	1.03±0.25	1.04±0.36	0.93±0.12
Posterior Thalamic Radiation R	0.43±0.06	0.46±0.04	0.47±0.05	1.25±0.32	1.08±0.23	1.05±0.22
Posterior Thalamic Radiation L	0.42±0.07	0.44±0.06	0.46±0.04	1.33±0.38	1.18±0.35	1.16±0.24
Sagittal Stratum R	0.4±0.06	0.44±0.05	0.44±0.06	1.19±0.25	1.04±0.17	1.01±0.13
Sagittal Stratum L	0.39±0.06	0.41±0.07	0.43±0.06	1.23±0.24	1.12±0.26	1.03±0.13
External Capsule R	0.4±0.04	0.41±0.04	0.41±0.03	0.8±0.07	0.78±0.04	0.77±0.04
External Capsule L	0.37±0.03	0.38±0.04	0.38±0.02	0.85±0.06	0.82±0.05	0.8±0.04
Cingulum (Cingulate Gyrus) R	0.37±0.09	0.38±0.09	0.37±0.05	0.83±0.05	0.82±0.06	0.8±0.05
Cingulum (Cingulate Gyrus) L	0.39±0.1	0.41±0.09	0.36±0.06	0.84±0.08	0.83±0.1	0.8±0.04
Cingulum (Hippocampus) R	0.32±0.05	0.34±0.05	0.32±0.05	1.07±0.18	1.05±0.22	1.05±0.15
Cingulum (Hippocampus) L	0.3±0.05	0.3±0.06	0.31±0.04	1.11±0.23	1.1±0.25	1.11±0.22
Fornix R	0.36±0.07	0.38±0.05	0.41±0.07	1.23±0.22	1.15±0.22	1.1±0.23
Fornix L	0.38±0.06	0.4±0.05	0.42±0.06	1.14±0.21	1.06±0.21	1.03±0.18
Superior Longitudinal Fasciculus R	0.41±0.03	0.42±0.03	0.42±0.03	0.78±0.05	0.76±0.03	0.75±0.04
Superior Longitudinal Fasciculus L	0.4±0.03	0.4±0.03	0.4±0.03	0.79±0.05	0.78±0.03	0.76±0.04
Superior Fronto Occipital Fasciculus R	0.33±0.1	0.34±0.08	0.35±0.06	1.03±0.39	0.97±0.44	0.92±0.23
Superior Fronto Occipital Fasciculus L	0.35±0.08	0.35±0.08	0.34±0.06	1.03±0.37	0.96±0.45	0.92±0.25
Uncinate Fasciculus R	0.48±0.07	0.48±0.08	0.49±0.06	0.77±0.07	0.74±0.08	0.75±0.04
Uncinate Fasciculus L	0.44±0.08	0.44±0.08	0.48±0.06	0.84±0.1	0.82±0.06	0.8±0.05
Tapetum R	0.27±0.15	0.35±0.15	0.4±0.15	2.33±0.63	2.07±0.53	1.82±0.64
Tapetum L	0.26±0.14	0.33±0.15	0.34±0.14	2.35±0.66	2.03±0.64	2.09±0.65
Caudate	0.26±0.05	0.26±0.05	0.26±0.04	1.66±0.34	1.57±0.34	1.61±0.27
Cerebellum	0.24±0.02	0.24±0.02	0.24±0.02	1.05±0.1	1.03±0.08	1.03±0.08
Frontal Lobe	0.21±0.01	0.21±0.01	0.21±0.01	1.22±0.13	1.15±0.13	1.15±0.11
Insula	0.22±0.02	0.23±0.02	0.23±0.02	1.22±0.15	1.15±0.12	1.12±0.13
Occipital Lobe	0.2±0.01	0.21±0.01	0.2±0.01	0.98±0.08	0.95±0.07	0.96±0.07
Parietal Lobe	0.21±0.01	0.22±0.01	0.22±0.01	1.19±0.12	1.13±0.09	1.14±0.12
Putamen	0.36±0.03	0.36±0.03	0.37±0.02	0.8±0.05	0.78±0.04	0.76±0.04
Temporal Lobe	0.21±0.01	0.21±0.01	0.21±0.01	1.19±0.1	1.13±0.09	1.13±0.08
Thalamus	0.33±0.03	0.33±0.04	0.33±0.03	1.19±0.1	1.13±0.09	1.13±0.08

Table 3.19: Kruskal Wallis test results.

Region	FA			p value
	PD-MCI	PD-CI	HC	
	Mean Std	Mean Std	Mean Std	
Pontine Crossing Tract	0.43±0.04	0.41±0.04	0.44±0.03	0.006
Corpus Callosum (Body)	0.46±0.08	0.47±0.11	0.51±0.03	0.03
Cerebral Peduncle L	0.55±0.05	0.55±0.04	0.59±0.04	0.006
Posterior Thalamic Radiation R	0.43±0.06	0.46±0.04	0.47±0.05	0.02
Sagittal Stratum R	0.4±0.06	0.44±0.05	0.44±0.06	0.03
Fornix R	0.36±0.07	0.38±0.05	0.41±0.07	0.05
Tapetum R	0.27±0.15	0.35±0.15	0.4±0.15	0.014
Tapetum L	0.26±0.14	0.33±0.15	0.34±0.14	0.047
Parietal Lobe	0.21±0.01	0.22±0.01	0.22±0.01	0.02
Region	MD			p value
	PD-MCI	PD-CI	HC	
	Mean Std(10^-3)	Mean Std(10^-3)	Mean Std(10^-3)	
Pontine Crossing Tract	0.74±0.05	0.74±0.05	0.71±0.03	0.05
Corpus Callosum (Splenium)	1.18±0.28	1.05±0.27	1.03±0.18	0.05
Cerebral Peduncle R	0.96±0.14	0.92±0.1	0.82±0.08	0.004
Cerebral Peduncle L	0.96±0.11	0.93±0.08	0.85±0.08	0.002
Posterior Limb of Internal Capsule L	0.79±0.05	0.78±0.08	0.75±0.04	0.045
Superior Corona Radiata R	0.84±0.12	0.82±0.14	0.77±0.06	0.04
Posterior Thalamic Radiation R	1.25±0.32	1.08±0.23	1.05±0.22	0.013
Sagittal Stratum R	1.19±0.25	1.04±0.17	1.01±0.13	0.005
Sagittal Stratum L	1.23±0.24	1.12±0.26	1.03±0.13	0.018
External Capsule L	0.85±0.06	0.82±0.05	0.8±0.04	0.01
Superior Longitudinal Fasciculus L	0.79±0.05	0.78±0.03	0.76±0.04	0.01
Tapetum R	2.33±0.63	2.07±0.53	1.82±0.64	0.04
Insula	1.22±0.15	1.15±0.12	1.12±0.13	0.02
Putamen	0.8±0.05	0.78±0.04	0.76±0.04	0.005
Temporal Lobe	1.19±0.1	1.13±0.09	1.13±0.08	0.04

Table 3.20: Mann Whitney rank sum test results.

Region	Group	FA Mean ± Std	p Value
Pontine Crossing Tract	PD-MCI/ PD-CI	0.43±0.04 / 0.41±0.04	p=0.04*
	PD-CI / HC	0.41±0.04 / 0.44±0.03	p=0.002**
Corpus Callosum (Body)	PD-MCI/ HC	0.46±0.08 / 0.51±0.03	p=0.005**
Cerebral Peduncle L	PD-MCI/ HC	0.55±0.05 / 0.59±0.04	p=0.002**
	PD-CI/ HC	0.55±0.04 / 0.59±0.04	p=0.02*
Posterior Thalamic Radiation R	PD-MCI/ HC	0.43±0.06 / 0.47±0.05	p=0.02*
	PD-MCI/PD-CI	0.43±0.06 / 0.46±0.04	p=0.03*
Saggital Stratum R	PD-MCI/ HC	0.4±0.06 / 0.44±0.06	p=0.03*
	PD-MCI/PD-CI	0.4±0.06 / 0.44±0.05	p=0.02*
Tapetum R	PD-MCI/ PD-CI	0.27±0.15 / 0.35±0.15	p=0.04*
	PD-MCI/HC	0.27±0.15 / 0.4±0.15	p=0.008**
Tapetum L	PD-MCI/ PD-CI	0.26±0.14 / 0.33±0.15	p=0.04*
	PD-MCI/HC	0.26±0.14 / 0.34±0.14	p=0.04*
Fornix R	PD-MCI/ HC	0.36±0.07 / 0.41±0.07	p=0.03*
Parietal Lobe	PD-MCI/ PD-CI	0.21±0.01 / 0.22±0.01	p=0.02*
	PD-MCI/ HC	0.21±0.01 / 0.22±0.01	p=0.02*
Region	**Group**	**MD Mean ± Std**	**p Value**
Pontine Crossing Tract	PD-MCI/ HC	0.74±0.05 / 0.71±0.03	p=0.02*
	PD-CI/ HC	0.74±0.05 / 0.71±0.03	p=0.03*
Corpus Callosum (Splenium)	PD-MCI/ HC	1.27±0.35 / 1.08±0.23	p=0.04*
Posterior Thalamic Radiation R	PD-MCI/ HC	1.13±0.28 / 0.96±0.21	p=0.01**
	PD-MCI/PD-CI	1.13±0.28 / 0.98±0.19	p=0.04*
Posterior Limb of Internal Capsule L	PD-MCI/ HC	0.77±0.06 / 0.73±0.04	p=0.014**
Saggital Stratum R	PD-MCI/ HC	1.13±0.26 / 0.94±0.11	p=0.01**
	PD-MCI/PD-CI	1.13±0.26 / 0.98±0.14	p=0.014**
Saggital Stratum L	PD-MCI/ HC	1.15±0.22 / 0.98±0.11	p=0.01**
Cerebral Peduncle R	PD-MCI/ HC	1.08±0.23 / 0.88±0.14	p=0.003**
	PD-CI /HC	1.02±0.17 / 0.88±0.14	p=0.003**
Cerebral Peduncle L	PD-MCI/ HC	1.08±0.2 / 0.89±0.12	p=0.001**
	PD-CI /HC	1.03±0.16 / 0.89±0.12	p=0.004**
Tapetum R	PD-MCI/ HC	2.14±0.71 / 1.6±0.69	p=0.02*
Superior Longitidunal Fasciculus L	PD-CI / HC	0.78±0.04 / 0.75±0.04	p=0.01**
	PD-MCI/ HC	0.79±0.04 / 0.75±0.04	p=0.01**
Superior Corona Radiata R	PD-MCI/ HC	0.81±0.09 / 0.76±0.05	p=0.02*
External Capsule L	PD-MCI/ HC	0.86±0.06 / 0.75±0.04	p=0.003**
Temporal Lobe	PD-MCI/ HC	1.1±0.1 / 1.03±0.09	p=0.02*
Insula	PD-MCI/ HC	1.28±0.16 / 1.16±0.14	p=0.015**
Putamen	PD-MCI/ HC	0.82±0.05 / 0.78±0.04	p=0.003**
	PD-MCI/ PD-CI	0.82±0.05 / 0.8±0.04	p=0.02*
*trend, **p<0.05/3			

Table 3.21: TBSS results of FA maps (+:Difference exists,−:Difference does not exist.)

	Region	PD-MCI HC	PD-MCI PD-CI	PD-CI HC
1	Middle Cerebellar Peduncle	+	-	-
2	Pontine Crossing Tract	+	-	-
3	Genu & Body of Corpus Callosum	+	+	-
4	Splenium of Corpus Callosum	+	+	-
5	Fornix	+	-	-
6	Corticospinal Tract R / L	+	-	-
7	Medial Lemniscus R / L	+	-	-
8	Inferior Cerebellar Peduncle R / L	+	-	-
9	Superior Cerebellar Peduncle R / L	+	-	-
10	Cerebral Peduncle R	+	-	-
11	Cerebral Peduncle L	+	+	-
12	Anterior Limb of Internal Capsule R / L	+	+	-
13	Posterior Limb of Internal Capsule R / L	+	+	-
14	Retrolenticular Internal Capsule R / L	+	+	-
15	(A,S,P) Corona Radiata R / L	+	+	-
16	Posterior Thalamic Radiation R / L	+	+	-
17	Sagittal Stratum R / L	+	+	-
18	External Capsule R / L	+	+	-
19	Cingulum (Cingulate Gyrus) R / L	+	+	-
20	Cingulum (Hippocampus) R	+	+	-
21	Cingulum (Hippocampus) L	+	-	-
22	Fornix R	+	-	-
23	Fornix L	+	+	-
24	Superior Longitudinal Fasciculus R / L	+	-	-
25	Superior Fronto-occipital Fasciculus R / L	+	-	-
26	Uncinate Fasciculus R / L	+	-	-
27	Tapetum R	+	-	-
28	Tapetum L	+	+	-

4. DISCUSSION

This study focused on the analysis of DW-MRI parameters in PD-MCI, PD-CI and HC groups with an overarching goal of defining DW-MRI based biomarkers of PD-MCI. Our results indicated that ACE-R test scores decrease as cognitive ability worsens. Similar results were found in Berankova et al.s' study, where PD-HC, PD-CI and PDD patients' test scores were compared and ACE-R test was reported as a successful tool of discriminating PD subtypes [66]. A significant reduction of SDMT scores between PD-MCI and PD-CI groups might be a sign of remarkable motor function loss as the disease progresses.

We have defined several correlations between regional mean FA or MD values and neuropsychological test scores. We should also add that association of cognitive deficits and neuroanatomical pathology remained unexplored [67]. Still, at this point we should consider the study of Zheng et al., where correlations of DTI and cognitive profiles were examined in a very similar pipeline to our study [68]. In this study, 16 PD patients' regional mean FA and MD values were calculated via FSL's tools and these values were linearly regressed to neuropsychological test scores. The study found positive correlations between all mean FA values and all cognitive domains, where negative correlations were found for mean MD values. In our study, when all groups including HC's, we also found positive correlations for FA values except GDS and STROOP tests, and for MD values all correlations were negative. Zheng et al. reported that executive function was directly correlated with FA and inversely correlated with MD at anterior corona radiata, left anterior limb of internal capsule and genu of corpus callosum. In our study, executive function was measured by STROOP test and a positive correlation with FA at posterior corona radiata and a negative correlation with MD at posterior limb of internal capsule was observed for PD-MCI group. Additionally, a negative correlation of STROOP test with MD was observed at splenium of corpus callosum for PD-CI group. In the same study, it was mentioned that non-verbal memory deficits were related to MD alterations in the fornix and

anterior corona radiata [68]. In our study, attention was measured by ACE-R, SDMT and STROOP tests, and a negative correlation between ACE-R scores and FA at both regions and a positive correlation with MD at fornix were found for the PD-MCI group. It was also reported that the strongest correlations between attention and brain regions were found at cingulate gyrus [68]. In our study, PD-MCI groups' ACE-R scores (when the test was used to measure attention) showed a positive correlation with MD values at left cingulate gyrus.

When regionwise mean FA and MD values were assessed, it was seen that as cognitive ability worsens mean FA values decreased and mean MD values increased. Many previous studies that compared two or more of the PDD, PD-MCI, PD-CI and HC groups also reported a decrease of FA values in PDD and PD-MCI groups compared to HC's at major WM tracts [61,69,70] with a simultaneous increase of MD values [69]. As disease progresses, white matter integrity decreases, causing a greater amount of cognitive dysfunction [61, 69, 71, 72].

As cognitive profile worsens, FA values decreased at prefrontal WM, genu of corpus callosum, superior and inferior longitudinal fasciculus, fronto occipital fasciculus, and uncinate fasciculus [61, 69, 70]. On a study carried out by Zhan et al., 51 PD-MCI and 66 PD-CI patients' DTI images were compared and a significant FA reduction was reported at fornix of PD-MCI patients [73]. Likewise, Deng et al. found reductions of FA at cinguate bundles, left/front and right temporal lobe [74] and Agosta et al. found reductions of FA at longitudinal fascicle [75]. Rae et al. found lower FA and higher MD at thalamic region [64]. Our results on the other hand, indicated lower FA at body of corpus callosum and right fornix. We noted higher MD values at the corpus callosum, left superior longitudinal fasciculus and temporal lobe.

Some of the previous studies found no differences of FA values between PD-CI and HC groups [61, 69]. Other studies reported FA reductions at substantia nigra [72, 76], lower part of putamen [72], left anterior cingulate gyrus [77], right superior longitudinal fasciculus and corpus callosum [77,78], and thalamus [78]. No MD changes were reported between these two groups at putamen, caudate and thalamus [78].

While most of the PD-MCI research focused on FA values, a study by Thillainadesan et al. presented MD changes similar to our results. In that study, 158 PD-MCI and 238 PD-CI subjects were compared, and PD-MCI patients were found to have higher MD at internal capsule, putamen and cingulate gyrus (cingulum) [79], but no differences were found for FA values.

Our results acquired from TBSS analyis correlates better with the previous studies. A study of Agosta et al. found that there was no differences between PD-CI and HC's [75], which was in agreement with our results. Moreover, differences were noted at corpus callosum and bilateral corona radiata, which was similar to our results. Anterior cingulate bundle was found to be different in a study of Deng et al.'s [74], which was also indicated in our analysis.

Our study had some limitations that could be tackled in the future. First of all, registration methods could be reviewed, where non-linear registration methods might provide better alignment and more successful overlay of the same structures. We should also note that brain WM changes due to the disease process made it harder to delineate the brain structures for some patients. At this point, increasing the number of patients could provide more accurate results.

This study made a great contribution on my engineering and research skills. In order to analyze the data set, I learned shell script coding, which was completely a new environment for me. From now on, I believe that I will be more comfortable in learning new coding languages. Apart from this, I had a chance to learn diffusion weighted magnetic resonance imaging principles on a larger extend and especially, broaden my point of view on Parkinson's disease and similar neurodegenerative diseases that might be a guide for me to do further studies in the future.

5. CONCLUSION

The aim of this study was to investigate the structural changes of the brain in PD-MCI by using DW-MRI. Our results indicated that FA and MD maps, derived from DW-MRI, could be used for defining biomarkers of PD-MCI. Future studies will include TBSS analysis of MD maps and detection of temporal changes of FA and MD in PD-MCI patients for defining possible patterns of evolution into PDD.

6. APPENDIX A. Software Packages

- FSL(http://fsl.fmrib.ox.ac.uk/fsl/fslwiki/)
- MATLAB (http://www.mathworks.com/downloads/)

7. APPENDIX B. FSL Scripts

All scripts are provided within the CD attached to the backpage.

8. ACKNOWLEDGMENTS

This study was supported by TUBITAK project #115S219 and the Ministry of Development project #2010K120330.

REFERENCES

1. Le Bihan, D., J. F. Mangin, C. Poupon, C. A. Clark, S. Pappata, N. Molko, and H. Chabriat, "Diffusion tensor imaging: concepts and applications," *J Magn Reson Imaging*, Vol. 13, no. 4, pp. 534–46, 2001.

2. Currie, S., N. Hoggard, I. J. Craven, M. Hadjivassiliou, and I. D. Wilkinson, "Understanding mri: basic mr physics for physicians," *Postgrad Med J*, Vol. 89, no. 1050, pp. 209–23, 2013.

3. Jacobs, M. A., T. S. Ibrahim, and R. Ouwerkerk, "Aapm/rsna physics tutorials for residents: Mr imaging: brief overview and emerging applications," *Radiographics*, Vol. 27, no. 4, pp. 1213–29, 2007.

4. Trip, S. A., and D. H. Miller, "Imaging in multiple sclerosis," *Journal of Neurology, Neurosurgery & Psychiatry*, Vol. 76, no. suppl 3, pp. iii11–iii18, 2005.

5. Roberts, T. P., and E. S. Schwartz, "Principles and implementation of diffusion-weighted and diffusion tensor imaging," *Pediatr Radiol*, Vol. 37, no. 8, pp. 739–48, 2007.

6. Robertson, R. L., and C. M. Glasier, "Diffusion-weighted imaging of the brain in infants and children," *Pediatr Radiol*, Vol. 37, no. 8, pp. 749–68, 2007.

7. Assaf, Y., and O. Pasternak, "Diffusion tensor imaging (dti)-based white matter mapping in brain research: a review," *J Mol Neurosci*, Vol. 34, no. 1, pp. 51–61, 2008.

8. Alexander, A. L., J. E. Lee, M. Lazar, and A. S. Field, "Diffusion tensor imaging of the brain," *Neurotherapeutics*, Vol. 4, no. 3, pp. 316–29, 2007.

9. Zhang, L., "Structural and functional magnetic resonance imaging in hepatic encephalopathy," 05 2014.

10. Mori, S., and J. Zhang, "Principles of diffusion tensor imaging and its applications to basic neuroscience research," *Neuron*, Vol. 51, no. 5, pp. 527–39, 2006.

11. Stejskal, E. O., and J. E. Tanner, "Spin diffusion measurements: spin echoes in the presence of a time-dependent field gradient," *The journal of chemical physics*, Vol. 42, no. 1, pp. 288–292, 1965.

12. Pierpaoli, C., and P. J. Basser, "Toward a quantitative assessment of diffusion anisotropy," *Magnetic Resonance in Medicine*, Vol. 36, no. 6, pp. 893–906, 1996.

13. Papadakis, N. G., D. Xing, G. C. Houston, J. M. Smith, M. I. Smith, M. F. James, A. A. Parsons, C. L. Huang, L. D. Hall, and T. A. Carpenter, "A study of rotationally invariant and symmetric indices of diffusion anisotropy," *Magn Reson Imaging*, Vol. 17, no. 6, pp. 881–92, 1999.

14. Ulug, A. M., and P. C. van Zijl, "Orientation-independent diffusion imaging without tensor diagonalization: Anisotropy definitions based on physical attributes of the diffusion ellipsoid," *Journal of Magnetic Resonance Imaging*, Vol. 9, no. 6, pp. 804–813, 1999.

15. Westin, C. F., S. E. Maier, H. Mamata, A. Nabavi, F. A. Jolesz, and R. Kikinis, "Processing and visualization for diffusion tensor mri," *Med Image Anal*, Vol. 6, no. 2, pp. 93–108, 2002.

16. Goldberg-Zimring, D., A. U. Mewes, M. Maddah, and S. K. Warfield, "Diffusion tensor magnetic resonance imaging in multiple sclerosis," *J Neuroimaging*, Vol. 15, no. 4 Suppl, pp. 68S–81S, 2005.

17. Sbardella, E., F. Tona, N. Petsas, and P. Pantano, "Dti measurements in multiple sclerosis: Evaluation of brain damage and clinical implications," *Mult Scler Int*, Vol. 2013, p. 671730, 2013.

18. Fujiyoshi, K., K. Hikishima, J. Nakahara, O. Tsuji, J. Hata, T. Konomi, T. Nagai, S. Shibata, S. Kaneko, A. Iwanami, S. Momoshima, S. Takahashi, M. Jinzaki, N. Suzuki, Y. Toyama, M. Nakamura, and H. Okano, "Application of q-space diffusion mri for the visualization of white matter," *J Neurosci*, Vol. 36, no. 9, pp. 2796–808, 2016.

19. Meireles, J., and J. Massano, "Cognitive impairment and dementia in parkinson's disease: clinical features, diagnosis, and management," *Front Neurol*, Vol. 3, p. 88, 2012.

20. DeMaagd, G., and A. Philip, "Parkinson's disease and its management:part 1:disease entity, risk factors, pathophysiology, clinical presentation, and diagnosis," *Pharmacy and Therapeutics*, Vol. 40, no. 8, p. 504, 2015.

21. Schrag, A., L. Horsfall, K. Walters, A. Noyce, and I. Petersen, "Prediagnostic presentations of parkinson's disease in primary care: a case-control study," *The Lancet Neurology*, Vol. 14, no. 1, pp. 57–64, 2015.

22. Braak, H., and E. Braak, "Pathoanatomy of parkinson's disease," *Journal of Neurology*, Vol. 247, pp. II3–II10, Apr 2000.

23. Kovari, E., J. Horvath, and C. Bouras, "Neuropathology of lewy body disorders," *Brain Research Bulletin*, Vol. 80, no. 4, pp. 203 – 210, 2009. Neurodegenerative diseases and mechanisms of cell death.

24. Braak, H., K. D. Tredici, U. Rub, R. A. de Vos, E. N. J. Steur, and E. Braak, "Staging of brain pathology related to sporadic parkinson's disease," *Neurobiology of Aging*, Vol. 24, no. 2, pp. 197 – 211, 2003.

25. Chaudhuri, K. R., and A. H. Schapira, "Non-motor symptoms of parkinson's disease: dopaminergic pathophysiology and treatment," *Lancet Neurol*, Vol. 8, no. 5, pp. 464–74, 2009.

26. Massano, J., and K. P. Bhatia, "Clinical approach to parkinson's disease: features, diagnosis, and principles of management," *Cold Spring Harb Perspect Med*, Vol. 2, no. 6, p. a008870, 2012.

27. Tolosa, E., C. Gaig, J. Santamaria, and Y. Compta, "Diagnosis and the premotor phase of parkinson disease," *Neurology*, Vol. 72, no. 7 Suppl, pp. S12–20, 2009.

28. Lim, S., S. H. Fox, and A. E. Lang, "Overview of the extranigral aspects of parkinson disease," *Archives of Neurology*, Vol. 66, no. 2, pp. 167–172, 2009.

29. Aarsland, D., K. Andersen, J. P. Larsen, A. Lolk, H. Nielsen, and P. Kragh-Sorensen, "Risk of dementia in parkinson's disease - a community-based, prospective study," *Neurology*, Vol. 56, no. 6, pp. 730–736, 2001.

30. Goetz, C. G., and G. T. Stebbins, "Risk factors for nursing home placement in advanced parkinson's disease," *Neurology*, Vol. 43, no. 11, pp. 2227–9, 1993.

31. Pai, M. C., and S. H. Chan, "Education and cognitive decline in parkinson's disease: a study of 102 patients," *Acta Neurol Scand*, Vol. 103, no. 4, pp. 243–7, 2001.

32. Caviness, J. N., E. Driver-Dunckley, D. J. Connor, M. N. Sabbagh, J. G. Hentz, B. Noble, V. G. H. Evidente, H. A. Shill, and C. H. Adler, "Defining mild cognitive impairment in parkinson's disease," *Movement Disorders*, Vol. 22, no. 9, pp. 1272–1277, 2007.

33. Petersen, R. C., R. Doody, A. Kurz, R. C. Mohs, J. C. Morris, P. V. Rabins, K. Ritchie, M. Rossor, L. Thal, and B. Winblad, "Current concepts in mild cognitive impairment," *Arch Neurol*, Vol. 58, no. 12, pp. 1985–92, 2001.

34. Litvan, I., J. G. Goldman, A. I. Troster, B. A. Schmand, D. Weintraub, R. C. Petersen, B. Mollenhauer, C. H. Adler, K. Marder, C. H. Williams-Gray, D. Aarsland, J. Kulisevsky, M. C. Rodriguez-Oroz, D. J. Burn, R. A. Barker, and M. Emre, "Diagnostic criteria for mild cognitive impairment in parkinson's disease: Movement disorder society task force guidelines," *Mov Disord*, Vol. 27, no. 3, pp. 349–56, 2012.

35. Yang, Y., B.-s. Tang, and J.-f. Guo, "Parkinson's disease and cognitive impairment," *Parkinson's Disease*, Vol. 2016, 2016.

36. Hobson, P., J. Gallacher, and J. Meara, "Cross-sectional survey of parkinson's disease and parkinsonism in a rural area of the united kingdom," *Movement disorders*, Vol. 20, no. 8, pp. 995–998, 2005.

37. Hershey, L. A., and G. M. Peavy, "Cognitive decline in parkinson disease how steep and crowded is the slope?," 2015.

38. Broeders, M., D. C. Velseboer, R. de Bie, J. D. Speelman, D. Muslimovic, B. Post, R. de Haan, and B. Schmand, "Cognitive change in newly-diagnosed patients with parkinson's disease: a 5-year follow-up study," *Journal of the International Neuropsychological Society*, Vol. 19, no. 6, pp. 695–708, 2013.

39. Pedersen, K. F., J. P. Larsen, O.-B. Tysnes, and G. Alves, "Prognosis of mild cognitive impairment in early parkinson disease: the norwegian parkwest study," *JAMA neurology*, Vol. 70, no. 5, pp. 580–586, 2013.

40. Berg, D., "Is pre-motor diagnosis possible? the european experience," *Parkinsonism & Related Disorders*, Vol. 18, pp. S195 – S198, 2012. Proceedings of WFN XIX World Congress on Parkinson's Disease and Related Disorders.

41. Postuma, R. B., D. Aarsland, P. Barone, D. J. Burn, C. H. Hawkes, W. Oertel, and T. Ziemssen, "Identifying prodromal parkinson's disease: Pre-motor disorders in parkinson's disease," *Movement Disorders*, Vol. 27, no. 5, pp. 617–626, 2012.

42. Litvan, I., D. Aarsland, C. H. Adler, J. G. Goldman, J. Kulisevsky, B. Mollenhauer, M. C. Rodriguez-Oroz, A. I. Troster, and D. Weintraub, "Mds task force on mild cognitive impairment in parkinson's disease: critical review of pd-mci," *Mov Disord*, Vol. 26, no. 10, pp. 1814–24, 2011.

43. Symms, M., H. R. Jager, K. Schmierer, and T. A. Yousry, "A review of structural magnetic resonance neuroimaging," *J Neurol Neurosurg Psychiatry*, Vol. 75, no. 9, pp. 1235–44, 2004.

44. Martinez-Martin, P., A. Gil-Nagel, L. M. Gracia, J. B. Gomez, J. Martinez-Sarries, and F. Bermejo, "Unified parkinson's disease rating scale characteristics and structure," *Movement Disorders*, Vol. 9, no. 1, pp. 76–83, 1994.

45. Tsoi, K. K. F., J. Y. C. Chan, H. W. Hirai, S. Y. S. Wong, and T. C. Y. Kwok, "Cognitive tests to detect dementia: a systematic review and meta-analysis.(report)," Vol. 175, September 2015.

46. Mioshi, E., K. Dawson, J. Mitchell, R. Arnold, and J. R. Hodges, "The addenbrooke's cognitive examination revised (ace-r): a brief cognitive test battery for dementia screening," *International journal of geriatric psychiatry*, Vol. 21, no. 11, pp. 1078–1085, 2006.

47. Cummings, J. L., "Depression and parkinson's disease: a review," *The American journal of psychiatry*, Vol. 149, no. 4, p. 443, 1992.

48. Weintraub, D., K. Saboe, and M. B. Stern, "Effect of age on geriatric depression scale performance in parkinson's disease," *Movement Disorders*, Vol. 22, no. 9, pp. 1331–1335, 2007.

49. Golden, C. J., "A group version of the stroop color and word test.," *Journal of Personality Assessment*, Vol. 39, no. 4, p. 386, 1975.

50. Montse, A., V. Pere, J. Carme, V. Francesc, and T. Eduardo, "Visuospatial deficits in parkinson's disease assessed by judgment of line orientation test: Error analyses and practice effects.," *Journal of Clinical and Experimental Neuropsychology*, Vol. 23, no. 5, p. 592, 2001.

51. AL, B., V. NR, and H. KS, "Visuospatial judgment: A clinical test," *Archives of Neurology*, Vol. 35, no. 6, pp. 364–367, 1978.

52. Lezak, M. D., *Neuropsychological assessment*, Oxford University Press, USA, 2004.

53. Sheridan, L. K., H. E. Fitzgerald, K. M. Adams, J. T. Nigg, M. M. Martel, L. I. Puttler, M. M. Wong, and R. A. Zucker, "Normative symbol digit modalities test performance in a community-based sample," *Archives of Clinical Neuropsychology*, Vol. 21, no. 1, pp. 23–28, 2006.

54. Smith, S. M., M. Jenkinson, M. W. Woolrich, C. F. Beckmann, T. E. Behrens, H. Johansen-Berg, P. R. Bannister, M. De Luca, I. Drobnjak, D. E. Flitney, R. K. Niazy, J. Saunders, J. Vickers, Y. Zhang, N. De Stefano, J. M. Brady, and P. M. Matthews, "Advances in functional and structural mr image analysis and implementation as fsl," *Neuroimage*, Vol. 23 Suppl 1, pp. S208–19, 2004.

55. Basser, P. J., and D. K. Jones, "Diffusion-tensor mri: theory, experimental design and data analysis - a technical review," *NMR Biomed*, Vol. 15, no. 7-8, pp. 456–67, 2002.

56. Bodammer, N., J. Kaufmann, M. Kanowski, and C. Tempelmann, "Eddy current correction in diffusion-weighted imaging using pairs of images acquired with opposite diffusion gradient polarity," *Magnetic Resonance in Medicine*, Vol. 51, no. 1, pp. 188–193, 2004.

57. Ashburner, J. T., and R. S. J. Frackowiak, *Human Brain Function*, Academic Press, 2 ed., 2004.

58. Wakana, S., A. Caprihan, M. M. Panzenboeck, J. H. Fallon, M. Perry, R. L. Gollub, K. Hua, J. Zhang, H. Jiang, P. Dubey, A. Blitz, P. van Zijl, and S. Mori, "Reproducibility of quantitative tractography methods applied to cerebral white matter," *NeuroImage*, Vol. 36, no. 3, pp. 630 – 644, 2007.

59. Wang, D., Y. Luo, V. C. Mok, W. C. Chu, and L. Shi, "Tractography atlas-based spatial statistics: Statistical analysis of diffusion tensor image along fiber pathways," *NeuroImage*, Vol. 125, pp. 301 – 310, 2016.

60. Smith, S. M., M. Jenkinson, H. Johansen-Berg, D. Rueckert, T. E. Nichols, C. E. Mackay, K. E. Watkins, O. Ciccarelli, M. Z. Cader, P. M. Matthews, and T. E. Behrens, "Tract-based spatial statistics: Voxelwise analysis of multi-subject diffusion data," *NeuroImage*, Vol. 31, no. 4, pp. 1487 – 1505, 2006.

61. Hattori, T., S. Orimo, S. Aoki, K. Ito, O. Abe, A. Amano, R. Sato, K. Sakai, and H. Mizusawa, "Cognitive status correlates with white matter alteration in parkinson's disease," *Human Brain Mapping*, Vol. 33, no. 3, pp. 727–739, 2012.

62. Nichols, T. E., and A. P. Holmes, "Nonparametric permutation tests for functional neuroimaging: A primer with examples," *Human Brain Mapping*, Vol. 15, no. 1, pp. 1–25, 2002.

63. Winkler, A. M., G. R. Ridgway, M. A. Webster, S. M. Smith, and T. E. Nichols, "Permutation inference for the general linear model," *Neuroimage*, Vol. 92, pp. 381–97, 2014.

64. Rae, C. L., M. M. Correia, E. Altena, L. E. Hughes, R. A. Barker, and J. B. Rowe, "White matter pathology in parkinson's disease: the effect of imaging protocol differences and relevance to executive function," *Neuroimage*, Vol. 62, no. 3, pp. 1675–1684, 2012.

65. Glantz, S. A., *Primer of Biostatistics*, USA: McGraw-Hill, Medical Publishing Division, 6th edition ed., 2014.

66. Berankova, D., E. Janousova, M. Mrackova, I. Eliasova, M. Kostalova, S. Skutilova, and I. Rektorova, "Addenbrooke's cognitive examination and individual domain cut-off scores for discriminating between different cognitive subtypes of parkinson's disease," *Parkinson's Disease*, Vol. 2015, 2015.

67. Atienza, M., K. Atalaia-Silva, G. Gonzalez-Escamilla, E. Gil-Neciga, A. Suarez-Gonzalez, and J. L. Cantero, "Associative memory deficits in mild cognitive impairment: the role of hippocampal formation," *Neuroimage*, Vol. 57, no. 4, pp. 1331–1342, 2011.

68. Zheng, Z., S. Shemmassian, C. Wijekoon, W. Kim, S. Y. Bookheimer, and N. Pouratian, "Dti correlates of distinct cognitive impairments in parkinson's disease," *Human brain mapping*, Vol. 35, no. 4, pp. 1325–1333, 2014.

69. Melzer, T., R. Watts, M. MacAskill, T. Pitcher, L. Livingston, R. Keenan, J. Dalrymple-Alford, and T. J Anderson, "White matter microstructure deteriorates across cognitive stages in parkinson disease," Vol. 80, 04 2013.

70. Kamagata, K., Y. Motoi, H. Tomiyama, O. Abe, K. Ito, K. Shimoji, M. Suzuki, M. Hori, A. Nakanishi, T. Sano, R. Kuwatsuru, K. Sasai, S. Aoki, and N. Hattori, "Relationship between cognitive impairment and white-matter alteration in parkinson's disease with dementia: tract-based spatial statistics and tract-specific analysis," *European Radiology*, Vol. 23, pp. 1946–1955, Jul 2013.

71. Madden, D. J., I. J. Bennett, and A. W. Song, "Cerebral white matter integrity and cognitive aging: contributions from diffusion tensor imaging," *Neuropsychology review*, Vol. 19, no. 4, p. 415, 2009.

72. Yoshikawa, K., Y. Nakata, K. Yamada, and M. Nakagawa, "Early pathological changes in the parkinsonian brain demonstrated by diffusion tensor mri," *Journal of Neurology, Neurosurgery & Psychiatry*, Vol. 75, no. 3, pp. 481–484, 2004.

73. Zhan, W., G. A. Kang, G. A. Glass, Y. Zhang, C. Shirley, R. Millin, K. L. Possin, M. Nezamzadeh, M. W. Weiner, J. Marks, W. J., and N. Schuff, "Regional alterations of brain microstructure in parkinson's disease using diffusion tensor imaging," *Mov Disord*, Vol. 27, no. 1, pp. 90–7, 2012.

74. Deng, B., Y. Zhang, L. Wang, K. Peng, L. Han, K. Nie, H. Yang, L. Zhang, and J. Wang, "Diffusion tensor imaging reveals white matter changes associated with cognitive status in patients with parkinson's disease," *American Journal of Alzheimer's Disease & Other Dementiasr*, Vol. 28, no. 2, pp. 154–164, 2013. PMID: 23271331.

75. Agosta, F., E. Canu, E. Stefanova, L. Sarro, A. Tomić, V. Špica, G. Comi, V. S. Kostić, and M. Filippi, "Mild cognitive impairment in parkinson's disease is associated with a distributed pattern of brain white matter damage," *Human brain mapping*, Vol. 35, no. 5, pp. 1921–1929, 2014.

76. Chan, L.-L., H. Rumpel, K. Yap, E. Lee, H.-V. Loo, G.-L. Ho, S. Fook-Chong, Y. Yuen, and E.-K. Tan, "Case control study of diffusion tensor imaging in parkinson's disease," *Journal of Neurology, Neurosurgery & Psychiatry*, Vol. 78, no. 12, pp. 1383–1386, 2007.

77. Karagulle Kendi, A., S. Lehericy, M. Luciana, K. Ugurbil, and P. Tuite, "Altered diffusion in the frontal lobe in parkinson disease," *American Journal of Neuroradiology*, Vol. 29, no. 3, pp. 501–505, 2008.

78. Gattellaro, G., L. Minati, M. Grisoli, C. Mariani, F. Carella, M. Osio, E. Ciceri, A. Albanese, and M. Bruzzone, "White matter involvement in idiopathic parkinson disease: A diffusion tensor imaging study," *American Journal of Neuroradiology*, Vol. 30, no. 6, pp. 1222–1226, 2009.

79. Thillainadesan, S., W. Wen, L. Zhuang, J. Crawford, N. Kochan, S. Reppermund, M. Slavin, J. Trollor, H. Brodaty, P. Sachdev, and et al., "Changes in mild cognitive impairment and its subtypes as seen on diffusion tensor imaging," *International Psychogeriatrics*, Vol. 24, no. 9, pp. 1483–1493, 2012.